



**Leave Extract from *Mitragyna speciosa* (Korth.) Havil. Attenuates
Methamphetamine Conditioned Place Preference of Mice**

Jakkrit Nukitram

**A Thesis Submitted in Partial Fulfillment of the Requirement for
the Degree of Doctor of Philosophy in Physiology**

Prince of Songkla University

2022

Copyright of Prince of Songkla University



**Leave Extract from *Mitragyna speciosa* (Korth.) Havil. Attenuates
Methamphetamine Conditioned Place Preference of Mice**

Jakkrit Nukitram

**A Thesis Submitted in Partial Fulfillment of the Requirement for
the Degree of Doctor of Philosophy in Physiology**

Prince of Songkla University

2022

Copyright of Prince of Songkla University

Thesis Title Leave Extract from *Mitragyna speciosa* (Korth.) Havil. Attenuates Methamphetamine Conditioned Place Preference of Mice
Author Mr. Jakkrit Nukitram
Major Physiology

Major advisor:

.....
 (Assoc. Prof. Dr. Ekkasit Kumarnsit)

Co-advisor:

.....
 (Asst. Prof. Dr. Dania Cheaha)

Examining Committee:

..... Chairperson
 (Prof. Dr. Banthit Chetsawang)

..... Committee
 (Assoc. Prof. Dr. Ekkasit Kumarnsit)

..... Committee
 (Asst. Prof. Dr. Dania Cheaha)

..... Committee
 (Dr. Nifareeda Samerphob)

..... Committee
 (Asst. Prof. Dr. Pissared Muangnil)

..... Committee
 (Asst. Prof. Dr. Chatchai Wattanapiromsakul)

..... Committee
 (Asst. Prof. Dr. Theerawit Wilaiprasitporn)

The Graduate School, Prince of Songkla University, has approved this thesis as a partial fulfillment of the requirement for the Doctor of Philosophy Degree in Physiology

.....
 (Prof. Dr. Damrongsak Faroongsarng)

Dean of Graduate School

This is to certify that the work here submitted is the results of the candidate's own investigations. Due acknowledge has been made of any assistance received.

..... Signature
(Assoc. Prof. Dr. Ekkasit Kumarnsit)
Major advisor

..... Signature
(Asst. Prof. Dr. Dania Cheaha)
Co-advisor

..... Signature
(Mr. Jakkrit Nukitram)
Candidate

I hereby certify that this work has not been accepted in substance for any degree and is not being currently submitted in candidature for any degree.

..... Signature

(Mr. Jakkrit Nukitram)

Candidate

ชื่อวิทยานิพนธ์ สารสกัดจากใบกระท่อมลดอาการอยากยาเมทแอมเฟตามีนในโมเดลชอบสถานที่
อย่างมีเงื่อนไขในหนูขนาดเล็ก

ผู้เขียน นายจักรกริช นุกิจรัมย์

สาขาวิชา สรีรวิทยา

ปีการศึกษา 2565

บทคัดย่อ

เมทแอมเฟตามีน (Methamphetamine, METH) เป็นยาเสพติดประเภทกระตุ้นประสาท ถึงแม้กลไกการติด METH ที่มีต่อระบบประสาทจะถูกรายงานออกมามากแล้ว แต่ยังคงขาดข้อมูลของสัญญาณศักย์ไฟฟ้าเฉพาะที่ (Local field potential, LFP) ของสมองส่วน basolateral amygdala (BLA) ดังนั้น การทดลองแรก จึงบันทึกและวิเคราะห์ LFP จากสมองส่วน BLA โดยใช้โมเดลชอบสถานที่อย่างมีเงื่อนไข (Condition place preference, CPP) เพื่อชักนำให้หนูติด METH และพบว่า หนูที่แสดงอาการติดยา จะลดค่า power ของ BLA LFP ที่ความถี่ theta และ alpha แต่เพิ่มค่า theta-gamma coupling ซึ่งการเปลี่ยนแปลงดังกล่าว คาดว่าบางส่วนเป็นผลมาจากการลดลงของสารสื่อประสาท serotonin แต่เพิ่มขึ้นของสารสื่อประสาท dopamine และการตอบสนองต่อความเครียด ซึ่งเป็นการเปลี่ยนแปลงทางสรีรวิทยาที่อาจสามารถเปลี่ยนกลับได้ด้วยฤทธิ์จากสารสกัดจากใบพืชกระท่อม

พืชกระท่อม (*Mitragyna speciosa* (Korth.) Havil.) (KT) เป็นพืชสมุนไพรที่มีรายงานการใช้ใบหรือสารสกัดจากใบ เพื่อบรรเทาอาการลงแดง ในช่วงของการถอนยาเสพติดหลายชนิด อย่างไรก็ตาม ยังไม่มีรายงานการใช้สารสกัดจากใบ KT ต่อการควบคุมอาการอยาก METH ดังนั้น การวิจัยในครั้งนี้ มีวัตถุประสงค์เพื่อศึกษาพฤติกรรมความอยากยา METH ในโมเดล CPP และรูปแบบ LFP ของสมองส่วน ventral tegmental area (VTA), hippocampus (HP) และ nucleus accumbens (NAc) ที่ตอบสนองต่อการให้ KT ผลการทดลองพบว่า KT ช่วยลดความแรงของการติดยา METH ในสัตว์ทดลอง ซึ่งประเมินโดยใช้ค่า CPP score ผ่านการลด VTA delta power, HP delta power และ NAc gamma I power ในขณะเดียวกันเมื่อศึกษาการสอดคล้องกันของ LFP ระหว่างสมอง (Coherence) พบว่า KT ยังช่วยลด gamma I coherence ในแกน VTA-NAc และ HP-NAc แต่จะเพิ่ม alpha coherence ในแกน VTA-HP

การลดลงของพฤติกรรมติดสารเสพติด ที่ชักนำด้วย METH CPP และรูปแบบ LFP ที่เปลี่ยนไป อาจเป็นหลักฐานที่ช่วยยืนยันถึงการใช้ KT เป็นยาทางเลือกเพื่อการรักษาอาการติดและถอน METH ได้

Thesis Title Leave Extract from *Mitragyna speciosa* (Korth.) Havil.
Attenuates Methamphetamine Conditioned Place
Preference of Mice
Author Mr. Jakkrit Nukitram
Major Program Physiology
Academic Year 2022

Abstract

Methamphetamine (METH) is a psychostimulant drug that can induce rewarding behaviors. Although its mechanism acting on the central nervous system has been proposed, there is no evidence reported about the local field potential (LFP) pattern in the basolateral amygdala (BLA) in response to METH dependence. The first experiment was conducted to record and analyze LFP in the BLA in METH conditioned place preference (CPP). The results exposed that addition-related mice suppressed BLA theta and alpha power but enhanced theta-gamma coupling. These changes were hypothesized to involve stress response, dopamine release, and serotonin clearance. All these physiological alterations may be reversed by the effects of kratom leave extract.

Mitragyna speciosa (Korth.) Havil. locally called kratom (KT) is a medicinal plant. Its leave extract has been proposed to attenuate many withdrawal symptoms induced by the abuse of drugs. However, using KT leaves on METH-induced CPP remained largely unexplored. This experiment aimed to examine animal behaviors as well as LFP patterns in the ventral tegmental area (VTA), hippocampus (HP), and the nucleus accumbens (NAc) in response to KT leave extract treatment in METH CPP mice. The results revealed that KT leaves extract at 80 mg/kg effectively ameliorated the CPP score via attenuating VTA delta power, HP delta power, and NAc gamma I power. Simultaneously, it also changes the pattern of brain connectivity expressed as coherence by lowering gamma I coherence in the VTA-NAc and HP-NAc axes but escalating alpha coherence in the VTA-HP axis.

Altogether, the evidence-based study may suggest that KT leave extract may be suitable to develop as an alternative drug for METH craving therapy.

Acknowledgments

There were many people who brought me to accomplish the goals of this thesis. Without their assistance and support from them, this work would have not been achieved perfectly. Firstly, I would like to express my deeply sincere thanks to my core advisor, Assoc. Prof. Dr. Ekkasit Kumarnsit passes his warm encouragement and insightful guidance to me since I was an undergrad internship from Khon Kaen University until finishing my Ph.D. research. During the rough road of my Ph.D. journey, I always obtained excellent and positive comments from him to allow me to get through unexpected obstacles. I also require declaring a big appreciation to my co-advisor, Asst. Prof. Dr. Dania Cheaha, who sent me very great attitudes frequently. I am indebted to all thesis defense committees, Prof. Dr. Bantthit Chetsawang, Asst. Prof. Dr. Chatchai Wattanapiromsakul, Asst. Prof. Dr. Dania Cheaha, Dr. Nifareeda Samerphob, Asst. Prof. Dr. Pissared Muangnil, and Asst. Prof. Dr. Theerawit Wilaiprasitporn, who give critical and valuable suggestions and comments to my thesis dissertation.

I desired to show my appreciation to the Human Resource Development in Science Project (Science Achievement Scholarship of Thailand, SAST) and the Physiology program, Division of Health and Applied Science, Prince of Songkla University which offered the finance for this project. Moreover, I couldn't omit to thank the research team from the Biosignal Research Center for Health for the exchange and transfer of their valuable experiences of animal surgery and signal processing that everyone has been practicing intensively and for a long time.

Lastly but most importantly, I would like to dedicate the goodness and benefits resulting from this research to my parents and my beloved family who have been continuously educating, supporting, and encouraging me. They often push me both spiritually and physically to allow me to reach a good education as currently, Thank you.

Jakkrit Nukitram

List of Contents

Contents	Page
List of Figures	x
List of Abbreviations	xii
List of original publications	xiv
1. Conceptual framework of the experiments	1
2. Background and METH problems	2
3. Basic information on LFP signal parameters	4
3.1 Power spectral density (PSD)	5
3.2 Phase-amplitude couplings (PAC)	6
3.3 Coherence	6
4. Objective of the METH CPP experiment	7
5. Materials and Methods for the METH CPP experiment	7
5.1 Animals	7
5.2 Drugs and chemicals	7
5.3 Animal surgery for implanting the LFP electrodes	7
5.4 CPP apparatus and paradigm	8
5.5 Recording of LFP signals and animal locomotor activity	10
5.6 Statistical analyses	11
6. Results of the METH CPP experiment	11
6.1 Locomotor activity	11
6.2 METH conditioned place preference	11
6.3 PSD in the BLA of METH conditioned place preference	12
6.4 PAC in the BLA of METH conditioned place preference	14
7. Discussion of the METH CPP experiment	17
8. Conclusion of the METH CPP experiment	20
9. Kratom extract as a candidate drug for treatment METH CPP craving	21
9.1 KT extract and stress response	21
9.2 KT extract and 5-HT levels	21
9.3 KT extract and anti-DA activity	22
10. Objective of the METH CPP experiment treated with KT leaves extract	27
11. Materials and methods of METH CPP experiment treated with KT leaves extract	22
11.1 Plant materials	22
11.2 Preparation of crude alkaloid extract and phytochemical characterization	22
11.3 Animals	23
11.4 Drugs and chemicals	23
11.5 Animal surgery for implanting the LFP electrodes	24
11.6 CPP apparatus and paradigm	24
11.7 The processing of LFP signals and locomotor activity	26
11.8 Statistical analyses	27

Contents	Page
12. Results of the METH CPP experiment treated with KT leaves extract	28
12.1 Animal movement and Locomotor activity	28
12.2 CPP Score	29
12.3 LFP oscillation in the VTA, HP, and the NAc	32
12.4 Activities of the coherences	36
13. Discussion of the METH CPP experiment treated with KT leaves extract	40
14. Conclusion of the METH CPP experiment treated with KT leaves extract	45
Significant findings of all experiments	47
Further direction	48
References	49
Appendices	62
Appendix A Original article	63
Appendix B Ethical approval of using the animal for scientific purposes	87
VITAE	89

List of Figures

Figures	Page
1 A flowchart exhibits the overall work of two experiments	1
2 Interconnections of the brain regions in the reward circuit	2
3 Type of brain signals from the extracellular recording	4
4 Component of signal oscillation	4
5 The composition of LFP signals in different amplitudes, frequencies, and phases of each sine wave, and the principle of the FFT transformation	5
6 Overview of data transformation from time to frequency domain under the function of FFT	5
7 The procedures for PAC analysis	6
8 The ideal phenomena of signals between areas that contained a high degree of coherence at 40 Hz	6
9 The protocol for characterization of LFP pattern and PAC rhythm in the BLA of mice in METH-induced CPP	9
10 Locomotor activity of animals in a CPP apparatus	11
11 Locomotor tracking of exploratory behavior of representative mice and CPP scores	12
12 Raw LFP signals of representative mice during pre-conditioning and post-conditioning phases of the METH group	13
13 Averaged LFP spectral powers of control and METH groups	14
14 Phase-amplitude cross-frequency couplings of control and METH group	15
15 Modulation indices of the BLA of control group during pre-conditioning and post-conditioning phases	16
16 Modulation indices of the BLA of METH group during pre-conditioning and post-conditioning phases	17
17 An overview of the key findings of the BLA LFP oscillations following METH CPP induction	20
18 Experimental protocol for investigation of KT alkaloid extract effects on METH CPP	26
19 Locomotor activity of mice during pre-conditioning and post-conditioning phases of control group and METH groups treated with various solutions	29
20 Locomotor tracking of animal exploration in CPP apparatus during pre-conditioning and post-conditioning phases of control and METH groups treated with various solutions	31
21 Raw LFP signals of representative mice from each group during pre-conditioning and post-conditioning phases of control and METH groups treated with various solutions	32

Figures	Page
22 Effects of the treatments with KT alkaloid extract on LFP spectral powers in the VTA	33
23 Effects of the treatments with KT alkaloid extract on LFP spectral powers in the HP	34
24 Effects of the treatments with KT alkaloid extract on LFP spectral powers in the NAc	36
25 Effects of the treatments with KT alkaloid extract on LFP spectral coherence between the VTA and the HP	37
26 Effects of the treatments with KT alkaloid extract on LFP spectral coherence between the VTA and the NAc	38
27 Effects of the treatments with KT alkaloid extract on LFP spectral coherence between the HP and the NAc	39
28 Schematic diagrams of integrated coherence activity among the VTA, HP and NAc during METH CPP expression and after KT extract administration	40
29 Novel discovery of LFP signals associated with the attenuation of METH CPP treated with KT leaves extract	46

List of Abbreviations

5-HT	Serotonin
AMY	Amygdala
ANOVA	Analysis of variance
AP	Antero-posterior
BLA	Basolateral nuclei of amygdala
BP	Bupropion
CFC	Cross-frequency coupling
CMC	Carboxymethyl cellulose
CNS	Central nervous system
COR	Corticosterone
CPP	Conditioned place preference
DA1	Dopamine receptor type 1
DA2	Dopamine receptor type 2
DA	Dopamine
DAT	Dopamine transporter
DRn	Dorsal raphe nuclei
DV	Dorso-ventral
FFT	Fast Fourier Transform
FLU	Fluoxetine
FST	Force swimming test
HP	Hippocampus
HPA	Hypothalamic-pituitary-adrenal
KT	Kratom
LFP	Local field potential
METH	Methamphetamine
MI	Modulation index
ML	Medio-Lateral
mPFC	medial Prefrontal cortex
MT	Mitragynine
MTPD	Methylphenidate
NAc	Nucleus accumbens core
NT	Neurotransmitter
PAC	Phase-amplitude coupling
PSD	Power spectral density
SEM	Standard Error of Mean
SSRI	Selective serotonin reuptake inhibitor
STR	Striatum

TST Tail suspension test
VTA Ventral tegmental area

List of original publications

This dissertation is comprised of some research outputs that have been already published in international journals. The publishers are kindly allowed to include those data in the thesis. The publications have existed as attached documents in appendices in the last section of this thesis. The referred publications were listed as follows.

Nukitram, J., Cheaha, D., & Kumarnsit, E. (2021). Spectral power and theta-gamma coupling in the basolateral amygdala related with methamphetamine conditioned place preference in mice. *Neuroscience letters*, 756, 135939.
(Reprinted with permission of Elsevier)

Nukitram, J., Cheaha, D., Sengnon, N., Wungsintaweekul, J., Limsuwanchote, S., & Kumarnsit, E. (2022). Ameliorative effects of alkaloid extract from *Mitragyna speciosa* (Korth.) Havil. leaves on methamphetamine conditioned place preference in mice. *Journal of Ethnopharmacology*, 284, 114824.
(Reprinted with permission of Elsevier)

Leave extract from *Mitragyna speciosa* (Korth.) Havil. attenuates methamphetamine conditioned place preference of mice

1. Conceptual framework of the experiments

The overview of this research was summarized and exhibited in **Figure 1**. It contained two continuous works initiated from establishing the methamphetamine (METH) conditioned place preference (CPP) model to obtain possible mechanisms underlying this model. The following experiment was conducted to test the effects of the selected drug on METH CPP.

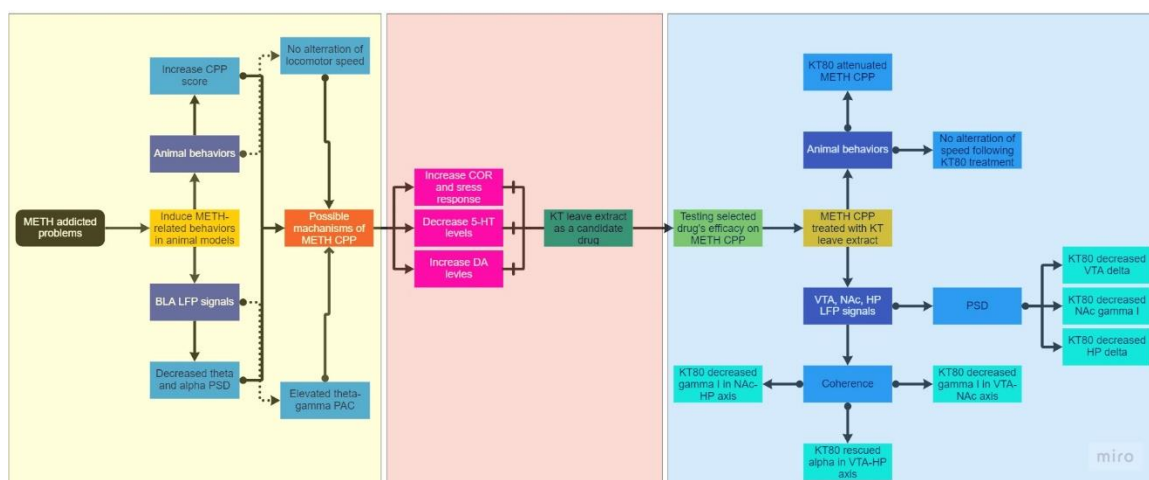


Figure 1 A flowchart exhibits the overall work of two experiments. Yellow, red, and blue boxes represent the METH CPP experiment to find a possible mechanism underlying the METH CPP, the transitional stage involved in surveying candidate drugs for METH CPP therapy and testing the effects of the selected drug on the treatment for METH CPP.

2. Background and METH problems

The evidence of public health problems from misuse and overdose of METH does exist ¹. METH is a stimulant drug acting on the central nervous system (CNS) as a sympathomimetic agent. Chronic METH administration adversely affects body functions² and psychological consequences, including depression and schizophrenia ³. These psychological disorders partially result from the elevation of monoamine neurotransmission-induced monoamine neurotransmitter (NT) remodeling known as neuroplasticity, primarily in the mesolimbic dopaminergic (DA) system ⁴. Additionally, negative consequences of METH use were found to affect behavioral and social aspects of the adolescent population ⁵. Although the deleterious effects of METH use on health exist, the current solution is not satisfied.

The DA cell populations of the mesolimbic DA system located in the ventral tegmental area (VTA) play a crucial role in addictive functions and pleasure behaviors. Fundamentally, several brain regions, including, the nucleus accumbens core (NAc), hippocampus (HP), and the amygdala (AMY), are primarily innervated by DA pathways from the VTA ⁶ (**Figure 2**). In humans, emotion and cognition were interrelated with neural processing from the AMY ⁷. However, the feature of the AMY is not a single complete unit. It comprises various sub-regions, e.g., the centromedial nuclei or basolateral nuclei (BLA) ⁸.

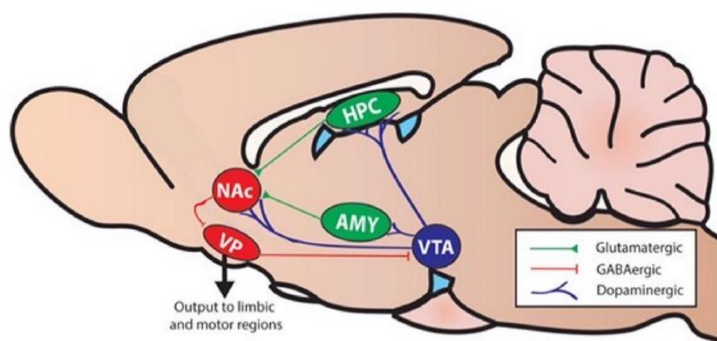


Figure 2 Interconnections of the brain regions in the reward circuit (Modified from Russo and Nestler, 2013)

Neural processing in the BLA is related to reward learning and addiction ⁹. Previously, permanent BLA lesion disrupted the effect of conditioned-cued reinstatement in cocaine self-administration. The attenuation of reinstatement was observable in a classical interference method that inactivated the BLA by using dopamine type 1 (DA1) receptors antagonist. This effect was reversible by intra-infusion of amphetamine, a psychostimulant drug, to the BLA directly ^{10,11}. It was found that decreased BLA activity by intra-injection with AP5, an NMDA receptor antagonist, could block amphetamine

CPP acquisition and extinction¹². These findings indicated that the BLA plays a critical role in neural mechanisms associated with some aspects of drug addiction and craving.

Modulation of the BLA that facilitates drug-seeking behaviors remains to be explored. Although a significant role of the BLA engaged with addictive activities has been proposed. Most previous studies were performed using molecular techniques such as immunoreactive staining, western blotting, and microdialysis^{13,14} which the data outputs were limited in terms of temporal resolution and sensitivity. For example, detecting brain activity modulated within a time fraction in milliseconds is impractical. Therefore, the solution to this problem has already been addressed by the previous demonstration using electrical brain wave recording and analyses¹⁵.

Fundamentally, electrical transmission is a predominant feature of brain communication. Neuronal responses produced by substances such as drugs or neurotransmitters are primarily generated from the interaction between functional domains of various biomolecular molecules (e.g., receptors, channels, enzymes)¹⁶. These substances change downstream signaling pathway modulation, alternate ion conductance pattern of neurons (e.g., increase or decrease firing rate) and elicit local field potential (LFP). LFP signals can be recorded, analyzed, and depicted in various aspects, such as power spectral density (PSD) and phase-amplitude coupling (PAC), which are extensively used to identify clinical profiles of drugs of interest in rodents¹⁷ and humans¹⁸. Moreover, unique LFP patterns can also be used to reflect and represent the specific condition of stimulation, or some certain tasks performed. Previously, elevation in delta and theta powers and theta-high gamma PAC in the hippocampal CA1 of mice were detected in response to repeated exposure to palatable food¹⁹. Moreover, mPFC oscillation in theta and gamma frequency bands and theta-high gamma PAC was associated with heroin addiction, validated by CPP behavioral method²⁰.

In general, multiple factors such as drug conditions, users with a genetic vulnerability, and the properties of drugs themselves can facilitate an addictive state²¹. Additionally, the former factor is decisive because its effect is stored as long-term memory for an extended period. To mimic METH-associated environment-induced rewarding effects and CBs in laboratory models, the CPP paradigm has been extensively deployed²²⁻²⁵.

Several experiments were carried out using the CPP paradigm according to its highly standardized quality for testing addictive properties of drug candidatures²⁶. In particular, it has been widely used as a reliable animal model for investigating brain mechanisms associated with drug-seeking and rewarding behavior in laboratory animals induced by various psychomotor stimulants such as amphetamine, cocaine, and METH^{25,27,28}. Drug craving and seeking behavior are generated by the contextual stimuli related to drug administration. Mostly, the addicts are vulnerable to relapse in response to the

incentives associated with drug intake. However, brain mechanisms and signaling underlying these phenomena have been largely unexplored.

3. Basic information on LFP signal parameters

The electrodes inserted into the extracellular space of neuronal populations in deep areas can capture brain signals that contain two components superimposed on each other. Firstly, spike potential refers to the high-frequency signals from 0.6–1 to 3 kHz²⁹. Another is LFP which is the signals that fluctuate at low-frequency voltage (<200 Hz) (**Figure 3**). It was recognized as the output from the neural ensemble and dendritic processing of the local neural networks³⁰. Processed LFP signals are often illustrated in aspects such as PSD, PAC, and coherence.

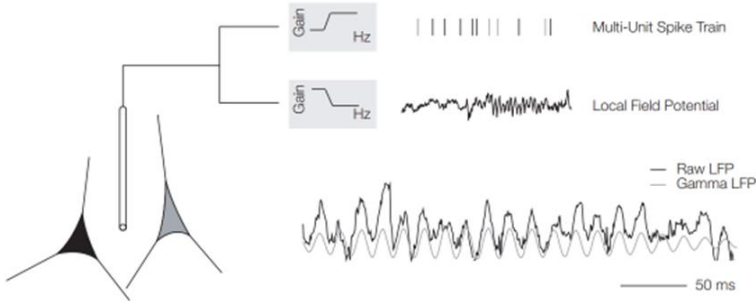


Figure 3 Type of brain signals from the extracellular recording (Modified from (Berens et al., 2008))

Any signal oscillation may contain three portions primarily: frequency, phase, and power (**Figure 4**). Frequency represents the speed of signal oscillated per second, while the definition of phase is the position or angle on a sine wave in a given time. It is often measured in radians or degrees. The energy of the distinct frequency is referred to as power.



Figure 4 Component of signal oscillation (Modified from (Cohen, 2019)³¹)

3.1 Power spectral density (PSD)

LFP signals were established by the aggregation of noises and several sine waves containing the difference in amplitudes, frequencies, and phases (**Figure 5A**). Band filter was performed to extract sine wave into 3 and 8 Hz and mix of 3-Hz-8Hz signal (**Figure 5B in panels A1, B1, and C1, respectively**). The Fast Fourier Transform (FFT) was deployed to convert data from time to the frequency domain, as shown in the bottom panels. The data transformation over time will appear in the continuous histogram (**Figure 5B in panel C2**) to demonstrate the area under the curve of **Figure 6C**. In other words, signal power (**Figure 6C**) results from the principle of FFT working via side-view observation in the horizontal plane of signals in the time domain (**Figure 6B**).

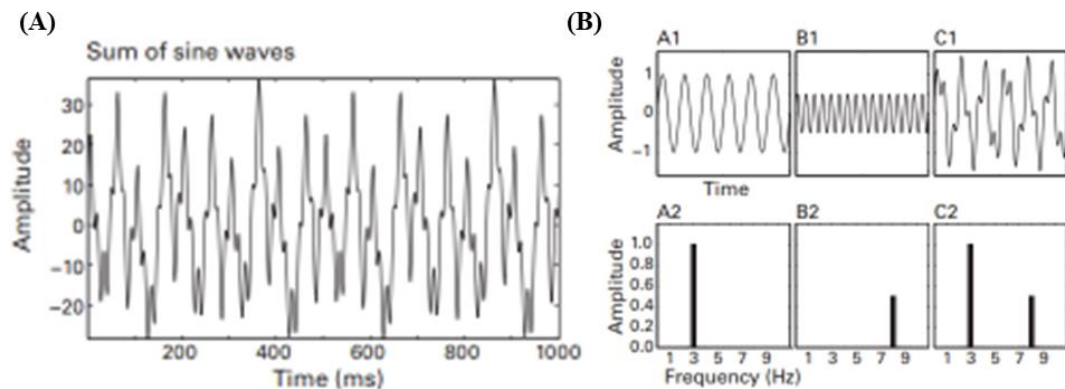


Figure 5 LFP signals are composed of different amplitudes, frequencies, and phases of each sine wave (A). The FFT transformed data from time to frequency domain (B) (Modified from (Cohen, 2019)).

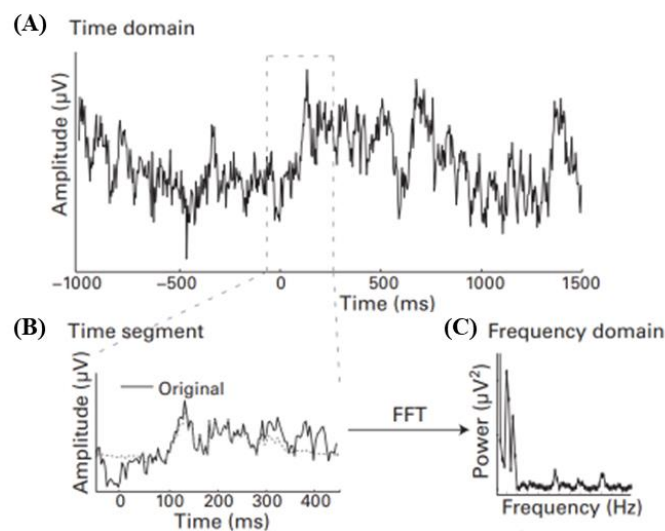


Figure 6 Overview of data transformation from time to frequency domain under the function of FFT (Modified from (Cohen, 2019))

3.2 Phase-amplitude couplings (PAC)

PAC was applied to assess whether a slow oscillation's phase modulates a fast oscillation's amplitude. Strong PAC usually represents a form of high modulation index (MI) (Figure 7).

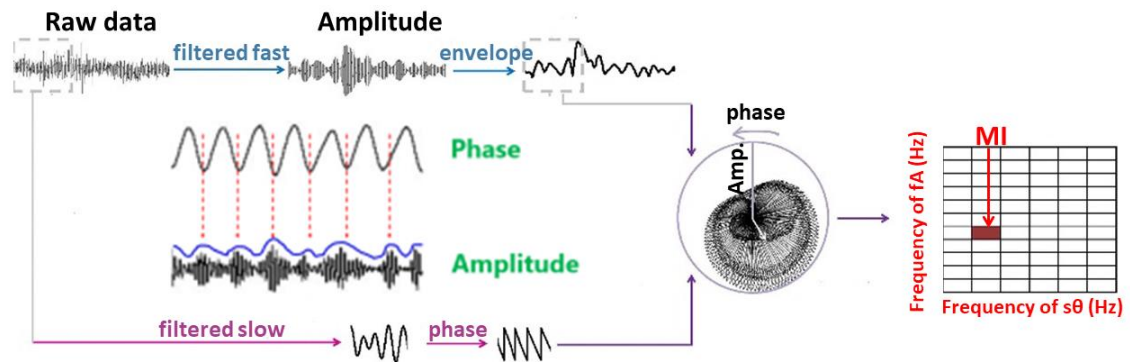


Figure 7 The procedures for PAC analysis (Modified from (Samiee and Baillet, 2017))

3.3 Coherence

Brain working was recognized as a network system functioning by integrating and processing information from many regions. Signals in different sites interacted through the power spectrum over many frequencies and expressed the yield of signal interactions as the degree of coherence. The degree ranged from 0 – 1 to determine that no interaction was seen between the signals originating from a couple of areas and vice versa (Figure 8)

32

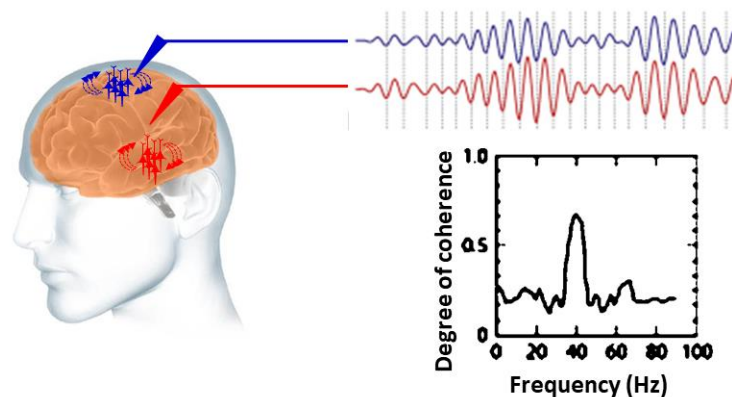


Figure 8 The ideal phenomena of signals between areas that contained a high degree of coherence at 40 Hz (Modified from (Shinohara et al., 2013))

4. Objective of the METH CPP experiment

This study aimed to characterize and clarify LFP spectral powers and PAC patterns in the BLA of mice induced by the METH CPP paradigm.

5. Materials and Methods for the METH CPP experiment

5.1 Animals

This animal study was conducted under the guidelines of the European Science Foundation (Use of Animals in Research, 2001) and ARRIVE (Animal Research: Reporting of In Vivo Experiments) to protect animals used in scientific research. The experimental procedures and protocols were approved by the Institute Animal Care and Use Committee, Prince of Songkla University [project license number: MHESI 6800.11/845 and reference number: 57/2019]. Male Swiss albino ICR mice (7–8 weeks old) were obtained from the National Laboratory Animal Center, Mahidol University, Thailand. To acclimatize and minimize animal stress, all animals were pre-handled for one week before the initiation of the experiment at the Southern Laboratory Animal Facility, Prince of Songkla University. The animals were housed in an individual stainless-steel cage (17 x 28.5 x 17 cm) with a standard environment (12/12 h light/dark cycle, 22 ± 3 °C, and $55 \pm 10\%$ relative humidity). Commercial food pellets and water were available ad libitum. All experiments were carried out between 8 a.m. and 4 p.m.

5.2 Drugs and chemicals

METH hydrochloride was provided by the Food and Drug Administration, Thailand, with a standard purity (95.8%) for research purposes. In addition, METH at 1 mg/kg diluted in physiological saline solution (0.9% w/v NaCl) was intraperitoneally injected with a fixed volume per body weight of mice at 10 ml/kg. The concentration of METH was selected under a dose that produced conditioned place preference in this strain of mice²⁵.

5.3 Animal surgery for implanting the LFP electrodes

The process of intracranial electrode implantation has already been described previously³³. At the start of the experiment, animals were approximately four months after birth with a body weight of 45.0 ± 2.4 g. They were deeply anesthetized with an intraperitoneal injection of 16 mg/kg xylazine hydrochloride (Xylavet, Sigma-Aldrich International GmbH, Switzerland) and 50 mg/kg zoletil (Tiletamine – zolazepam, Vibac Ah, Inc., USA) cocktail. Following a period of unconsciousness, animals' heads were then fixed with stereotaxic apparatus. Lignocaine (20 mg/ml) (Lidocaine, M & H manufacturing Co., Ltd., Thailand), a local analgesic drug, was administered subcutaneously before making the midline incision of the scalp on the dorsal head to

expose the skull. The position on the skull above the BLA was marked for a drilling hole. Therefore, the electrode was stereotaxically positioned on the left hemisphere of the brain, defined from bregma to the BLA (AP; -1.7 mm, ML; 3 mm; DV; 4.8 mm) according to the mouse brain atlas³⁴. The reference also used as a ground electrode was implanted on the skull at the midline over the cerebellum (AP; -6.0 mm, ML; 0.0 mm; DV; 1.5 mm). Additional holes were drilled for stainless steel screws as anchors for extra stability. All silver wire electrodes (0.381 mm in diameter) were secured permanently with dental acrylic (Unifast Trad, GC Dental Industrial Corp., Tokyo, Japan). The antibiotic ampicillin (100 mg/kg) (General Drug House Co., Ltd., Bangkok, Thailand) was applied intramuscularly for three days to prevent infection. The animals were allowed to fully recover in an individual cage for at least two weeks before the start of the experiment.

5.4 CPP apparatus and paradigm

CPP paradigm has been employed to assess environment-induced drug-seeking behaviors in laboratory animals. The CPP apparatus was modified from the previous study³⁵ and made from plexiglass in a Y-shape (**Figure 9**). There were three rectangular compartments (25 cm x 18 cm x 25 cm) connected with and separated from each other by removing or placing removable walls between each compartment and triangular central zone. Two compartments located laterally had identical shapes and sizes to the central zone but had different floor textures and wall shading. One lateral compartment had vertical strips lined on the wall and a smooth floor. The other lateral compartment had grid strips attached to the wall and textured the floor. The third compartment on the base was a neutral zone used as a starting position for animal exploration. The overall schedule of drug injection was modified from the recent study²⁵. The experiment's protocol was shown in a time sequence (**Figure 9**). In brief, the CPP paradigm primarily began with habituation and continued with three phases of CPP, which included a pre-conditioning, a conditioning, and a post-conditioning phases.

5.4.1 Habituation and pre-conditioning phase

Animals were acclimatized to the experimental room. They were brought to a place in the room for at least 30 min before the start of the experiments. During the habituation (days 1 and 2), animals were intraperitoneally injected with normal saline solution and immediately placed in the starting position in the chamber. Then, animals were individually allowed to explore all compartments of the CPP apparatus freely for 15 min. During a period of pre-conditioning (day 3), the animals were treated and trained in the same manner as during the habituation periods. The time animals spent in each compartment was assessed and expressed as a CPP score. CPP score for each animal was calculated by subtraction of the time that each animal spent in the METH-paired compartment with time spent in the normal saline-paired compartment. Tossing a coin was a method to divide all mice into two sub-groups to receive either normal saline or

METH. Moreover, two compartment sides were randomly paired with METH or saline to avoid bias.

5.4.2 Conditioning phase

The conditioning phase took ten consecutive days (days 4 - 13). Mice of the METH group ($n = 7$) were given METH and saline injection on alternative days (1 mg/kg METH on an odd day and saline on an even day during this phase). Subsequently, they were confined to the assigned compartment for 30 min to learn to pair with different treatments (METH and saline) and specific details of the assigned compartments. On the other hand, control mice ($n = 10$) were administered with normal saline daily for both compartments. After the animals completed the session each day, they were moved back to their home cage.

5.4.3 Post-conditioning phase

The post-conditioning phase was done on day 14 (post-conditioning day1). The procedure of this phase was the same as that of the pre-conditioning phase. For testing, mice from both groups were given neither METH nor normal saline. They were individually allowed to survey the entire CPP apparatus freely for 15 min. After that, the calculation of the CPP score was carried out.

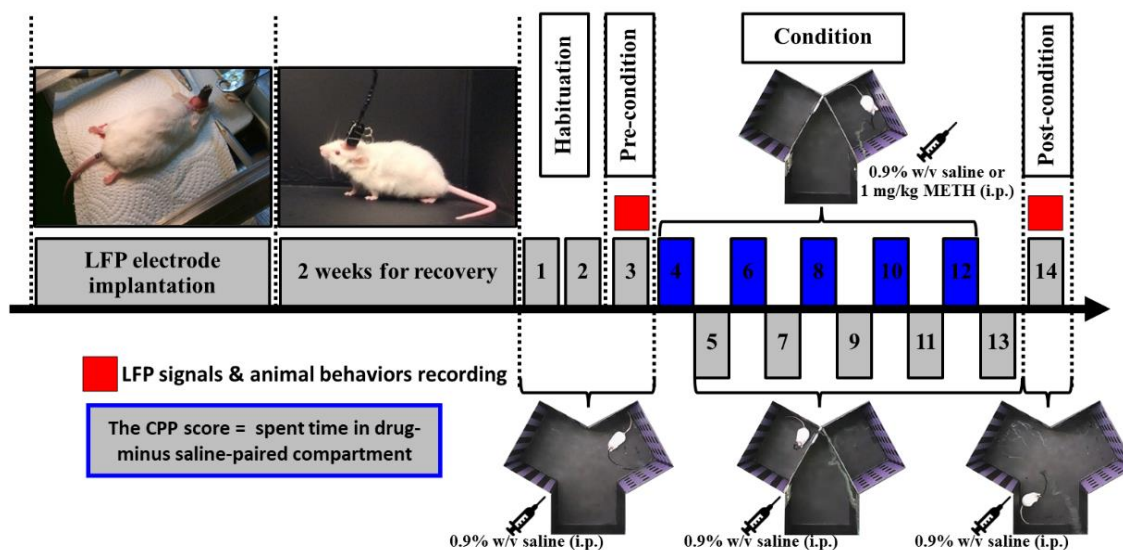


Figure 9 The protocol for characterization of LFP pattern and PAC rhythm in the BLA of mice in METH-induced CPP. Animals were handled through the processes of electrode implantation, recovery period, and three phases of a CPP paradigm: habituation and pre-conditioning, conditioning, and post-conditioning phases during days 1-3, 4-13, and 14, respectively.

5.5 Recording of animal locomotor activity and LFP signals

LFP signals and locomotor activities of individual animals were recorded simultaneously during the pre-conditioning and post-conditioning phases. For LFP signal recording, after 50 Hz power line and spontaneously electrical artifact rejection, signals were harvested with 1.024 s duration in sweeps, and the size of sampling frequency was 2 kHz. Therefore, the sampling frequency was 2.048 kHz, well over the Nyquist sampling rate. All LFP signals were amplified with low-pass 1 kHz and high-pass 0.3 Hz by Dual Bio Amp (AD Instruments, Castle Hill, NSW, Australia). A PowerLab 16/35 system (AD Instruments, Castle Hill, NSW, Australia) with 16-bit A/D performed the conversion from analog signals to digital data. LFP signal analysis was processed through 1–100 Hz band-pass digital filtering. For locomotor activity, the spontaneous animal movement was captured by a webcam camera vertically fixed on the top of the recording chamber. All data were deposited in a computer through LabChart 7.3.7 pro software. Data were selected explicitly during 5-15 min of this recording to monitor LFP oscillations and PAC patterns of mice under an addictive state induced by METH treatment.

5.5.1 Locomotor activity analysis

The analysis of locomotor activities of animals was validated by using the open source toolbox OptiMouse³⁶ to capture the body position of mice. The alternations of locomotor activity in the assigned period and time spent in each compartment of the apparatus were illustrated and expressed as mean \pm Standard Error of Mean (SEM).

5.5.2 LFP signal analysis

For data analysis, the FFT algorithm (Hanning window cosine transform) with 50% window overlap and 0.976 Hz of power spectra resolution was used for generating PSD from digitized data stored in a PC via the LabChart 7.3.7 pro software. Subsequently, each discrete frequency band of the PSD was averaged and depicted as a log percentage of total power in frequency domains with eight defined signal frequency ranges (delta: 1.0-3.9 Hz, theta: 4.7-8.7 Hz, alpha: 9.8–12.7 Hz; beta: 13.6-29.3 Hz, gamma I-IV: 30-90 (increase in 15 Hz in order))

Cross-frequency coupling (CFC) was used to evaluate the interactions between different frequency ranges of the neural signal. This study focused on PAC, one of the most typical representatives of CFC, to analyze the strength of coupling between 2 frequency bands of interest. The results were expressed as MI extracted from comodulograms or coupling maps to present faster wave amplitude driven by a slower frequency phase. Therefore, PAC was deployed to analyze LFP data during drug-seeking behaviors. Theta-gamma coupling was explicitly focused. All raw data were run via toolbox Brainstorm3³⁷.

5.6 Statistical analyses

All parameters were shown and analyzed as mean \pm Standard Error of Mean (SEM). All parameters were processed under the function of two-way repeated measure analysis of variance (ANOVA). Conditioning states or trials were used as within-subject factors, and inter-subject factors with or without METH treatment were considered inter-subject factors defined as a group. A P-value < 0.05 was defined as statistically significant.

6. Results of the METH CPP experiment

6.1 Locomotor activity

Locomotor activity was monitored for a period of 15 min recording. Data were analyzed for a parameter of locomotor speed (**Figure 10A**). Values during pre- and post-conditioning phases of control and METH groups were shown. The results showed high fluctuations, particularly during the early period. The speed levels were relatively stable from the middle to the end of the recording period of both the control and METH groups. Statistical analysis revealed non-significant differences between groups and pre-conditioning and post-conditioning phases (**Figure 10B**). Therefore, raw signals from a period of 5 to 15 min recording were selected for analyses of all data in this study.

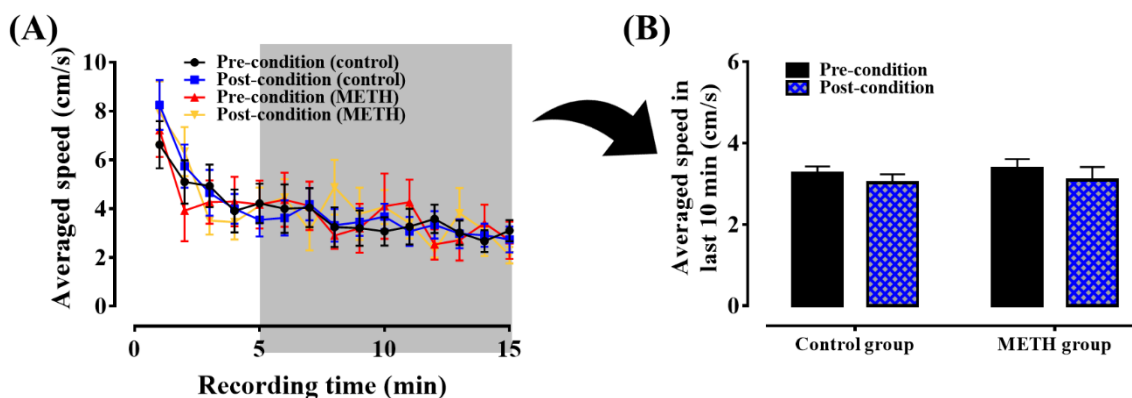


Figure 10 Locomotor activity of animals in a CPP apparatus, Averaged speed during pre-conditioning and post-conditioning phases of control ($n = 10$) and METH ($n = 7$) groups were monitored. Values were calculated every 1-min bin (A). Averaged speeds during 5-15 min were selected for investigation (B).

6.2 METH conditioned place preference

Time spent on animals in saline-paired and METH-paired compartments during pre- and post-conditioning phases of control and METH groups were analyzed. Both control and METH animals explored all compartments relatively evenly during the pre-conditioning phase. No obvious side preference in their exploratory patterns was seen

(Figure 11A). However, during the post-conditioning phase, the control group maintained the same pattern of exploration, whereas the METH group clearly showed a side preference for the METH-paired compartment. Therefore, time spent values were converted into CPP scores and statistically analyzed. During the pre-conditioning phase, control and METH groups had CPP scores at 1.59 ± 16.03 s and -6.70 ± 20.42 s, respectively. During the post-conditioning phase, control and METH groups produced CPP scores at 10.07 ± 50.20 s and 258.48 ± 48.83 s, respectively. Two-way repeated measure ANOVA revealed significant effects of trial [$F(1, 15) = 13.712, P = 0.002$], group [$F(1, 15) = 11.334, P = 0.004$] and group x trial interactions [$F(1, 15) = 12.065, P = 0.003$]. Multiple comparisons revealed significant increases in CPP score during post-conditioning phase of METH group compared to pre-conditioning phase of METH group [$F(1, 15) = 21.888, P < 0.001$] and post-conditioning phase of control group [$F(1, 15) = 13.145, P = 0.002$] (Figure 11B). No significant difference was found between the pre- and post-conditioning phases of the control group and between the pre-conditioning phases of the control and METH groups. Altogether, the present data confirmed the establishment of METH-conditioned place preference.

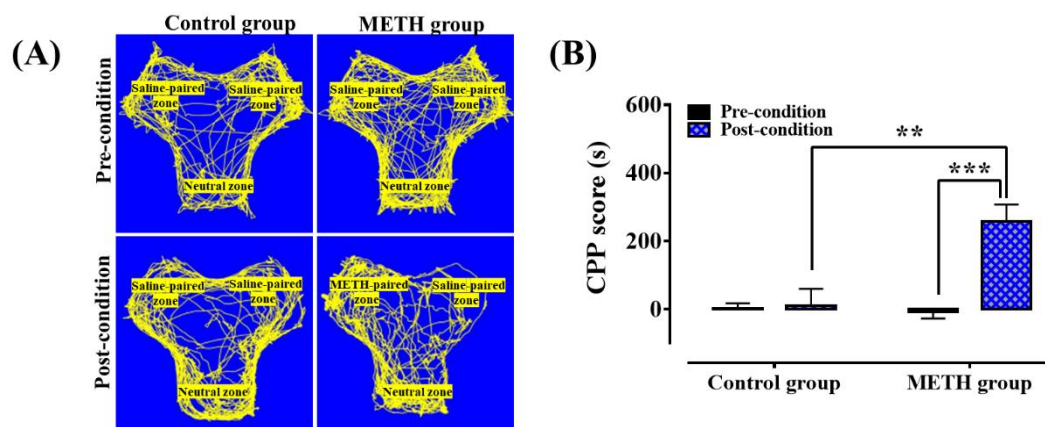


Figure 11 Locomotor tracking of exploratory behavior of representative mice (A) and averaged CPP scores (B) of control and METH groups during pre- and post-conditioning phases in the CPP apparatus are shown. Data were expressed as mean \pm SEM. **, *** $P < 0.01, 0.001$ for comparisons with each paired result.

6.3 PSD in the BLA of METH conditioned place preference

Visual inspection was performed to observe the oscillatory patterns of raw LFP signals and spectrograms during pre-conditioning and post-conditioning phases. Baseline LFP patterns of the pre-conditioning phase were shown with normal components of frequency activity. During the post-conditioning phase, slow wave activities were absent intermittently from time domain signals of METH groups. No apparent change between

the pre-conditioning and post-conditioning phases was seen in the control group (**Figure 12**).

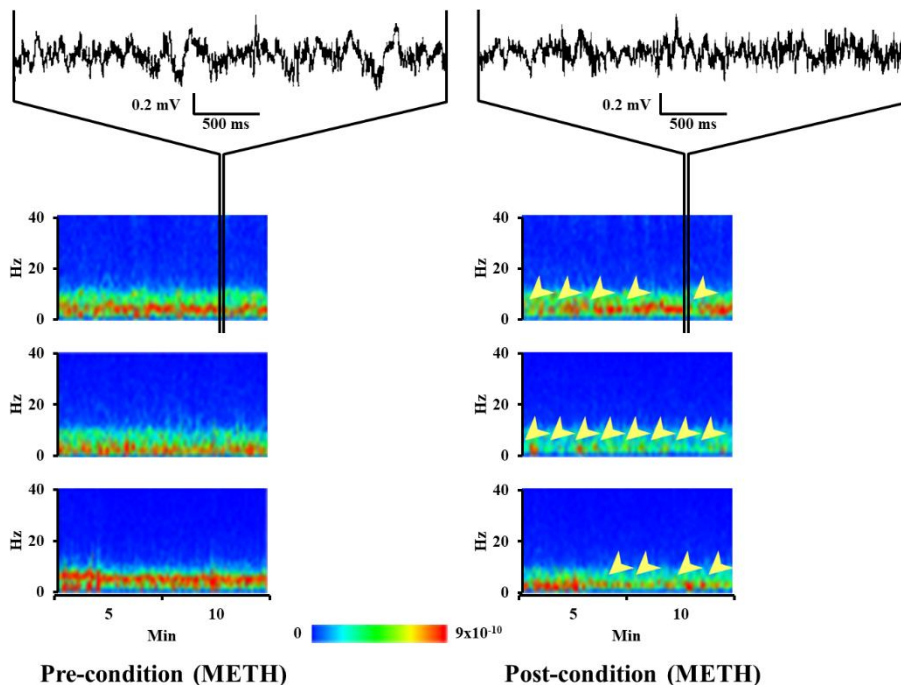


Figure 12 Raw LFP signals of representative mice during pre-conditioning (left panel) and post-conditioning phases (right panel) of the METH group. Raw signals were also converted and shown in spectrograms. Frequency spectral power was demonstrated with color code. Blue and red colors represented the lowest and highest LFP powers, respectively. Arrowheads indicate the disappearance of slow frequency oscillations, particularly in theta and alpha ranges.

Therefore, LFP signals were transformed into the frequency domain for quantitative analysis as LFP spectral powers (**Figure 13A and 13C for control and METH groups, respectively**). Two-way repeated measures ANOVA demonstrated significant effects of trial [$F(1, 15) = 4.776, P = 0.045$] and trial x group interactions [$F(1, 15) = 5.342, P = 0.035$] but not effects of group on the theta wave. Moreover, significant effect was found only on trial [$F(1, 15) = 5.714, P = 0.030$] of alpha wave. The Control group did not show any significant change following the conditioning paradigm (**Figure 13B**). In METH group, significant decreases in theta [$F(1, 15) = 8.593, P = 0.010$] and alpha [$F(1, 15) = 6.220, P = 0.025$] frequency powers during post-conditioning phase compared to pre-conditioning levels were seen (**Figure 13D**). The present data indicated specific changes in theta and alpha frequency ranges in the BLA during the post-conditioning phase of METH CPP.

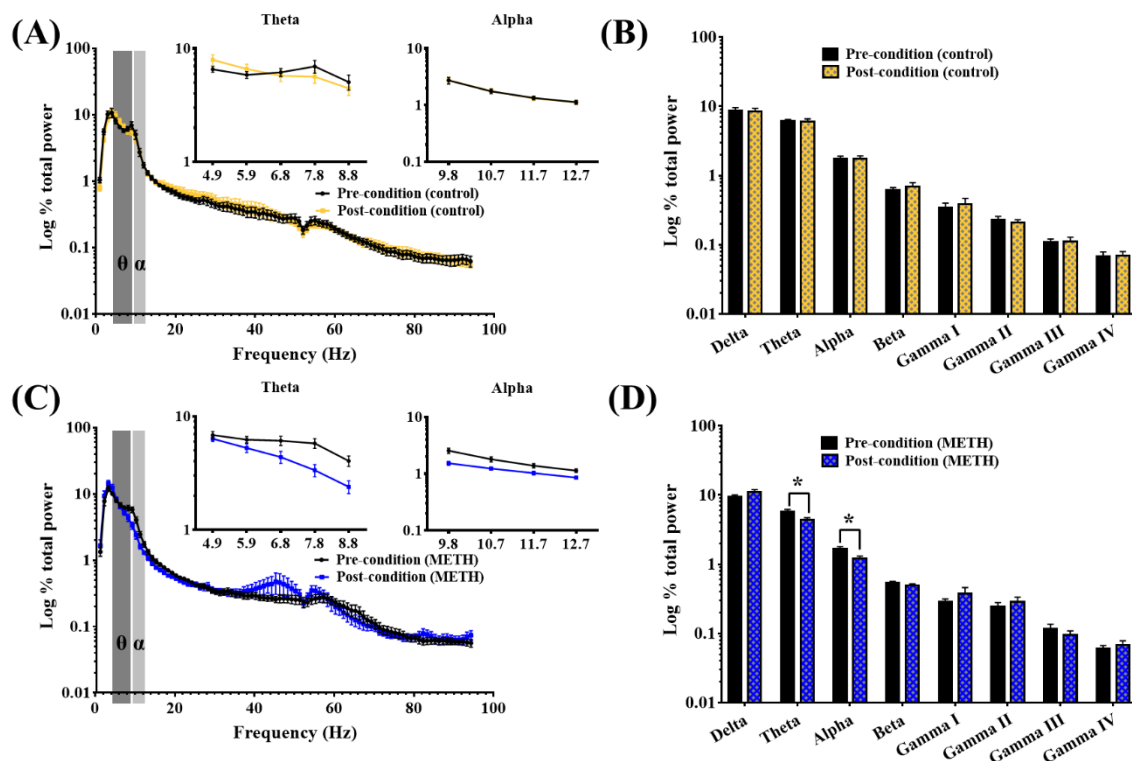


Figure 13 Averaged LFP spectral powers of control (A) and METH groups (C). Data were normalized as percent total power and illustrated on a log scale. Theta and alpha powers were depicted in small sub-plots. LFP powers of control (B) and METH groups (D) were divided into eight discrete frequency bands ranging from delta (1.0-3.9 Hz), theta (4.7-8.7 Hz), alpha (9.8–12.7 Hz), beta (13.6-29.3 Hz), and gamma I-IV (30-90 Hz with an increase in 15 Hz in order). Data were expressed as mean \pm SEM. Asterisks indicate significant differences at *: $P < 0.05$ performed by two-way repeated measure ANOVA.

6.4 PAC in the BLA of METH conditioned place preference

Comodulograms of PAC from the BLA of mice during pre-conditioning and post-conditioning phases were visualized. In the control group, no obvious change was seen. In the METH group, different patterns between comodulograms of pre-conditioning and post-conditioning phases were found (**Figure 14A**). Two-way repeated measures ANOVA demonstrated significant influence of trial [$F(1, 15) = 15.195, P = 0.001$], group [$F(1, 15) = 11.488, P = 0.004$], and trial \times group interactions [$F(1, 15) = 11.039, P = 0.005$] on maximal modulation index (MI). Pairwise comparisons revealed significant increases in MI during post-conditioning phase compared to pre-conditioning phase of METH group [$F(1, 15) = 24.620, P < 0.001$] and post-conditioning phase of control group [$F(1, 15) = 12.254, P = 0.003$] (**Figure 14B**). No significant difference was observed between the pre-

conditioning and post-conditioning phases of the control group and between the pre-conditioning phases of the control and METH groups.

Additionally, significant effects of trial [$F(1, 15) = 5.498, P = 0.033$], and trial \times group interactions [$F(1, 15) = 5.498, P = 0.033$], but not the effects of group, were seen in frequency for phase of slow wave. Multiple comparisons confirmed significant increase in METH group during post-conditioning phase compared to pre-conditioning phase [$F(1, 15) = 10.386, P = 0.006$] and compared to post-conditioning phase of control group [$F(1, 15) = 9.476, P = 0.008$] (**Figure 14C**).

The analysis of frequency for amplitude of fast wave revealed a significant effect of group [$F(1, 15) = 4.735, P = 0.046$] but not trial [$F(1, 15) = 0.094, P = 0.764$] and trial \times group interactions [$F(1, 15) = 2.580, P = 0.129$]. Multiple comparisons indicated a significant difference in frequency for the amplitude of fast waves between post-conditioning levels of METH and control groups [$F(1, 15) = 9.173, P = 0.008$] but not within any group (**Figure 14D**).

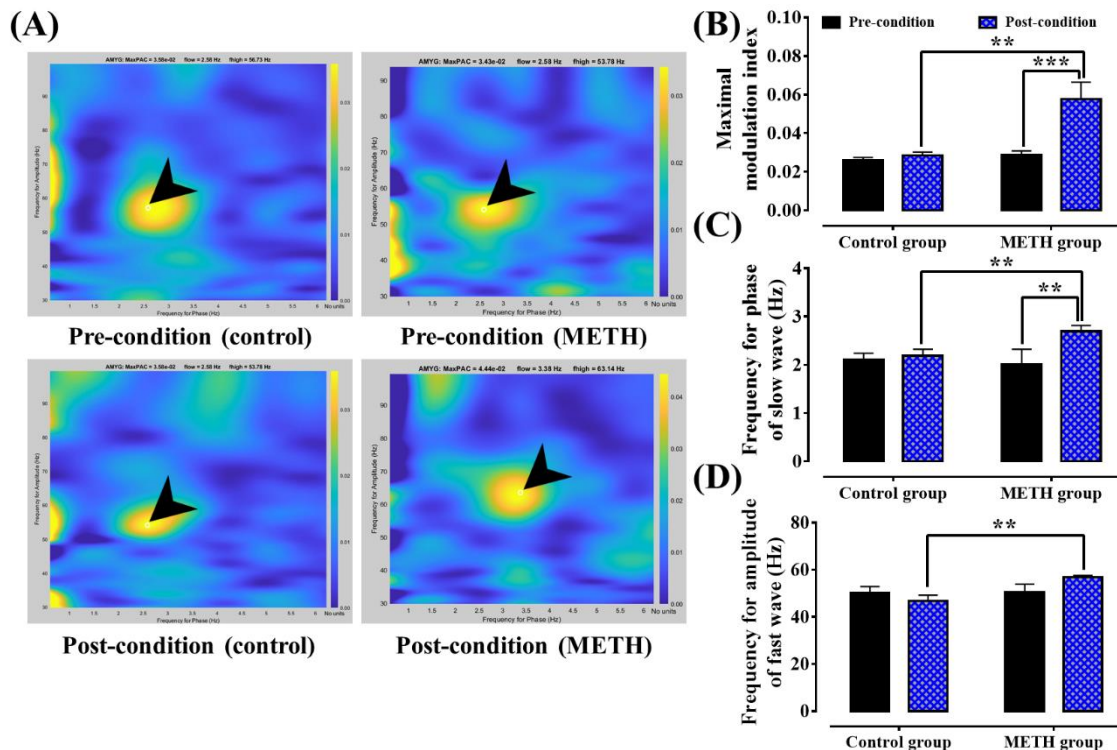


Figure 14 Phase-amplitude cross (PAC) frequency couplings of control and METH group, Comodulograms of PAC in the BLA of the representative mouse from control (left panel) and METH group (right panel) during pre-conditioning (top panel) and post-conditioning phase (bottom panel) are shown. Black arrows indicate the maximal modulation indices in each condition (A). PAC values were analyzed in terms of maximal

modulation index (B), the frequency for the phase of slow oscillation (C), and frequency for the amplitude of fast wave activity (D) extracted from comodulograms. All data were expressed as mean \pm SEM. A two-way repeated measure ANOVA was performed, ** $P < 0.01$, *** $P < 0.001$.

Therefore, broad frequency ranges for phase and amplitude were sub-divided for testing PAC induced during the post-conditioning phase. Frequency for phase was focused on theta and alpha ranges, whereas frequency for amplitude was focused on gamma I, II, and III. MI values were analyzed. The results displayed no significant difference between MI values of pre- and post-conditioning phases in the control group (**Figure 15A-I**). However, two-way repeated measure ANOVA revealed a significant influence of trial [$F(1, 15) = 10.670, P = 0.005$] but not trial \times group interaction [$F(1, 15) = 2.830, P = 0.113$] and group [$F(1, 15) = 0.259, P = 0.618$] on theta-gamma II (45-60 Hz) PAC. Moreover, a significant difference was seen in theta-gamma II [$F(1, 19) = 8.294, P = 0.010$] but not in other PAC couplings of the METH group (**Figure 16A-I**). The MI value of theta-gamma II was significantly increased during the post-conditioning phase compared to the pre-conditioning level. Altogether, these results indicated the enhanced MI of theta-gamma II PAC in the BLA of mice associated with METH CPP.

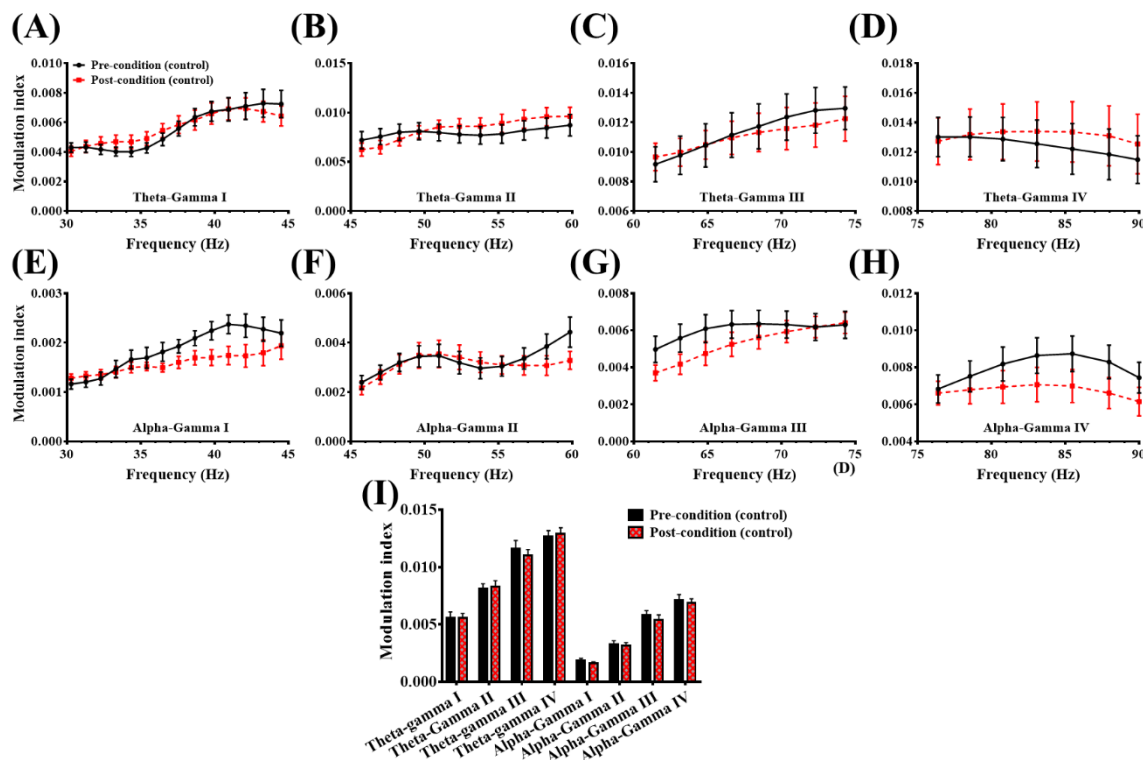


Figure 15 Modulation indices of the BLA of the control group during pre-conditioning and post-conditioning phases, Line graphs of modulation indices calculated from multiple couplings of frequency for the amplitude of the faster wave (gamma I-IV) (A-H) driven

by phase of theta wave (A-D) and alpha wave (E-H), respectively. Modulation indices of each coupling were averaged and expressed as bar graphs for statistical analysis (I). Data are shown as mean \pm SEM and analyzed by two-way repeated measure ANOVA.

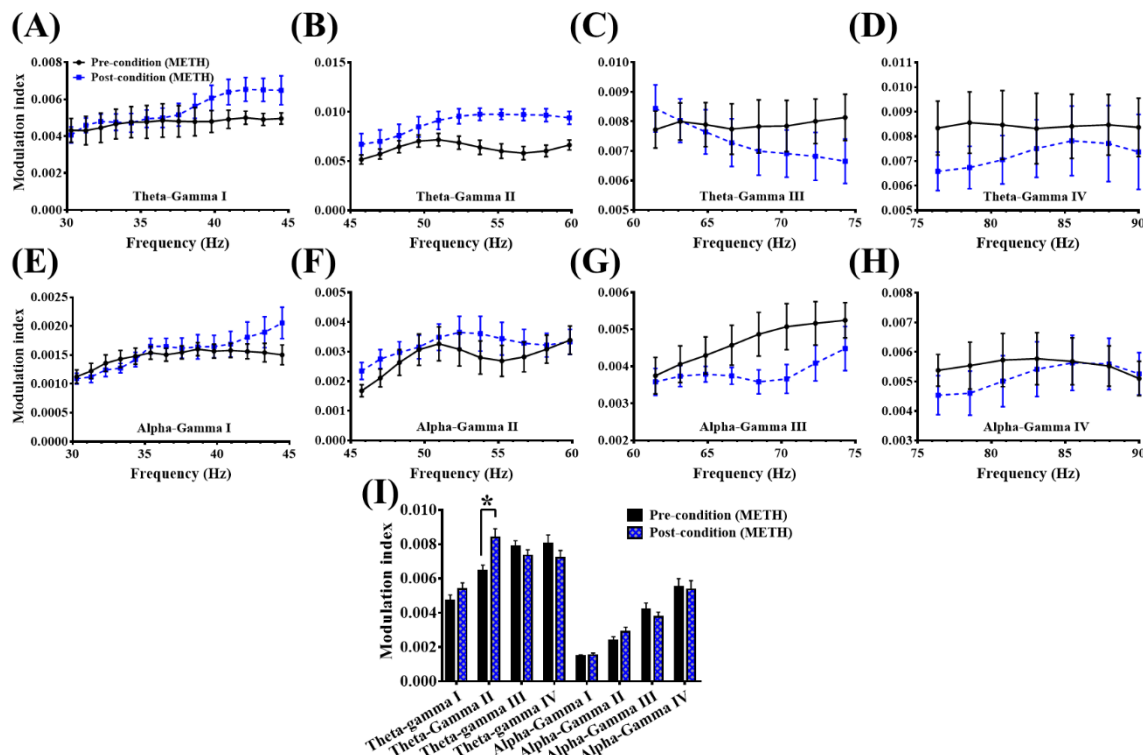


Figure 16

Modulation indices of the BLA of the METH group during pre-conditioning and post-conditioning phases, Line graphs of modulation indices calculated from multiple couplings of frequency for the amplitude of the faster wave (gamma I-IV) (A-H) driven by phase of theta wave (A-D) and alpha wave (E-H), respectively. Modulation indices of each coupling were averaged and expressed as bar graphs for statistical analysis (I). Data are shown as mean \pm SEM and analyzed by two-way repeated measure ANOVA, *P<0.05.

7. Discussion of the METH CPP experiment

The present study demonstrated METH CPP and changes in LFP activities of the BLA following repeated sessions of METH administration in the CPP paradigm. The CPP score of METH and changes in LFP oscillatory pattern in the BLA were highlighted as neural processing of METH CPP through associative learning. METH CPP scores confirmed the addictive property of the drug. The increased time spent in the METH-

paired compartment induced by METH-related cues in the CPP chamber was similar to that produced by standard drugs such as cocaine²⁷, heroin³⁸, or amphetamine²⁸.

The expression of METH CPP was believed to be induced by the memory-associated cue of METH administration. Basically, locomotor movement caused by psychostimulant drugs could interfere with CPP outcomes. Previously, the fluctuation of animals' movement was found to impact LFP signal generation and oscillation³⁹. Therefore, data recorded during a stable period of 5 to 15 min were selectively analyzed.

Apart from the direct effect of addictive drugs, some factors facilitate addiction, such as the genetic vulnerability of the users and drug-associated conditions²¹. In particular, the latter factor is decisive for the reward learning process of addictive drugs. Previously, the BLA was engaged with the reconsolidation of drug-associated memories⁴⁰. It was involved in cocaine-related memory reconsolidation⁴¹. Moreover, the relationship between BLA action and drug-seeking behaviors induced by drug-related cues has been evidenced⁴². Using the CPP paradigm, the contextual cues of the drug (e.g., drug paraphernalia) were demonstrated to elicit craving⁴³. This could explain why METH-associated cues increased CPP scores during the post-conditioning phase.

The BLA closely connects with the mesolimbic DA system for neural processing in response to reward-related stimuli. Previously, a disruption of the brain reward circuitry was found to result in mood disorders⁶. Several experiments have been conducted to demonstrate the critical role of the BLA in addiction. Altogether, alleviation of drug-seeking behaviors was correlated with the BLA activity suppression¹⁰⁻¹². The present data highlighted the decreased theta and alpha spectral powers and the increased MI of theta-gamma II cross-frequency coupling in the BLA. These LFP oscillatory patterns would likely predict drug craving and seeking.

Previously, theta desynchronization in the BLA was believed to relate to fear learning impairment via serotonin (5-HT) clearance^{44,45}. Escalation of craving and freezing behaviors evaluated by CPP and contextual fear conditioning paradigm was found to accompany the enhancement of stress hormones release (e.g., adrenocorticotrophic hormone, corticosterone (COR))^{46,47}. This may imply that a lower level of 5-HT seems to promote the expression of rewarding behaviors by inducing COR release because plasma 5-HT also declines during the abstinent period of alcohol dependence⁴⁸. In contrast, citalopram, a 5-HT reuptake inhibitor, was found to alleviate cue-induced drug craving and correlate with the availability of DA receptors⁴⁹. Altogether, it could be suggested that reduced BLA theta power may partially result from a decreased level of 5-HT, which is the physiological changes contributed to facilitating craving in the CPP paradigm.

Alpha power was decreased during the post-conditioning phase. The controlling of DA neurons projecting from the VTA to the BLA has been proposed to mediate

pleasure feeling⁵⁰. Activating the subset of GABAergic interneurons in the VTA could promote the disinhibition of DA neurons⁵¹, which can be induced by reward-predictive cues⁵². This, in turn, may facilitate hyperpolarized DA neurons and DA release in the nerve terminal (e.g., BLA, NAc, mPFC). Previously, the attenuation of alpha synchronization in the frontal cortex was postulated to associate with DA release^{53,54}. Moreover, it was found that amygdala connectivity was found to interact with many sub-regions in the frontal cortex during cocaine cues reactivity⁵⁵. Wholly, it could be indicated that dopamine fluctuation in the BLA would be a direct effect of BLA alpha power modulation.

The PAC, one of the most studied types of cross-frequency coupling, was analyzed following METH repeated exposures in the CPP paradigm. An increase in theta-gamma sub-band II (45-60 Hz) was observed. Theta-gamma PAC is a critical maker of neural processing that supports learning and memory in animals⁵⁶ and humans⁵⁷ and appears to be associated with memory formation and synaptic plasticity⁵⁸. So far, the critical role of theta-gamma coupling in the brain reward circuits implicated with drug dependence has not been well described. Previously, a significantly remarkable elevation in theta-gamma coupling (6–8 Hz with 50-55 Hz) was seen in the mPFC following cocaine treatment²⁰. In addition, cross-frequency coupling appeared to mediate network-level dynamical computations during the performance of T-maze task⁵⁹. Collectively, the mPFC and BLA couplings may be considered functional interactions that motivate drug-seeking behaviors. The gamma range coupled with the theta mentioned above was below 60 Hz. On the other hand, theta-high gamma (60-100 Hz) coupling was also involved in other motivated behaviors such as food seeking induced by chocolate cues after repeated chocolate sessions¹⁹. These data may suggest the underlying brain mechanisms in different degrees of motivation for food- or drug-induced seeking behaviors. In terms of mechanism, stress condition provoked by fear learning⁴⁷ was reported to escalate the BLA theta-gamma PAC⁶⁰. DA release resulted from VTA GABAergic neurons modulation induced by the prediction of positive reinforcement⁵² and stress condition⁶¹ may increase this kind of PAC in the BLA and NAcc, a brain located in the mesolimbic DA system³⁹. In addition, the BLA reactivity was proposed as the overlap mechanism underlying the conditions that responded to drug withdrawal and conditioned stressors exposures⁶². Altogether, the present PAC results might suggest possible changes in the brain circuits of memory and cognitive functions induced by METH dependence. Moreover, these findings may provide new information on LFP rhythmic oscillations in the BLA as evidence-based mechanisms consistent with METH-induced neural plasticity, neuronal transmission, and the transduction of intracellular pathways during METH dependence^{63–65}.

8. Conclusion of the METH CPP experiment

In summary, this study demonstrated the LFP spectral powers and PAC in the BLA during the post-conditioning phase of METH CPP (**Figure 17**). These findings were found in parallel with the induced METH CPP that could reflect the METH craving and seeking behavior of mice in the CPP paradigm. These electrical brain signals in the BLA are believed to support the process of learning association between METH effects and the assigned environment paired with METH administration. These BLA LFP oscillations might represent brain mechanisms that underlie drug craving and seeking behavior which is crucial for finding and assigning novel drugs for dependence therapy.

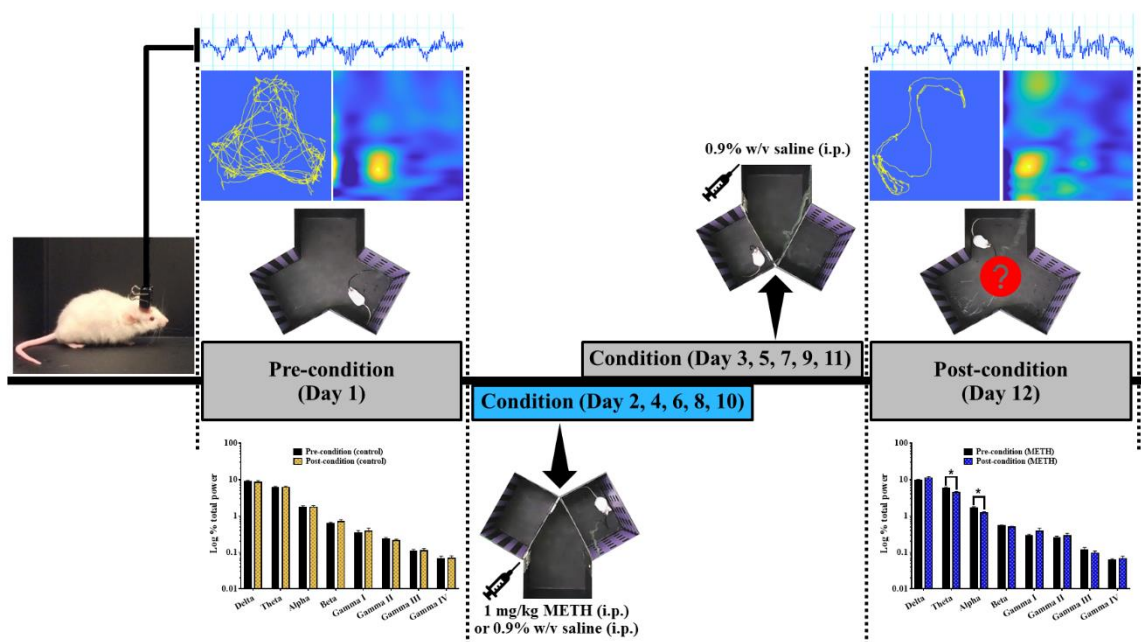


Figure 17 An overview of the key findings of the BLA LFP oscillations following METH CPP induction

The analysis of LFP signals in the BLA may be a more understandable mechanism for rewarding behaviors induced by METH CPP, as provided in the abovementioned discussions. It found that the capability to facilitate METH CPP may be partially involved in the inability to control stress response, lowering 5-HT levels, and DA over-release. Interestingly, kratom leaves extract could deal with these problems.

9. Kratom extract as a candidate drug for treatment METH CPP craving

Mitragyna speciosa (Korth.) Haval., commonly known as Kratom (KT), is a medicinal plant of the family Rubiaceae and abundantly found in Malaysia and Thailand⁶⁶. It has been widely used in folk medicines to cure many illnesses for several decades⁶⁷. KT leaves contain varieties of indole alkaloids that have been isolated and chemically identified such as mitragynine (MT), a major alkaloid, or 7-hydroxymitragynine (7-HMT), a minor constituent. These molecules exert their functions partially via opioid receptor activation in both peripheral and central organs^{68,69}. Traditionally, KT leaves consumption produces remedies for the mitigation of chronic musculoskeletal pain and fatigue, attenuation of an inflammatory response, and reduction of diarrhea and mood swings^{70,71}. Recently, MT was found to reduce neuropathic pain in rats via α -adrenoceptor mechanism⁷².

Moreover, during the past decades, KT extract possesses its efficacy in various aspects both centrally and peripherally to attenuate withdrawal symptoms in many abused drugs as described in the following details.

9.1 KT extract and stress response

Excessive levels of COR can be detectable in depressed rats⁷³. The forced swimming test (FST) and tail suspension test (TST) are the paradigms widely used to assess the antidepressant effect of novel substances. However, any drug that exhibits hyperkinesia typically fails to have positive results in FST and TST⁷⁴ due to the reduced period that both tests are immobile⁷⁵. In terms of therapeutic aspect, major alkaloid MT accumulated in the KT leaves effectively attenuates COR-induced depression⁷³. In addition, leave extract of KT also had no effects on locomotor activity^{33,76}. These may imply that KT leave extract could suppress COR-induced depressive symptoms.

9.2 KT extract and 5-HT levels

Biosynthesis of 5-HT originated from the dorsal raphe nuclei (DRn), the main site activated by KT extract⁷⁷. These effects may contribute to enhancing 5-HT in the nerve terminals. Furthermore, fluoxetine (FLU) is a selective serotonin reuptake inhibitor (SSRI) which leads to escalated extracellular 5-HT for an extended time in the synaptic clefts⁷⁸. Previously, FLU and KT extract demonstrated positive results in ethanol withdrawal symptoms^{79,80}. Altogether, these may indicate that KT extract may alter the 5-HT on both activating 5-HT synthesis and mimicking SSRI properties.

9.3 KT extract and anti-DA activity

The anti-DA activity of KT extract and its chemical constituents are apparently seen in various organs. Although, the people with long-term KT consumption produce darkening skin even if they remain indoors⁸¹. A classical investigation exposed that the attenuation of α -melanocyte stimulating-like peptides release was accompanied by the activation of dopamine type 2 (DA2) receptors on the pituitary gland⁸². From this result, it is possible that KT extract could block DA2 receptors to show hyperpigmentation in KT users. To support this effect, the MT also possesses its action via DA2 receptors inhibition (54.22%) assessed by radioligand binding assay⁸³. The stimulation of the DA2 receptor predominantly seen in the vas deference increases this organ contraction. However, the incubation of KT extract with the vas deference shows a reversed outcome⁸⁴.

Altogether, all these data may be sufficient to support the hypothesis that KT extract may be capable of attenuating METH craving induced by CPP.

10. Objective of the METH CPP experiment treated with KT leaves extract

This study was designed to examine and characterize the effects of KT leave extract on rewarding behavior and electrical brain wave induced by METH CPP.

11. Materials and methods of METH CPP experiment treated with KT leaves extract

11.1 Plant materials

Mature leaves of KT were collected from natural sources in Songkhla and Satun provinces, Thailand. Plant materials were then identified by Assist. Prof. Dr. Niwat Kaewpradub and stored at the herbarium in the Department of Pharmacognosy and Pharmaceutical Botany, Faculty of Pharmaceutical Sciences, Prince of Songkla University, Thailand, where a voucher specimen (no. PCOG/MS001-002) has been deposited.

11.2 Preparation of crude alkaloid extract and phytochemical characterization

The extraction and isolation of KT alkaloid extract were performed as described in previous study⁸⁵ with the following modifications. In brief, KT leaves were cleaned, dried at 45–50 °C, powdered, and macerated with methanol. The filtrate was evaporated in vacuo. The residue was dissolved in 10% (v/v) acetic acid solution, filtrated, and washed with petroleum ether, then made into alkaline (pH 9) with 25% (v/v) ammonia solution and extracted with chloroform. The combined chloroform fractions were washed

with brine solution and dried over anhydrous sodium sulfate. After evaporated to dryness, the KT alkaloid extract was obtained with a yield of 0.25% (w/w) based on dried weight. The authentic MT was isolated. The crude alkaloid extract was loaded on the top of the silica-gel column eluting with CHCl₃: MeOH (95:5). The structure of MT was identified using spectroscopic methods (MS, IR, ¹H NMR, and ¹³C NMR). The results were in agreement with the data from previous investigations^{85,86}. The MT purity was estimated at approx. 98% pure.

The characteristic of the KT alkaloid extract was determined using the validated HPLC method as described⁸⁷. The HPLC Shimadzu Prominence i 2030C (Kyoto, Japan) connected with VertiSep™ USP C18 HPLC column (4.6×250 mm, 5 μm; Vertical, Bangkok, Thailand) was used. The column was eluted isocratically with 20 mM ammonium acetate (pH 6): acetonitrile; 35:65 (% v/v). The flow rate was 1 mL/min. The injection volume was 20 μL. The photodiode array detector-UV was set at 225 nm.

11.3 Animals

This investigation was carried out under the guidelines of the European Science Foundation (Use of Animals in Research, 2001) and the ARRIVE (Animal Research: Reporting of In Vivo Experiments) for protecting animals used in scientific research. The experimental procedures and protocols were approved by the Institute Animal Care and Use Committee, Prince of Songkla University [project license number: MHESI 6800.11/845 and reference number: 57/2019]. Male Swiss albino ICR mice (7–8 weeks old) were obtained from the Nomura Siam International Company, Bangkok, Thailand. To minimize the stress in animals, all animals were handled for one week before the beginning of the experiment at the Southern Laboratory Animal Facility, Prince of Songkla University. The animals were individually housed in single stainless-steel cages (17 x 28.5 x 17 cm) with the standard environmental condition (12/12 h light/dark cycle, 22 ± 3 °C, and 55 ± 10% relative humidity). Commercial food pellets and water were available ad libitum. All experiments were conducted between 8 a.m. and 4 p.m.

11.4 Drugs and chemicals

METH hydrochloride with a standard purity (95.8%) for research purposes was provided by the Food and Drug Administration, Thailand. Moreover, 1 mg/kg METH dissolved in 0.9% w/v NaCl was used for intraperitoneal (i.p.) injection. METH concentration was selected according to the dose that definitely produced addictive behavior in the same strain of mice^{22,25}. The 40 (KT40) and 80 (KT80) mg/kg KT alkaloid extracts and standard drug bupropion (BP) at 20 mg/kg (Sigma-Aldrich, St.Louis, MO, USA) were diluted in 1%w/v of sodium carboxymethyl cellulose (CMC) solution and administered orally (p.o). Intragastric administration was accomplished using a smooth ball-tipped stainless steel gavage needle with a fixed volume per body weight of mice at 10 ml/kg.

11.5 Animal surgery for implanting the LFP electrodes

The process of intracranial electrode implantation was modified from the previous study^{22,33}. At approximately four months after birth, mice with an initial body weight of 45.0 – 52.0 g were deeply anesthetized with intramuscular injection of a mixed solution of 16 mg/kg xylazine hydrochloride (Xylavet, Sigma-Aldrich International GmbH, Switzerland) and 50 mg/kg zoletil (Tiletamine – zolazepam, Vibac Ah, Inc., USA). Animals' heads were then held with stereotaxic apparatus. Lignocaine (20 mg/ml) (Lidocaine, M & H manufacturing Co., Ltd., Thailand), a local analgesic drug, was applied subcutaneously before making the incision to the midline of the scalp on the dorsal head. The skull was drilled for the electrodes to be stereotaxically positioned on the left hemisphere of the brain, defined from bregma to the VTA (AP; -3 mm, ML; 0.5 mm; DV; 4.2 mm), HP (AP; -2.5 mm, ML; 2 mm; DV; 1.5 mm), and the NAc (AP; +1.3 mm, ML; 1.0 mm; DV; 4.2 mm) according to the mouse brain atlas³⁴. The reference and ground electrodes were implanted at the midline skull over the cerebellum (AP; -6.0 mm, ML; 0.0 mm; DV; 1.5 mm). After that, holes were drilled for stainless steel screws as anchors. All electrodes (0.381 mm diameter, coated) were secured in place for permanent with dental acrylic (Unifast Trad, GC Dental Industrial Corp., Tokyo, Japan). The antibiotic ampicillin (100 mg/kg) (General Drug House Co., Ltd., Bangkok, Thailand) and carprofen (10 mg/kg) (Best Equipment Center Co., Ltd., Thailand) were administered subcutaneously once a day for three days to prevent infection and alleviate pain, respectively. The animals were allowed at least two weeks to recover from the surgery in their separated cages fully.

11.6 CPP apparatus and paradigm

The equipment has been employed to evaluate condition-induced drug craving behaviors in the CPP paradigm known as the CPP apparatus. The CPP apparatus in this experiment was modified from the previous investigations^{22,35}. In brief, it was made from plexiglass to have three rectangular compartments (25 cm x 18 cm x 25 cm) (compartments A, B, and C) arranged radially at 120° to each other. Each rectangular compartment was accessible from a triangular zone located centrally. The compartments had identical shapes and sizes but different floor textures and wall shading. The ornamentation for floor texture and wall shading were designed in the following details, respectively: A) medium rough, vertical strips; B) rough, grid strips; and C) smooth, black color (**Figure 18**). Compartment C was a starting or neutral zone where individual animals were placed and allowed to explore the CPP apparatus freely. The overall schedule of drug administration was modified from the previous experiment^{22,25}, as depicted in figure 18. Briefly, after habituation, the CPP paradigm mainly consisted of three consecutive periods initiating from pre-conditioning to conditioning and post-conditioning phases in sequence.

11.6.1 Habituation and pre-conditioning phase

Mice were brought to a recording room for at least half an hour before the initiation of the experiments. During the habituation (day 1 and 2) period, animals were intraperitoneally injected with normal saline solution to attenuate the stress from the pain of drug injection and then immediately placed in the starting zone. Next, they were allowed to freely explore all CPP apparatus compartments for 15 min. During the pre-conditioning phase (day 3), the animals were subjected to the same protocol of the habituation period. The time animals spent in each compartment was recorded and expressed as a CPP score. CPP score was calculated from the difference in time that each animal spent in METH-paired and normal saline-paired compartment. Tossing a coin was a method to randomly divide all mice into five groups defined as control, METH+CMC, METH+KT40, METH+KT80, and METH+BP groups. Each group contained ten mice. However, three n numbers of the METH+CMC and METH+KT40 group and two n numbers of METH+KT80 and METH+BP groups showed an initial bias of side preference. They spent more than 80% of the time in one compartment. Altogether, ten mice were rejected from the CPP procedure after the pre-conditioning phase.

11.6.2 Conditioning phase

Animals were subjected to training sessions that took ten consecutive days (from day 4 - 13) that began the day after the pre-conditioning phase. To trigger the addictive behavior, mice were given intraperitoneal (i.p.) injection of 1 mg/kg METH and normal saline solution on alternative days (odd and even days for METH and saline, respectively). Animals were immediately confined to the assigned compartment for 30 min to learn to associate the context of the unique condition of each compartment and the specific effect of METH or saline injection. Animals in the control group were administered with normal saline (both odd and even days) for pairing with all compartments. After the animals completed the session each day, they were returned to their home cage.

11.6.3 Post-conditioning phase

The post-conditioning phase was taken on day 14 to evaluate the efficacy of KT alkaloid extract and BP on the expression of METH CPP. 40 mg/kg KT (n = 7), 80 mg/kg KT (n = 8), 20 mg/kg BP (n = 8) and 10 ml/kg 1%w/v CMC (n = 7) were administered orally to the assigned groups of mice 60 min before CPP testing. After that, time spent in each compartment was analyzed for CPP score.

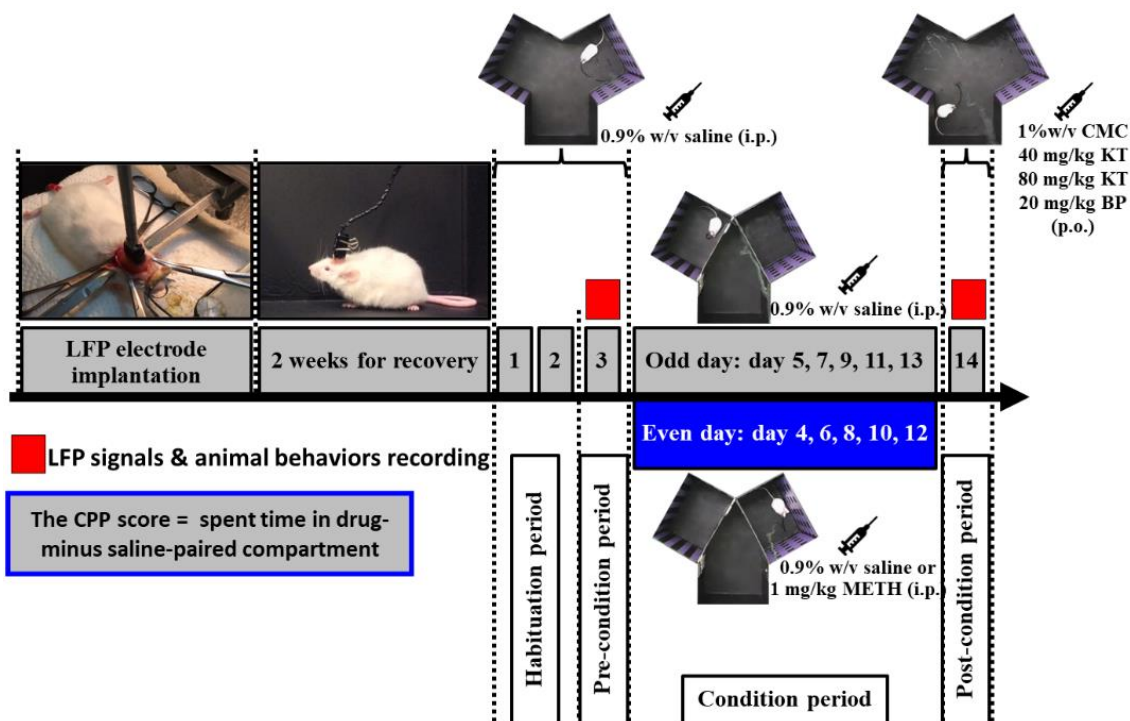


Figure 18 Experimental protocol for the investigation of KT alkaloid extract effects on METH CPP. Animals were handled through the processes of surgery for LFP electrode implantation into the brain and a recovery period of at least two weeks. Following the habituation, the CPP paradigm consisted of three phases: habituation and pre-conditioning, conditioning, and post-conditioning period scheduled on days 1-3, 4-13, and 14, respectively. In the post-conditioning phase, animals were administered orally with either two concentrations of KT alkaloid extract or standard drug bupropion (BP) 60 min before testing METH CPP and LFP patterns.

11.7 The processing of locomotor activity and LFP signals

During the pre-conditioning and post-conditioning phases, LFP signals and locomotor activities of individual mice in the CPP apparatus were recorded simultaneously for 15 min. For LFP signal processing, raw LFP signals were amplified and converted from analog to digital data by Dual Bio Amp (AD Instruments, Castle Hill, NSW, Australia) and a PowerLab 16/35 system (AD Instruments, Castle Hill, NSW, Australia) with 16-bit A/D, respectively. Additionally, signals were harvested with 1.024 s duration in sweeps, and the sampling frequency was 2 kHz. LFP signal analysis was processed through 1–100 Hz band-pass digital filtering. Notch filtering at 50 Hz was deployed to reject the noise from power line artifacts. For locomotor activity, a webcam mounted vertically on the top of the CPP apparatus was used to capture and monitor the spontaneous movement of animals. All data were stored on a PC through LabChart 7.3.7 Pro software for offline analysis.

11.7.1 Locomotor activity analysis

Each video record of locomotor activities from an individual mouse deposited in a PC was analyzed to evaluate the animal movement. The method was validated using the open source toolbox OptiMouse³⁶ to detect the translocation of the center position of the animal body. The basic principle of animal detection was designed based on the contrast between the black color of the background (floor & wall of the CPP apparatus) and the white color of animals' bodies. The alternations of locomotor activity, tracking of animal exploration, and time spent in each compartment of the apparatus during the assigned period were the parameters to be specifically focused on.

11.7.2 LFP signal analysis

PSD values were computed from LFP raw data stored in the LabChart software using the Hanning window cosine transform function with 50% window overlap and 0.976 Hz of power spectra resolution. The analysis of frequency power was processed by using the FFT algorithm and expressed in powers of the frequency domain in 6 discrete frequency bands, which included delta (1.0-3.9 Hz), theta (4.7-8.7 Hz), alpha (9.8–12.7 Hz), beta (13.6-29.3 Hz), low gamma or gamma I (30.0-44.9 Hz), and high gamma or gamma II (60.5-95.7 Hz). Data were normalized as percent relative powers of a particular frequency range ($P_{(f)}$) by the following equation;

$$\% \text{ Relative power} = \frac{P_{(f)} \text{ at Post-condition} - P_{(f)} \text{ at Pre-condition}}{P_{(f)} \text{ at Post-condition} + P_{(f)} \text{ at Pre-condition}} \times 100$$

For coherence analysis, the values were obtained by running raw data via toolbox Brainstorm3³⁷. Then, data were normalized as percent relative coherence to quantify the strength of signal communication between 2 separate brain regions in particular frequency ($C_{(f)}$) according to the provided equation;

$$\% \text{ Relative coherence} = \frac{C_{(f)} \text{ at Post-condition} - C_{(f)} \text{ at Pre-condition}}{C_{(f)} \text{ at Post-condition} + C_{(f)} \text{ at Pre-condition}} \times 100$$

11.8 Statistical analyses

All parameters were analyzed and illustrated as mean \pm Standard Error Mean (SEM). For locomotor activities and CPP scores, a two-way repeated analysis of variance (ANOVA) was used to determine the influence of an interaction between two factors (Treatment x Condition), followed by a post hoc Bonferroni test for multiple comparisons. Conditioning states were used as within-subject factors, and with or without METH treatment were considered as inter-subject factors were defined as treatment. The rest of the parameters from considered brain regions induced by drug treatment with statistically significant output were specified using one-way ANOVA in comparison to data of the

control condition. Different symbols were used to indicate significant differences at $p < 0.05$ according to Tukey's post hoc. Multiple comparisons were performed for data expressed in %relative power and %relative coherence. All data were analyzed using the temporarily available software GraphPad 7.0 (Graphpad Software, Inc., USA).

12. Results of the METH CPP experiment treated with KT leaves extract

12.1 Animal movement and Locomotor activity

The spontaneous movement of each animal was recorded for 15 min for both the pre-conditioning and post-conditioning phases. Videos that captured mice exploration in the CPP apparatus were next analyzed and displayed for locomotor tracking patterns, velocity parameters, and time spent in each compartment. Locomotor speeds of each group were averaged with one min-bin and illustrated (**Figure 19A**). The results revealed relatively higher speed during the first 5 min and slowed down movement after that. To avoid movement-related effects on LFP signal generation, the analysis of averaged speed during 15 min of data recording was next performed. The results found no alternation of speed in pre-conditioning and post-conditioning phases in all treatments. Two-way repeated measures ANOVA also confirmed a non-significant difference of locomotor speed among groups [$F(4, 35) = 0.152, P = 0.961$] and between pre-conditioning and post-conditioning phases [$F(4, 35) = 0.475, P = 0.754$] (**Figure 19B**).

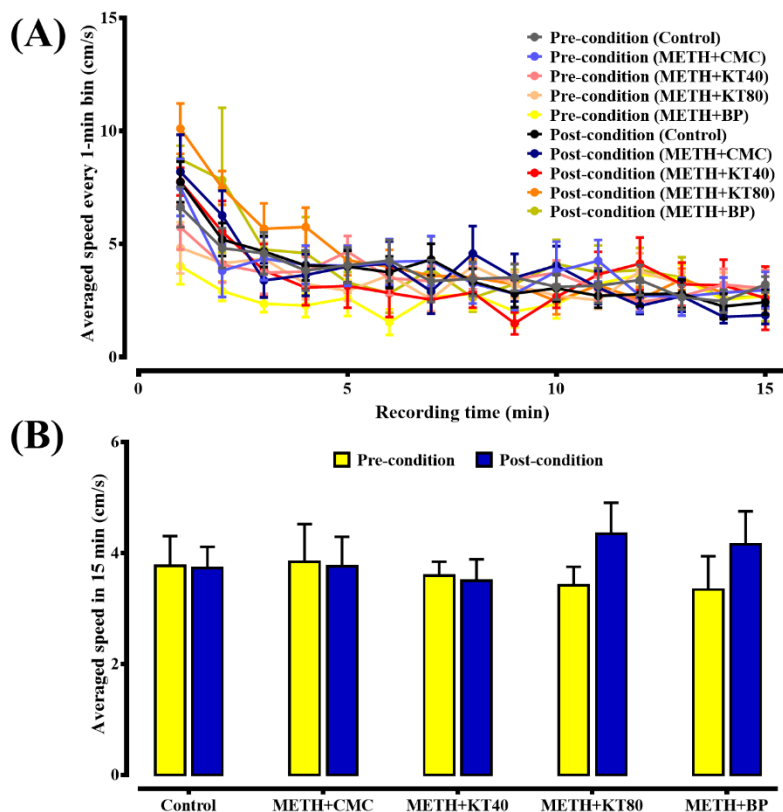


Figure 19 Locomotor activity of mice during pre-conditioning and post-conditioning phases of the control group (n=10) and METH groups treated with solvent (METH+CMC) (n=7), 40 mg/kg KT alkaloid (METH+KT40) (n=7), 80 mg/kg KT alkaloid (METH+KT80) (n=8), and a standard drug bupropion (BP) (METH+BP) (n=8), Mean values of locomotor speed in each group were calculated every 1-min bin (A). Averaged speed during a 15-min of exploration in the CPP apparatus was analyzed (B).

12.2 CPP Score

The effects of KT alkaloid extract and BP were measured during the expression of METH CPP. Data were analyzed as locomotor tracking patterns and CPP scores. Representative locomotor tracking of 5 groups was shown in comparisons between different treatments and between pre-conditioning and post-conditioning phases (**Figure 20A**). During the pre-conditioning phases, all five groups explored and visited all three compartments relatively equally. During the post-conditioning period, control animals maintained the same pattern exploring all three compartments equally, whereas the METH+CMC group clearly preferred to visit neutral and METH-paired compartments more than the saline-paired compartment. METH+KT40 group also visited the saline-paired compartment less than the control group but more than the METH+CMC group. However, normal patterns were found in the METH+KT80 group which animals visited

all three compartments equally. Unexpectedly, the METH+BP group clearly preferred the METH-paired compartment more than the other two compartments.

Therefore, CPP scores were statistically analyzed (**Figure 20B**). Two-way repeated measures ANOVA revealed significant effects of condition [$F(4, 35) = 34.576$, $P < 0.001$], treatment [$F(4, 35) = 4.545$, $P = 0.005$] and treatment x condition interaction [$F(4, 35) = 6.486$, $P < 0.001$]. Multiple comparisons using a post hoc Bonferroni test indicated significant in CPP scores during post-conditioning phase in METH+CMC ($P = 0.002$), METH+KT40 ($P = 0.001$) and METH+BP ($P < 0.001$) but not METH+KT80 group compared with pre-conditioning score of each group. In comparisons among groups during post-conditioning phase, significant increases in CPP score were seen in METH+CMC ($P = 0.001$), METH+KT40 ($P < 0.001$) and METH+BP ($P < 0.001$) but not METH+KT80 group compared to control level. Interestingly, addiction-related mice treated with KT80 (METH+KT80) significantly attenuated the CPP score as compared to the post-conditioning phase of the METH+CMC group ($P < 0.001$). These data confirmed that METH at 1 mg/kg significantly produced addictive behaviors. However, 80 mg/kg KT significantly ameliorated METH CPP in mice, whereas a standard drug BP at 20 mg/kg failed to suppress the CPP score.

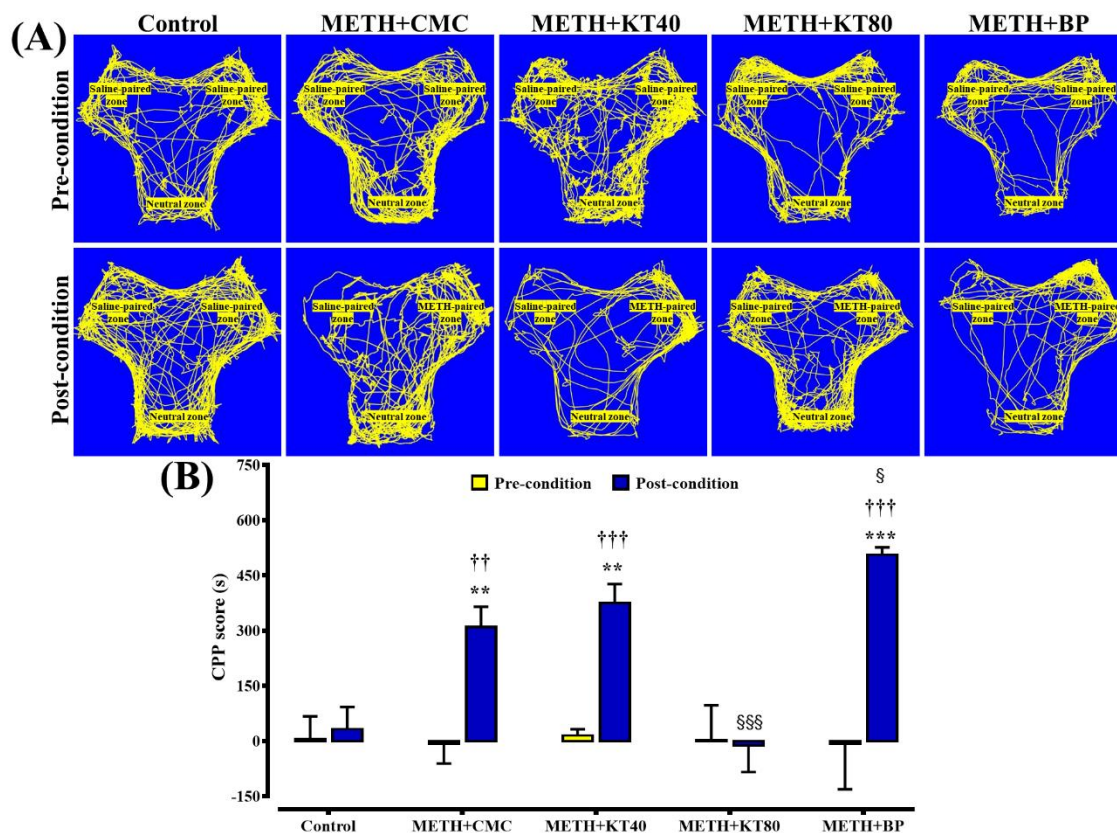


Figure 20 Locomotor tracking of animal exploration in CPP apparatus during pre-conditioning and post-conditioning phases. Each group's locomotor tracking of representative animals was shown for comparison (A). Data of time spent in a specific compartment were calculated and expressed as CPP scores for statistical analysis for the effects of 40 mg/kg KT alkaloid (METH+KT40) (n=7), 80 mg/kg KT alkaloid (METH+KT80) (n=8), and a reference drug BP at 20 mg/kg (METH+BP) (n=8), compared to that treated with vehicle (METH+CMC) (n=7) (B). CPP scores were calculated by subtracting the time that mice spent in the METH-paired zone from the time spent in the saline-paired zone. Data were expressed as mean \pm SEM. **, *** P<0.01, 0.001 for significant analyses using two-way repeated ANOVA followed by post hoc Bonferroni test for multiple comparisons between pre-conditioning and post-conditioning phases. ††P<0.01, †††P<0.001 compared with the post-conditioning phase of the control group. §P<0.05, §§§P<0.001 compared with the post-conditioning phase of the METH+CMC group.

12.3 LFP oscillation in the VTA, HP, and the NAc

Visual inspection was performed to overview the oscillations of raw LFP signals (Figure 21). The effects of KT alkaloid extract and BP on LFP patterns in the VTA, HP, and the NAc during METH CPP were illustrated. In the HP and the VTA, relatively similar patterns of LFP oscillation were seen among groups during the pre-conditioning and post-conditioning phases. General patterns in the NAc were identical among groups during the pre-conditioning phase. Therefore, the patterns appeared to be different during the post-conditioning phase, in which additional fast wave activity was superimposed in METH+CMC and METH+BP groups.

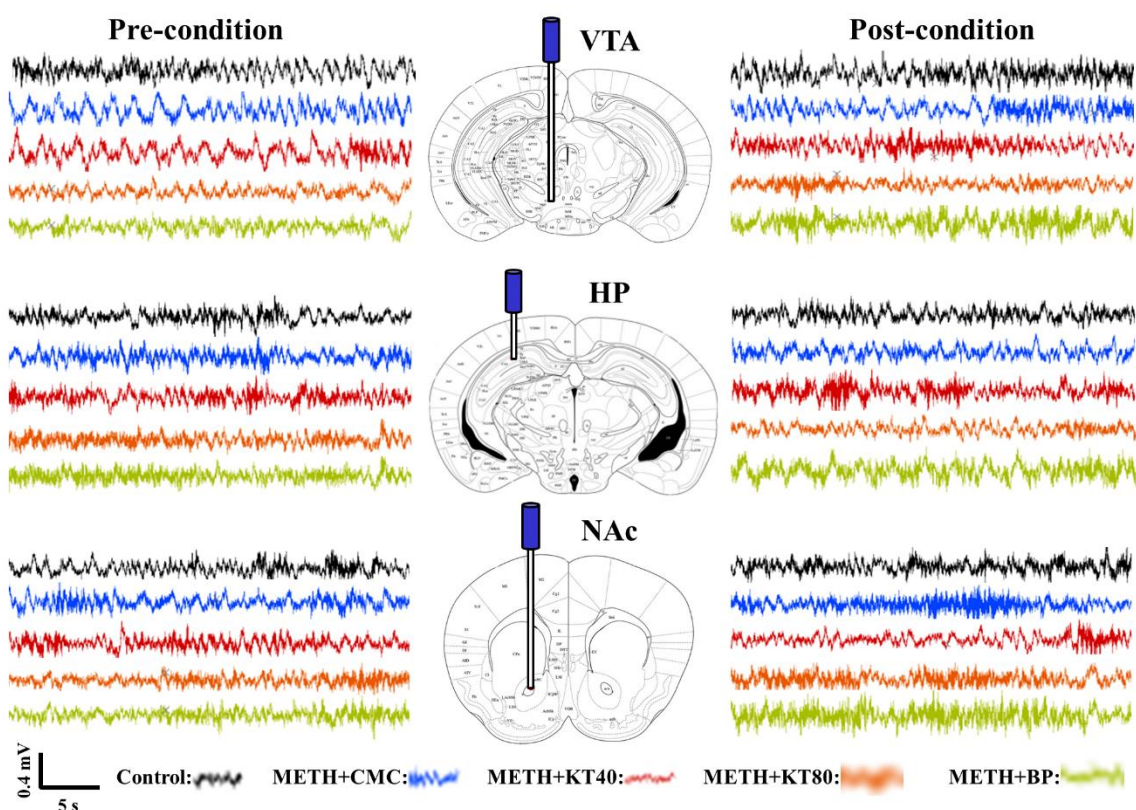


Figure 21 Raw LFP signals of representative mice from each group during pre-conditioning (left panel) and post-conditioning (right panel) phases of control and METH groups treated with vehicle (CMC), 40 mg/kg KT alkaloid, 80 mg/kg KT alkaloid, and 20 mg/kg BP. Raw signals were recorded from the ventral tegmental area (VTA), the hippocampus (HP), and the nucleus accumbens (NAc).

12.3.1 VTA powers

Therefore, raw LFP signals in the VTA during post-condition in the time domain were computed and transformed into LFP power spectra (%Relative power) in the frequency domain. A high fluctuation can be detected at a frequency lower than 20 Hz (**Figure 22A**). When the statistical analyses were performed. It was exposed that significant alteration apparently seen in the delta [$F(4, 35) = 7.098, P < 0.001$] and gamma I [$F(4, 35) = 6.088, P = 0.001$]. Under the delta power values, post hoc comparison showed the well increases in METH+CMC ($P = 0.003$) and METH+BP ($P = 0.043$) but this effect was neutralized by KT80 treatment ($P = 0.001$). A significant change in gamma I was observed only in the METH+BP group ($P < 0.001$) (**Figure 22B**).

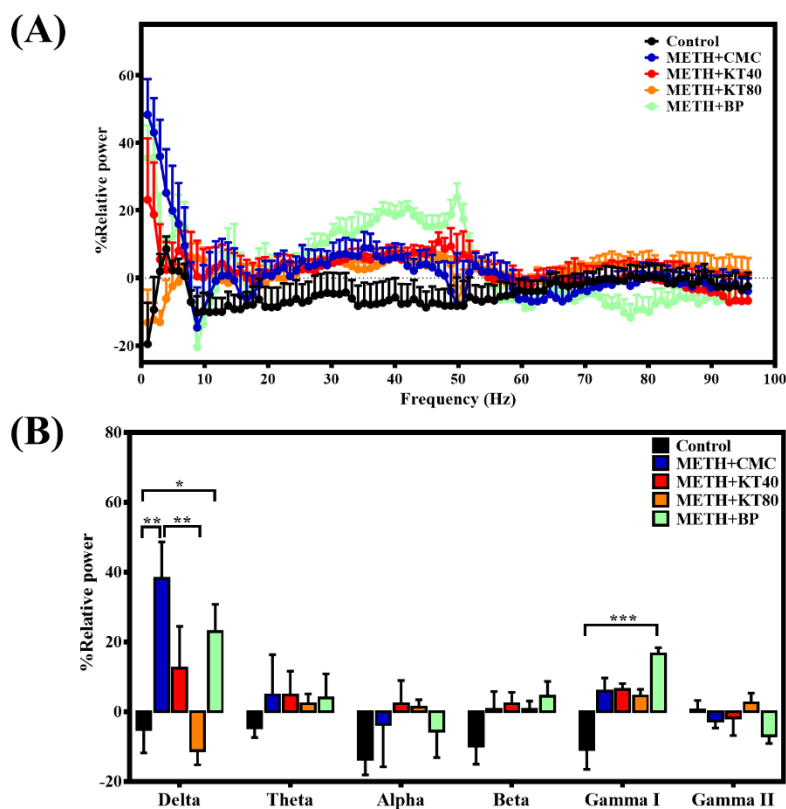


Figure 22 Effects of the treatments with KT alkaloid extract on LFP spectral powers in the VTA. Animals were treated with KT alkaloid extract (40 and 80 mg/kg) and BP (20 mg/kg). Data were normalized as percent relative power (A). LFP spectral powers were divided into powers of 6 discrete frequency bands (B). All data were expressed as mean \pm SEM and statistically analyzed using one-way ANOVA followed by Tukey's post hoc test. * $P < 0.05$, ** $P < 0.01$, *** $P < 0.001$.

12.3.2 HP powers

In the HP, the LFP power spectra of these five groups were shown for comparison. Dramatical differences among groups appeared in slow frequency activities below 20 Hz (**Figure 23A**). Relatively equal powers were seen for higher frequency waves. One-way ANOVA revealed significant differences only in delta wave [$F(4, 35) = 10.660$, $P < 0.001$]. Multiple comparisons confirmed significant increases in delta power seen in METH+CMC ($P = 0.001$) and METH+BP ($P = 0.003$) groups compared to that of control group (**Figure 23B**). Interestingly, this elevated delta power seen METH+CMC group was significantly suppressed by the treatment with both 40 mg/kg ($P = 0.001$) and 80 mg/kg ($P < 0.001$) KT alkaloid extract. Altogether, KT extract prevented the increase in delta power induced by METH-conditioning. This LFP pattern in the HP was positively correlated with the data of CPP scores that might reflect the attenuation effect of the extract on the intensity of METH CPP.

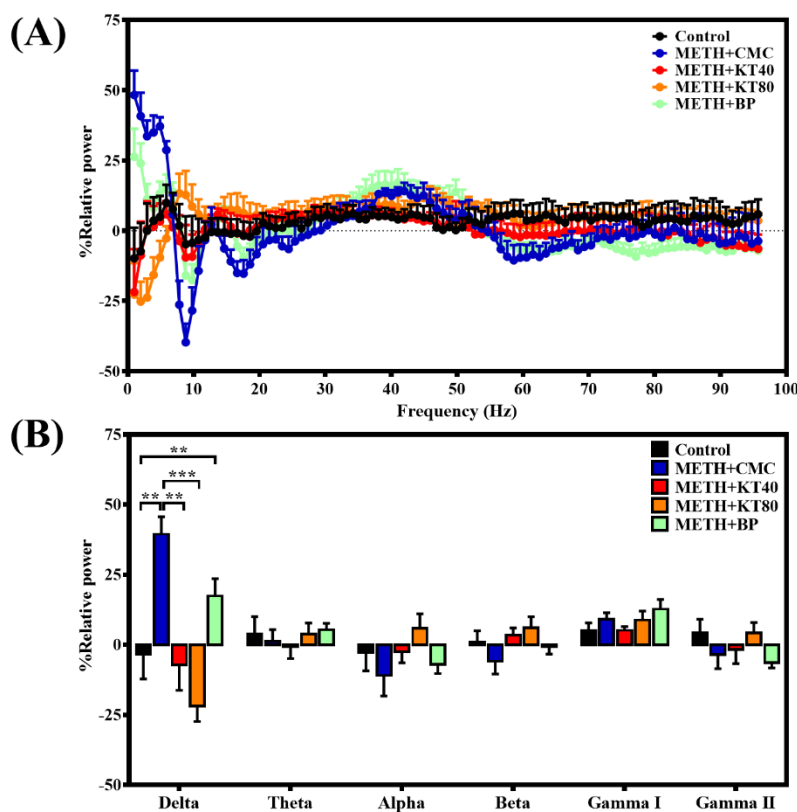


Figure 23 Effects of the treatments with KT alkaloid extract on LFP spectral powers in the HP. Animals were treated with KT alkaloid extract (40 and 80 mg/kg) and BP (20 mg/kg). Data were normalized as percent relative power (A). LFP spectral powers were divided into powers of 6 discrete frequency bands (B). All data were expressed as mean \pm

SEM and statistically analyzed using one-way ANOVA followed by Tukey's post hoc test. **P<0.01, ***P<0.01.

12.3.3 NAc powers

NAc power spectra of control, METH+CMC, METH+KT40, METH+KT80, and METH+BP groups were shown for comparison (**Figure 24A**). Statistical analysis confirmed significant differences found in delta [$F(4, 35) = 4.458, P = 0.005$], theta [$F(4, 35) = 5.194, P = 0.002$], alpha [$F(4, 35) = 3.306, P = 0.021$], gamma I [$F(4, 35) = 11.547, P < 0.001$], and gamma II [$F(4, 35) = 5.512, P = 0.002$] bands (**Figure 24B**). Tukey's post hoc analysis indicated a significant increase in gamma I ($P = 0.001$) and a decrease in gamma II ($P = 0.012$) induced by METH conditioning. However, 80 mg/kg KT alkaloid extract significantly reversed the increased gamma I power ($P = 0.033$). No significant difference was seen among the control, METH+KT40, and METH+KT80 groups for gamma I and II. It was noted that METH+KT80 group significantly produced opposite effects to that of METH+CMC in delta ($P = 0.002$), theta ($P = 0.001$), and alpha ($P = 0.015$) bands. Moreover, the METH+BP group produced significant differences from control levels in gamma I ($P < 0.001$) and gamma II ($P = 0.001$). The standard drug BP failed to reverse the effects of METH conditioning seen in gamma I and II powers of the METH+CMC group.

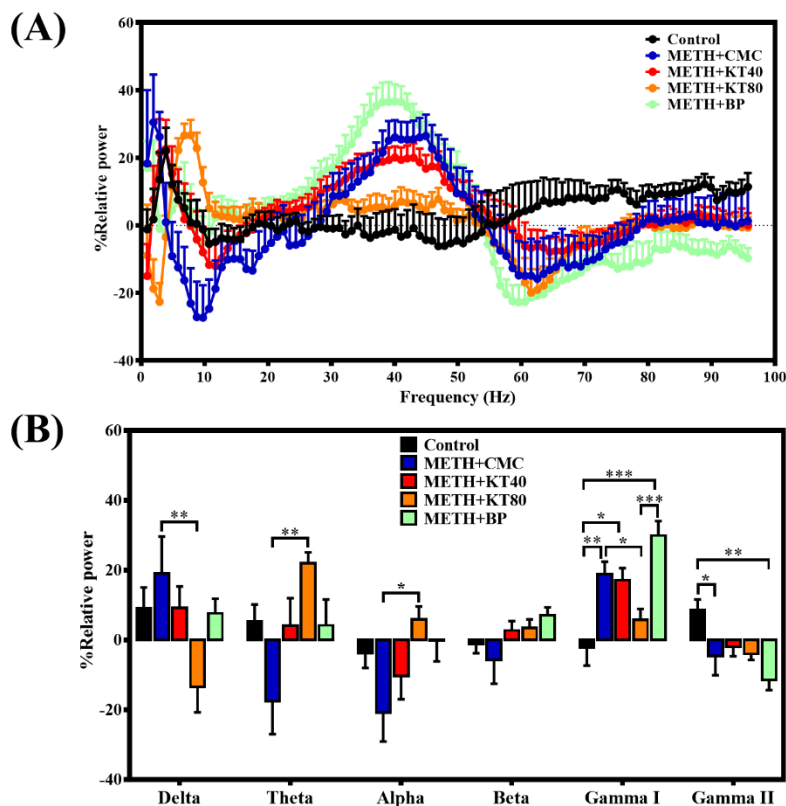


Figure 24 Effects of the treatments with KT alkaloid extract on LFP spectral powers in the NAc. Animals were treated with KT alkaloid extract (40 and 80 mg/kg) and BP (20 mg/kg). Data were normalized as percent relative power (A). LFP spectral powers were divided into powers of 6 discrete frequency bands (B). All data were expressed as mean \pm SEM and statistically analyzed using one-way ANOVA followed by Tukey's post hoc test. * $P < 0.05$, ** $P < 0.01$, *** $P < 0.001$.

12.4 Activities of the coherences

The effects of KT alkaloid extract and BP on coherence activity among the VTA, HP, and the NAc during the post-conditioning phase were analyzed and compared among groups. Data were expressed as percent relative coherence in the frequency domain (Figures 25, 26, and 27).

12.4.1 Coherence in the VTA-HP axis

Spectral coherences were analyzed over 100 Hz, and dominant oscillation in various frequencies was seen (Figure 25A). However, it remained to be confirmed statistically. The results revealed that significant changes found in the alpha [$F(4, 35) = 13.558$, $P < 0.001$], gamma I [$F(4, 35) = 2.793$, $P = 0.041$], and gamma II [$F(4, 35) = 4.550$, $P = 0.005$] coherences. Tukey's post hoc comparison exhibited the suppression in

alpha coherence in METH+CMC ($P = 0.006$) and METH+BP ($P = 0.008$) mice. Interestingly, this predisposition was rescued in the METH+KT80 group ($P < 0.001$). Reaching the significant increase and decrease was produced by METH+BP and METH+KT40 in gamma I ($P = 0.029$) and gamma II ($P = 0.006$) coherences, respectively (**Figure 25B**).

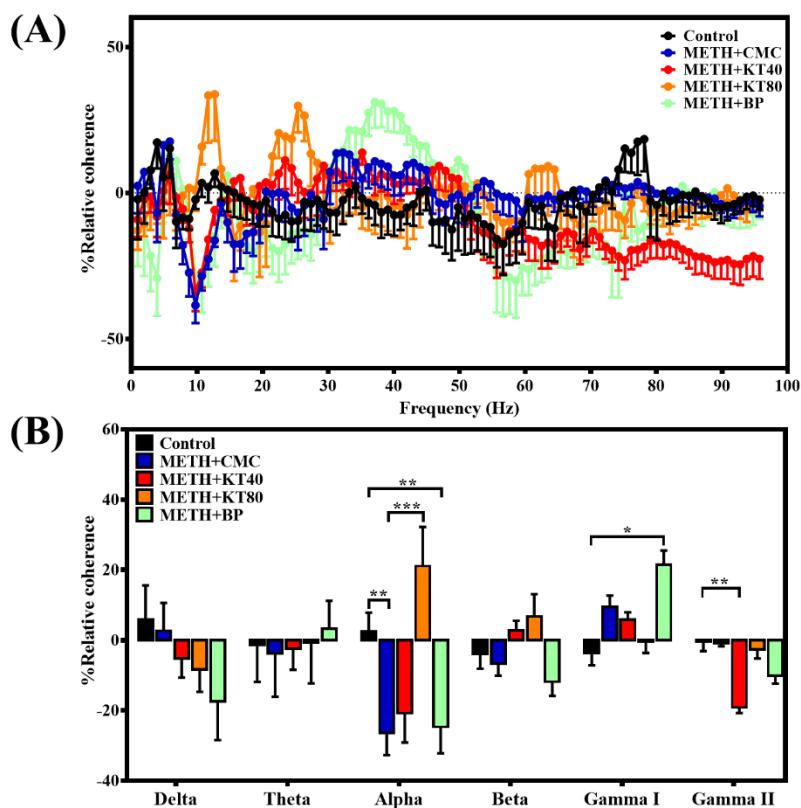


Figure 25 Effects of the treatments with KT alkaloid extract on LFP spectral coherence between the VTA and the HP in the frequency domain (1 – 100 Hz). Animals were treated with KT alkaloid extract (40 and 80 mg/kg) and BP (20 mg/kg). Data were normalized as percent relative coherence and expressed as mean \pm SEM (A). Data of each group were averaged in 6 discrete frequency bands (B). Statistical analyses were performed using one-way ANOVA followed by Tukey's post hoc test. * $P < 0.05$, ** $P < 0.01$, *** $P < 0.001$.

12.4.2 Coherence in the VTA-NAc axis

Coherences were processed and exhibited a relatively high fluctuation from 30 – 50 Hz approximately (**Figure 26A**). To confirm this phenomenon, a statistical assessment was done. The data indicated a significant change in gamma I [$F(4, 35) = 9.934$, $P < 0.001$] coherence. Multiple comparison tests specified that mice in METH+CMC ($P = 0.022$) and METH+BP ($P < 0.001$) produced a remarkable increase in this parameter. However, this was reversed by the remedy with KT80 ($P = 0.031$) (**Figure 26B**).

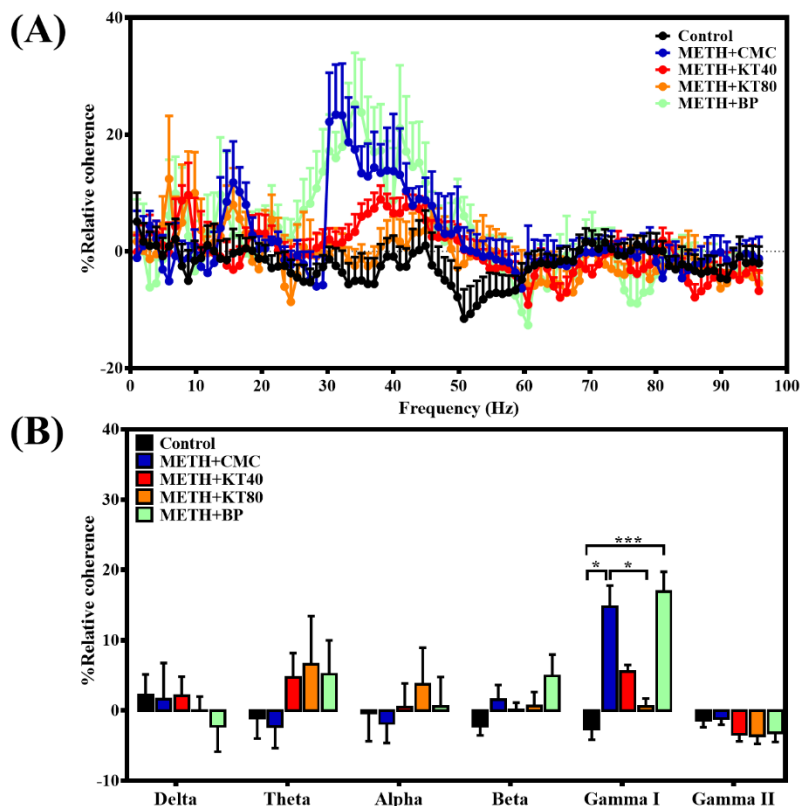


Figure 26 Effects of the treatments with KT alkaloid extract on LFP spectral coherence between the VTA and the NAc in the frequency domain (1 – 100 Hz). Animals were treated with KT alkaloid extract (40 and 80 mg/kg) and BP (20 mg/kg). Data were normalized as percent relative coherence and expressed as mean \pm SEM (A). Data of each group were averaged in 6 discrete frequency bands (B). Statistical analyses were performed using one-way ANOVA followed by Tukey's post hoc test. * $P < 0.05$, *** $P < 0.001$.

12.4.3 Coherence in the HP-NAc axis

In the HP-NAc axis, the results showed obvious differences in coherence activity, mostly in a frequency range approximately between 30 – 50 Hz (**Figure 27A**). Therefore, statistical analyses revealed significant differences only in gamma I band [$F(4, 35) = 9.934$, $P < 0.001$] (**Figure 27B**). Tukey's posthoc test confirmed significantly increased coherence values in the gamma I band of the METH+CMC group ($P = 0.022$). However, this increased coherence was significantly reversed only by treatment with KT80 ($P = 0.031$). No such effect was produced by treatment with BP, a standard drug for METH withdrawal treatment. Instead, the METH+BP group dramatically enhanced the coherence activity in the gamma I band compared to the control ($P < 0.001$). The increased coherence produced by BP treatment was even further than in the METH+CMC group.

Coherence reactivities in the VTA-HP-NAC loop during METH CPP expression (Figure 28A) and KT treatment (Figure 28B) compared with control and METH+CMC groups, respectively, were provided in **Figure 28**.

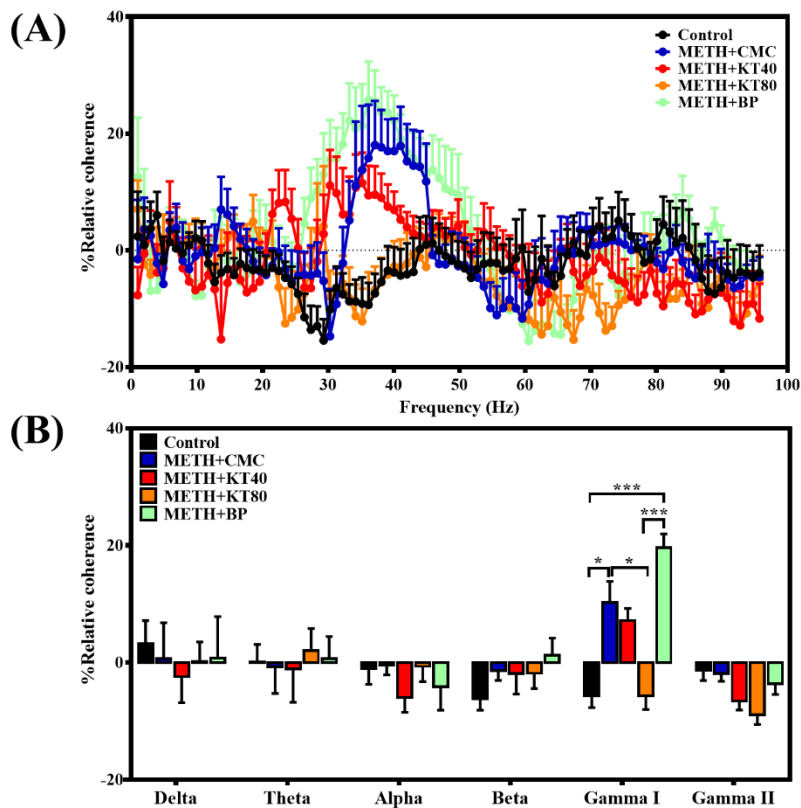


Figure 27 Effects of the treatments with KT alkaloid extract on LFP spectral coherence between the HP and the NAc in the frequency domain (1 – 100 Hz). Animals were treated with KT alkaloid extract (40 and 80 mg/kg) and BP (20 mg/kg). Data were normalized as percent relative coherence and expressed as mean \pm SEM (A). Data of each group were averaged in 6 discrete frequency bands (B). Statistical analyses were performed using one-way ANOVA followed by Tukey's post hoc test. *P<0.05, ***P<0.001.

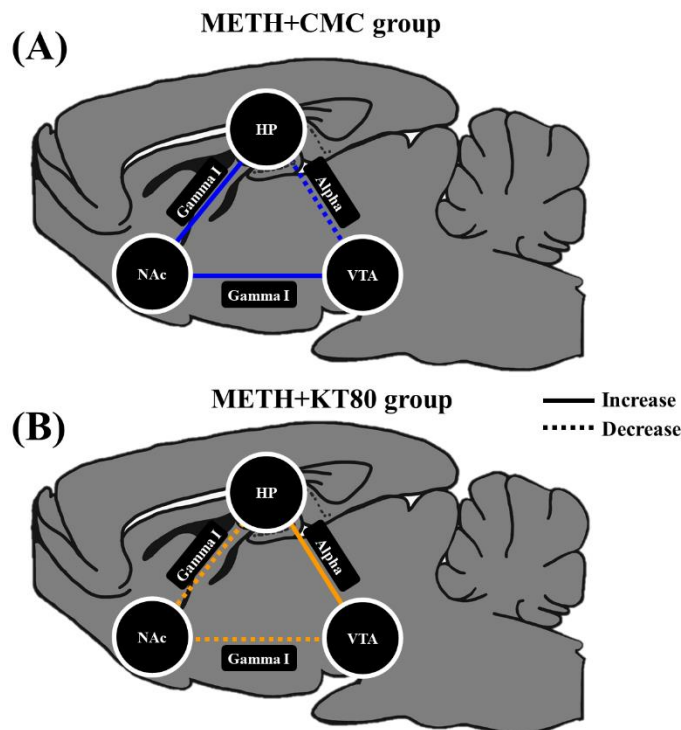


Figure 28 Schematic diagrams of integrated coherence activity among the VTA, HP, and NAc during METH CPP expression (A) and after KT extract administration (B). Solid and dashed lines represent significant increases and decreases, respectively.

13. Discussion of the METH CPP experiment treated with KT leaves extract

The effects of KT alkaloid extract and BP were measured during the expression of METH CPP. The present study highlighted that KT extract prevented METH CPP and changes in LFP oscillations induced by METH conditioning. At 80 mg/kg, KT alkaloid extract exhibited significant effects on all parameters, suggesting its efficacies on both physical and mental symptoms. CPP score reflects drug craving and seeking behaviors. In contrast, neural signaling induced during the post-conditioning phase suggests the brain mechanism underlying withdrawal symptoms.

Several mental disorders, including depression and anxiety, were detected during METH and ethanol withdrawal periods^{1,3,5,88}. Thus, potential substances for drug addiction treatment need to be determined whether they have CNS action with anti-depressive and anxiolytic effects. Previously, KT alkaloid extract was found to produce an LFP pattern and effectively attenuate the severity of ethanol withdrawal symptoms, similar to the standard antidepressant drug fluoxetine⁷⁹. KT aqueous extract also attenuated ethanol withdrawal-induced depressive behavior, probably through its

antidepressant-like activity⁸⁸. Therefore, KT alkaloid extract and BP were hypothesized to treat METH dependence in this CPP paradigm effectively.

Changes in behavior, emotion, learning, and the cognitive process are typically in response to DA depletion. In this study, the antidepressant BP was deployed as a reference drug to compensate for DA depletion induced by METH exposures. BP was used to cure METH-dependent patients as a DA transporter (DAT) inhibitor and increased DA concentration in the synaptic cleft for more robust receptor activation⁸⁹. It was also expected to improve depressive symptoms and mood swings during METH withdrawal period⁹⁰. However, the present data showed that BP did not prevent or attenuate behavioral change and neural signaling induced METH conditioning. This may be discussed regarding the METH concentration used for the CPP paradigm. Previously, side preference in the CPP paradigm caused by METH at 0.125-1.0 mg/kg was diminished by pretreatment with high dose METH that would induce neurotoxicity and decrease DA level in the striatum (STR)⁹¹. The dose of METH at 1.0 mg/kg in the present study was not likely to produce DA deficiency. It is possible that treatment with the DAT blocker could elicit excessively long-lasting overstimulation on DA receptors in the METH+BP group, as seen in CPP scores and LFP oscillatory patterns. Taken together, the alterations of parameters during the post-conditioning phase might partially be mediated through modulation in the DA system. Moreover, the present findings were consistent with a previous report that the other DAT blocker, methylphenidate (MTPD), also failed to produce beneficial results in treating amphetamine/METH dependence⁹². These data may suggest that DAT blockers (e.g., BP and/or MTPD) may be carefully used only in specific conditions of METH dependence. Aside from these aspects, BP is also reported as a novel substance inhibiting VTA GABAergic interneuron⁹³, a common mechanism with morphine action⁵¹. This may be another reason for explaining why BP treatment could not cure METH CPP in this experiment.

The expression of METH CPP has been found in response to a memory-associated cue of METH exposures. Any drugs that alter animal movement could have some impact on CPP outcomes. Apart from affecting the CPP score, the fluctuation of animals' locomotor activity was also found to interfere with LFP signal generation and oscillation^{39,94}. Therefore, it was necessary to exclude this confounding factor. Previous data revealed that 80 mg/kg KT alkaloid extract per se did not alter the animal's locomotor activity³³. It means that the KT alkaloid extract at this concentration was clearly effective on METH CPP and clean from disturbance produced by the motor activity of mice.

In traditional use, whole alkaloid constituents of KT are ingested by chewing and drinking tea from KT leaves. KT alkaloid extract, prepared in this study, had 47.1 mg MT per gram extract and was administered orally to the mice. The phytochemical analysis confirmed the presence of MT as a major alkaloid in the KT extract, which agrees with

the previous investigation³³. It has been reported that lyophilized tea (containing 25 mg/g MT) exhibited better oral bioavailability than feeding with MT alone⁹⁵.

Previously, KT extract's toxicity profile has been intensively investigated⁹⁶⁻⁹⁸. To determine the effective doses, preliminary tests were performed. The doses found to attenuate CPP scores by more than 50% obviously were remarkably lower than the LC50 dose⁷⁶. Moreover, KT extract was proposed to induce CPP, the sign of addiction only at higher doses (>500 mg/kg, p.o.)²⁶ or containing MT at 10 mg/kg⁹⁹. A large margin among effective (containing 3.8 mg/kg MT), lethal, and CPP doses suggest a safe use of the KT extract in attenuating METH dependence. Additionally, the doses of the KT extract selected followed the KT concentration that had beneficial effects in the treatment of morphine dependence³³.

The CPP paradigm is a standard model routinely used to screen drug candidates or herbal extracts on addictive substances-induced reward behaviors in experimental animals. Various psychostimulant drugs such as METH, amphetamine, and cocaine were used as positive substances that produced addictive behaviors^{22,25,27,28}. CPP is a form of Pavlovian conditioning used to measure the motivational effects of learning experiences¹⁰⁰. Pairing repeated drug use with a specific environment is believed to link with the conditioning context in the drug's delivery. They were allowing animals to re-expose with drug-related context after the condition development can trigger craving behaviors. Animals were found to spend more time in an environment with contextual cues and addictive drug delivery. The present study clearly showed the high CPP score of the METH+CMC group during the post-conditioning phase. This phenomenon appeared to have underlying mechanisms in many brain regions, including the VTA, HP, and the NAc functioning together as neural networks¹⁰¹⁻¹⁰³. Previously, reward-seeking behavior driven by the modulation of the VTA-NAc, VTA-HP, and the HP-NAc axes has also been proposed^{101,104,105}.

LFP spectral powers have been extensively analyzed as quantitative data for screening unidentified new drug compounds compared to standard drugs with known CNS action^{16,79}. With repeated exposure to METH learning sessions, VTA delta power was enhanced. METH+KT80 mice apparently reversed this. The mechanism underlying this phenomenon may be partially involved in the function of VTA GABAergic interneurons. Previous evidence proposed that the lowering activities of the VTA GABAergic neurons moderately correlated with delta power escalation¹⁰⁶. Micro-infusion of BP directly to the VTA⁹³ and a response to reward predicting stimuli⁵² appeared to reduce GABAergic neurons working. This eventually enhances DA release in nerve terminals (e.g., NAc, HP). To rescue the activity of this kind of neuron, KT80 was thus added. Inactivation of NMDA receptors by its antagonist located on the GABAergic neurons would finally enhance DA release and produce hyperactivation of DA2 receptors accompanied by social interaction impairment¹⁰⁷. Impressively, this abnormal behavior

was attenuated by pre-intervention with KT extract ⁸⁴. This may imply that KT extract may increase GABAergic neurons' activity via agonistic effects on the NMDA receptors.

Following multiple exposures to METH sessions, significant changes in delta oscillation in the HP were also highlighted. METH-induced considerable increase in HP delta power was consistent with the previous findings ⁶⁷. The olfactory cue of palatable food was found to increase delta power in the CA1, the sub-area of the HP ¹⁹. HP delta activity was associated with memory encoding through neocortical hippocampal crosstalk in animals ¹⁰⁸ and ¹⁰⁹. Delta oscillation in the HP was hypothesized to be part of neural mechanisms related to cognition and motivation. Changes in delta oscillation can be seen in humans responding to emotional stimuli ¹¹⁰ and processing reward-related conditions ⁶⁷. However, KT alkaloid extract treatment significantly reversed the enhanced HP delta power in this experiment. This result may partially be the outcome of the CNS action of KT alkaloid extract on the hypothalamic-pituitary-adrenal (HPA) axis. The HP is an important brain region that regulates stress response via the HPA axis modulation ¹¹¹. Having to face emotional stress during the post-conditioning phase would result in drug craving behaviors and COR secretion ⁴⁶. These stress responses, especially the HPA axis hyperreactivity and forced swimming-induced COR secretion were reduced by the treatment with MT, a potent alkaloid from KT leaves ⁷³. Moreover, MT was able to suppress low-frequency rhythms in the HP, including delta, and fix the CPP score remaining in the normal state ⁶⁷. These findings may suggest the alternative mechanism that the HP delta rhythm reflects the brain mechanism of motivation for METH-seeking behavior. With the mechanism of MT, KT alkaloid extract, which contains MT as a major alkaloid constituent, would reduce stress, CPP score, and neural signaling patterns induced during METH post-conditioning phase.

The present experiment induced the increased gamma I LFP power in the NAc and CPP scores by METH contextual cue. However, these parameters were significantly ameliorated by the treatment with 80 mg/kg KT alkaloid extract. The activity of the gamma I frequency range in the NAc is believed to be related to DA release and addiction. Essentially, opioid receptor activation by its agonists such as a significant KT alkaloid composition MT or even morphine, a standard addictive drug, in the VTA was found to promote the over-release of DA and increase gamma I in the NAc. However, these phenomena were abolished by pretreatment with naloxone, an opioid receptor blocker ³⁹. A psychoactive substance such as pseudoephedrine was demonstrated to have sites of action in the DA pathway's NAc and STR ¹⁴. Amphetamine and METH also activate gene expression in the mesolimbic/mesostriatal pathways via DA1 and DA2 receptors ¹¹². Previously, the DRn was an origin of 5-HT projections that inhibit DA nigrostriatal neurons ¹¹³. A previous report confirmed that the DRn was activated by KT extract ⁷⁷, resulting in decreased DA release in the NAc because the NAc is a significant component of the ventral STR ¹¹⁴. Additionally, the involvement of the anti-DA mechanism from methanolic extract of KT leaves evaluated by measuring the DA level in the NAc was

also evidenced¹¹⁵. Aside from the lowering of DA release affected by DRn activation from KT extract, the partial effects may result from mimicking the NMDA receptor's agonistic action of KT extract, as mentioned⁸⁴. Thus, KT extract might alleviate withdrawal symptoms and decrease gamma I activity via reduced DA release in the NAc as a mechanism. Another extract from *Morinda citrifolia* Linn. that possess anti-DA activity also found to alleviate METH CPP and drug abuse-induced craving behaviors^{25,116,117}.

The present study showed the decreases in gamma II oscillation in the NAc during the post-conditioning phase only in METH+vehicle and METH+BP groups. A wide range of gamma II activities in the NAc has been evidenced^{39,118}. A palatable food cue-induced gamma II oscillation in CPP paradigm¹¹⁸. This frequency band activity may be associated with brain mechanism that supports seeking behavior driven by CPP. Moreover, the positive correlation between gamma II oscillation and neuronal coding of movement was also reported³⁹. The present CPP data clearly demonstrated that KT alkaloid extract at the effective dose did not induce a spontaneous psychoactive effect. This was consistent with the previous report that 80 mg/kg KT alkaloid extract did not alter the motor activities³³. Altogether, these findings partially proposed the attenuation effects of KT alkaloid extract on METH-induced addiction through DA modulation. Gamma I and II oscillations were sensitive to METH repeated exposures and treatment with KT alkaloid extract but not BP.

The regulation of each behavior may involve multiple brain areas functioning in coordination. The interrelationship of the VTA-HP-NAc loop was believed to mediate drug-related cue-induced seeking behaviors^{101,104,105}. Coherence analysis, a mathematical algorithm, was used to measure the strength of neural connection to assess the communication between separate brain regions following drug treatment. The present data revealed that the METH+CMC group increased both percent relative coherence in the gamma I frequency range in the VTA-NAc axis and CPP score. However, 80 mg/kg KT alkaloid extract reversed this coherence activity entirely. Previously, gamma I coherence in this axis was produced dose-dependent from morphine administration³⁹. It may involve morphine-induced hyperpolarization of DA neurons projecting from the VTA to the NAc via the modulation of VTA GABAergic interneurons⁵¹. Impressively, the predisposition of these interneurons would be neutralized with KT80 treatment by mimicking NMDA receptors agonist⁸⁴.

Alpha coherence in the VTA-HP axis decreased during METH CPP expression, a phase fulfilled with stress response⁴⁶. Impressively, this was rescued by the KT80 remedy. Disruption of coherence synchronization in various frequency bands (e.g., alpha) in the region connected with the HP can be seen during stress exposure¹¹⁹. Moreover, it reduced GABAergic activities^{120,121} and enhanced the release of excitatory neurotransmitters in the HP (e.g., glutamate (GLU), DA, or norepinephrine)^{122,123} produced by the stressors. Interestingly, MT, a significant constituent accumulated in the KT80, was found to suppress COR release and the symptoms of stress-induced

depression-like behaviors⁷³. Hence, this may imply that a change of alpha coherence in the VTA-HP axis may involve a stress response.

The METH+CMC group in the HP-NAc axis also saw an increase in gamma I coherence. The KT80 administration reversed this. Previously, the HP was demonstrated to contain a neuronal population of place cells that selectively burst in response to specific spatial contexts¹²⁴. This evidence-based finding strongly suggests HP's involvement in processing spatial navigation¹²⁵. With the coherence activity, signaling information could be sent through the projection from the CA1 region of the HP to the NAc¹²⁶. The analysis of the firing rate confirmed that place cells in the HP fired preferentially before reward-related neurons in the NAc. This finding indicated that place-reward information was carried from the HP to the NAc¹²⁷. Ultimately, the interaction between the HP and the NAc also plays a significant role in CPP acquisition¹²⁸. This may be associated with processing information in decision-making and reinforcement-based learning¹²⁹. The underlying mechanism of these changes may be partially related to the GLU NMDA receptor's control activity. Ketamine, a GLU receptor antagonist, induced gamma functional connectivity enhancement, was proposed to be targeted for treating schizophrenia¹³⁰, a common symptom produced by drug abuse¹³¹. Increased GABA, GLU, DA releases, and escalated CPP scores were accompanied by ketamine application^{107,132,133}. These alterations were reversed by KT80 treatment as it mimicked the action of NMDA receptors agonist clozapine⁸⁴. This study suggests that the elevated CPP score and coherence in the gamma I frequency range were triggered by the neural signal of the METH-associated cue sent from the HP to the NAc. Therefore, KT80 treatment may help attenuate METH dependence and reduce the inter-region connectivity.

14. Conclusion of the METH CPP experiment treated with KT leave extract

In summary, the present study proposed beneficial effects of 80 mg/kg KT alkaloid extract for the treatment of METH dependence. The data from the CPP paradigm revealed that the extract successfully reversed METH CPP scores. This would suggest the KT plant's therapeutic property in treating abnormal behaviors induced by METH dependence. Moreover, the analyses of LFP power spectra and coherence also provided additional data for a better understanding of possible brain mechanisms of KT alkaloid extract in the attenuation of METH CPP (**Figure 29**). Taken together, these findings strongly suggested that the KT alkaloid extract has promising effects for further development as an alternative compound for possible use in METH-addicted patients.

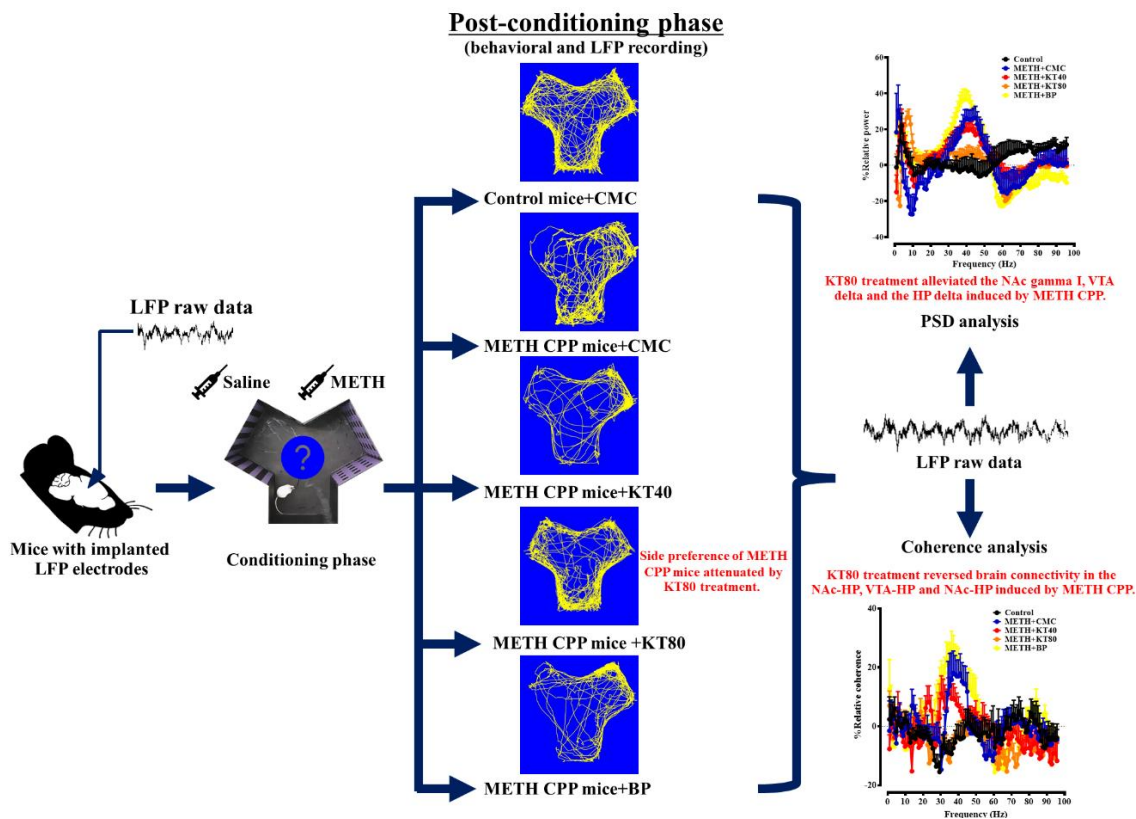


Figure 29 Novel discovery of LFP signals associated with the attenuation of METH CPP treated with KT leaves extract

Significant findings in summary

The BLA theta and alpha power desynchronizations and the BLA theta-gamma coupling may underly the brain mechanisms that responded to METH abstinent induced by the CPP paradigm. These may be important in drug discovery research to design and select the drugs for METH CPP therapy. From these findings, the effects of KT leave extract were hypothesized to deal with the aberrations of animal behaviors and brain wave oscillations. The confirmation was performed and exposed the neural signaling in the brain-related addicted behaviors in response to the attenuation of METH CPP cured with KT leave extract. KT leave extract ameliorated METH-induced CPP by decreasing power in the VTA delta, HP delta, NAc gamma I and alleviating coherence in the VTA-HP alpha, VTA-NAc gamma I, and HP-NAc gamma I. A wholly evidence-based study may provide additional data to support the development of KT leave extract as a standardized alternative drug for METH craving and seeking remedies.

Further direction

The effects of environment associated with drugs as the factor to motivate addiction-related behaviors in the CPP paradigm has been tested. However, these factors are also divided into two subtypes: alive and inanimate factors. This experiment has already conducted the effects of KT extract on inanimate factor induced CPP. Therefore, in further studies, the effects of KT extract might be determined whether it can suppress addiction-related behaviors induced by alive factors. To confirm this hypothesis, various experimental techniques such as microdialysis, immunohistochemistry staining, and western blotting might be integrated to precisely reach the exact mechanisms of KT leave extract in METH addiction treatment.

References

1. Halpin LE, Collins SA, Yamamoto BK. Neurotoxicity of methamphetamine and 3,4-methylenedioxymethamphetamine. *Life Sci.* 2013;97(1):37-44. doi:10.1016/j.lfs.2013.07.014
2. Turnipseed SD, Richards JR, Kirk JD, Diercks DB, Amsterdam EA. Frequency of acute coronary syndrome in patients presenting to the emergency department with chest pain after methamphetamine use. *J Emerg Med.* 2003;24(4):369-373. doi:10.1016/S0736-4679(03)00031-3
3. Wearne TA, Cornish JL. A comparison of methamphetamine-induced psychosis and schizophrenia: A review of positive, negative, and cognitive symptomatology. *Front Psychiatry.* 2018;9(491):1-21. doi:10.3389/fpsy.2018.00491
4. Korpi ER, den Hollander B, Farooq U, et al. Mechanisms of action and persistent neuroplasticity by drugs of abuse. *Pharmacol Rev.* 2015;67(4):872-1004. doi:10.1124/pr.115.010967
5. Embry D, Hankins M, Biglan A, Boles S. Behavioral and social correlates of methamphetamine use in a population-based sample of early and later adolescents. *Addict Behav.* 2009;34(4):343-351. doi:10.1016/j.addbeh.2008.11.019
6. Russo SJ, Nestler EJ. The brain reward circuitry in mood disorders. *Nat Rev Neurosci.* 2013;14(9):609-625. doi:10.1038/nrn3381
7. Phelps EA. Emotion and cognition: Insights from studies of the human amygdala. *Annu Rev Psychol.* 2006;57(Miller 2003):27-53. doi:10.1146/annurev.psych.56.091103.070234
8. Amunts K, Kedo O, Kindler M, et al. Cytoarchitectonic mapping of the human amygdala, hippocampal region and entorhinal cortex: Intersubject variability and probability maps. *Anat Embryol (Berl).* 2005;210(5-6):343-352. doi:10.1007/s00429-005-0025-5
9. Wassum KM, Izquierdo A. The basolateral amygdala in reward learning and addiction. *Neurosci Biobehav Rev.* 2015;57:271-283. doi:10.1016/j.neubiorev.2015.08.017
10. See RE, Fuchs RA, Ledford CC, McLaughlin J. Drug addiction, relapse, and the amygdala. *Ann N Y Acad Sci.* 2003;985:294-307. doi:10.1111/j.1749-6632.2003.tb07089.x
11. Meil WM, See RE. Lesions of the basolateral amygdala abolish the ability of drug associated cues to reinstate responding during withdrawal from self-administered cocaine. *Behav Brain Res.* 1997;87(2):139-148. doi:10.1016/S0166-4328(96)02270-X
12. Goodman J, Hsu E, Packard MG. NMDA receptors in the basolateral amygdala

- mediate acquisition and extinction of an amphetamine conditioned place preference. *Behav Neurosci.* 2019;133(4):428-436. doi:10.1037/bne0000323
13. You ZB, Wang B, Zitzman D, Wise RA. Acetylcholine release in the mesocorticolimbic dopamine system during cocaine seeking: Conditioned and unconditioned contributions to reward and motivation. *J Neurosci.* 2008;28(36):9021-9029. doi:10.1523/JNEUROSCI.0694-08.2008
 14. Kumarnsit E, Harnyuttanakorn P, Meksuriyen D, et al. Pseudoephedrine, a sympathomimetic agent, induces Fos-like immunoreactivity in rat nucleus accumbens and striatum. *Neuropharmacology.* 1999;38(9):1381-1387. doi:10.1016/S0028-3908(99)00054-4
 15. Dimpfel W. Pharmacological classification of herbal extracts by means of comparison to spectral EEG signatures induced by synthetic drugs in the freely moving rat. *J Ethnopharmacol.* 2013;149(2):583-589. doi:10.1016/j.jep.2013.07.029
 16. Dimpfel W, Schombert L, Gericke N. Electropharmacogram of Sceletium tortuosum extract based on spectral local field power in conscious freely moving rats. *J Ethnopharmacol.* 2016;177:140-147. doi:10.1016/j.jep.2015.11.036
 17. Christian EP, Snyder DH, Song W, et al. EEG-/ spectral power elevation in rat: A translatable biomarker elicited by GABA A2/3-positive allosteric modulators at non-sedating anxiolytic doses. *J Neuro-physiol.* 2015;113:116-131. doi:10.1152/jn.00539.2013.-Benzodiazepine
 18. Alonso JF, Romero S, Mañanas MÁ, Rojas M, Riba J, Barbanoj MJ. Evaluation of multiple comparison correction procedures in drug assessment studies using LORETA maps. *Med Biol Eng Comput.* 2015;53(10):1011-1023. doi:10.1007/s11517-015-1315-6
 19. Samerphob N, Cheaha D, Chatpun S, Kumarnsit E. Hippocampal CA1 local field potential oscillations induced by olfactory cue of liked food. *Neurobiol Learn Mem.* 2017;142:173-181. doi:10.1016/j.nlm.2017.05.011
 20. Zhu Z, Ye Z, Wang H, Hua T, Wen Q, Zhang C. Theta-gamma coupling in the prelimbic area is associated with heroin addiction. *Neurosci Lett.* 2019;701:26-31. doi:10.1016/j.neulet.2019.02.020
 21. Cadoret RJ, O'gorman TW, Troughton E, Heywood E. Alcoholism and antisocial personality: Interrelationships, genetic and environmental factors. *Arch Gen Psychiatry.* 1985;42(2):161-167. doi:10.1001/archpsyc.1985.01790250055007
 22. Nukitram J, Cheaha D, Kumarnsit E. Spectral power and theta-gamma coupling in the basolateral amygdala related with methamphetamine conditioned place preference in mice. *Neurosci Lett.* 2021;756(135939):1-10. doi:10.1016/j.neulet.2021.135939

23. Nukitram J, Cheaha D, Sengnon N, Wungsintaweekul J, Limsuwanchote S, Kumarnsit E. Ameliorative effects of alkaloid extract from *Mitragyna speciosa* (Korth.) Havil. leaves on methamphetamine conditioned place preference in mice. *J Ethnopharmacol.* 2022;284:114824. doi:10.1016/j.jep.2021.114824
24. Sun L, Song R, Chen Y, et al. A selective D3 receptor antagonist YQA14 attenuates methamphetamine-induced behavioral sensitization and conditioned place preference in mice. *Acta Pharmacol Sin* 2016 372. 2015;37(2):157-165. doi:10.1038/aps.2015.96
25. Pandey V, Wai YC, Amira Roslan NF, Sajat A, Abdulla Jallb AH, Vijeepallam K. Methanolic extract of *Morinda citrifolia* Linn. unripe fruit attenuates methamphetamine-induced conditioned place preferences in mice. *Biomed Pharmacother.* 2018;107(July):368-373. doi:10.1016/j.biopha.2018.08.008
26. Vijeepallam K, Pandey V, Murugan D, Kuppusamy M. Methanolic extract of *Mitragyna speciosa* Korth leaf exhibits place preference only at higher doses in mice. *Pharmacogn Mag.* 2020;16(71):449-454. doi:10.4103/pm.pm_62_20
27. Shen M, Jiang C, Liu P, Wang F, Ma L. Mesolimbic leptin signaling negatively regulates cocaine-conditioned reward. *Transl Psychiatry.* 2016;6(12):1-10. doi:10.1038/tp.2016.223
28. Bardgett ME, Downen T, Crane C, et al. Chronic risperidone administration leads to greater amphetamine-induced conditioned place preference. *Neuropharmacology.* 2020;179(August):108276. doi:10.1016/j.neuropharm.2020.108276
29. Gray CM, Maldonado PE, Wilson M, McNaughton B. Tetrodes markedly improve the reliability and yield of multiple single-unit isolation from multi-unit recordings in cat striate cortex. *J Neurosci Methods.* 1995;63(1-2):43-54. doi:10.1016/0165-0270(95)00085-2
30. Berens P, Keliris GA, Ecker AS, Logothetis NK, Tolias AS. Comparing the feature selectivity of the gamma-band of the local field potential and the underlying spiking activity in primate visual cortex. *Front Syst Neurosci.* 2008;2(JUN). doi:10.3389/neuro.06.002.2008
31. Cohen MX. *Analyzing Neural Time Series Data.*; 2019. doi:10.7551/mitpress/9609.001.0001
32. Castellanos NP, Makarov VA. Recovering EEG brain signals: Artifact suppression with wavelet enhanced independent component analysis. *J Neurosci Methods.* 2006;158(2):300-312. doi:10.1016/j.jneumeth.2006.05.033
33. Cheaha D, Reakkamnuan C, Nukitram J, et al. Effects of alkaloid-rich extract from *Mitragyna speciosa* (Korth.) Havil. on naloxone-precipitated morphine withdrawal symptoms and local field potential in the nucleus accumbens of mice. *J*

- Ethnopharmacol.* 2017;208:129-137. doi:10.1016/j.jep.2017.07.008
34. Paxinos G, Franklin KBJ. The mouse brain in stereotaxic coordinates. Published online 2001:120.
 35. Caillé S, Espejo EF, Reneric JP, Cador M, Koob GF, Stinus L. Total neurochemical lesion of noradrenergic neurons of the locus ceruleus does not alter either naloxone-precipitated or spontaneous opiate withdrawal nor does it influence ability of clonidine to reverse opiate withdrawal. *J Pharmacol Exp Ther.* 1999;290(2):881-892.
 36. Ben-Shaul Y. OptiMouse: A comprehensive open source program for reliable detection and analysis of mouse body and nose positions. *BMC Biol.* 2017;15(1):1-22. doi:10.1186/s12915-017-0377-3
 37. Tadel F, Baillet S, Mosher JC, Pantazis D, Leahy RM. Brainstorm: A user-friendly application for MEG/EEG analysis. *Comput Intell Neurosci.* 2011;2011:1-13. doi:10.1155/2011/879716
 38. Galaj E, Manuszak M, Babic S, Ananthan S, Ranaldi R. The selective dopamine D3 receptor antagonist, SR 21502, reduces cue-induced reinstatement of heroin seeking and heroin conditioned place preference in rats. *Drug Alcohol Depend.* 2015;156:228-233. doi:10.1016/j.drugalcdep.2015.09.011
 39. Reakkamnuan C, Cheaha D, Kumarnsit E. Nucleus accumbens local field potential power spectrums, phase-amplitude couplings and coherences following morphine treatment. *Acta Neurobiol Exp (Wars).* 2017;77:214-224. doi:https://doi.org/10.21307/ane-2017-055
 40. Hellemans KGC, Everitt BJ, Lee JLC. Disrupting reconsolidation of conditioned withdrawal memories in the basolateral amygdala reduces suppression of heroin seeking in rats. *J Neurosci.* 2006;26(49):12694-12699. doi:10.1523/JNEUROSCI.3101-06.2006
 41. Shi HS, Luo YX, Yin X, et al. Reconsolidation of a cocaine associated memory requires DNA methyltransferase activity in the basolateral amygdala. *Sci Rep.* 2015;5(August):1-13. doi:10.1038/srep13327
 42. Servonnet A, Hernandez G, Hage C El, Rompré PP, Samaha AN. Optogenetic activation of the basolateral amygdala promotes both appetitive conditioning and the instrumental pursuit of reward cues. *J Neurosci.* 2020;40(8):1732-1743. doi:10.1523/JNEUROSCI.2196-19.2020
 43. Kirby KC, Lamb RJ, Iguchi MY, Husband SD, Platt JJ. Situations occasioning cocaine use and cocaine abstinence strategies. *Addiction.* 1995;90(9):1241-1252. doi:10.1046/j.1360-0443.1995.90912418.x
 44. Bocchio M, McHugh SB, Bannerman DM, Sharp T, Capogna M. Serotonin,

- amygdala and fear: Assembling the puzzle. *Front Neural Circuits*. 2016;10(APR):1-15. doi:10.3389/fncir.2016.00024
45. Barkus C, Line SJ, Huber A, et al. Variation in serotonin transporter expression modulates fear-evoked hemodynamic responses and theta-frequency neuronal oscillations in the amygdala. *Biol Psychiatry*. 2014;75(11):901-908. doi:10.1016/j.biopsych.2013.09.003
 46. De Vries AC, Taymans SE, Sundstrom JM, Pert A. Conditioned release of corticosterone by contextual stimuli associated with cocaine is mediated by corticotropin-releasing factor. *Brain Res*. 1998;786(1-2):39-46. doi:10.1016/S0006-8993(97)01328-0
 47. Daviu N, Andero R, Armario A, Nadal R. Sex differences in the behavioural and hypothalamic-pituitary-adrenal response to contextual fear conditioning in rats. *Horm Behav*. 2014;66(5):713-723. doi:10.1016/j.yhbeh.2014.09.015
 48. Patkar A, Ashwin A, Gopalakrishnan R, et al. Changes in plasma noradrenaline and serotonin levels and craving during alcohol withdrawal. *Alcohol Alcohol*. 2003;38(3):224-231. doi:10.1093/alcalc/agg055
 49. Zorick T, Okita K, Mandelkern MA, London ED, Brody AL. Effects of citalopram on cue-induced alcohol craving and thalamic D2/3 dopamine receptor availability. *Int J Neuropsychopharmacol*. 2019;22(4):286-291. doi:10.1093/ijnp/pyz010
 50. Juarez B, Han MH. Diversity of dopaminergic neural circuits in response to drug exposure. *Neuropsychopharmacology*. 2016;41(10):2424. doi:10.1038/NPP.2016.32
 51. Johnson SW, North RA. Opioids excite dopamine neurons by hyperpolarization of local interneurons. *J Neurosci*. 1992;12(2):483-488. doi:10.1523/jneurosci.12-02-00483.1992
 52. Pan WX, Brown J, Dudman JT. Neural signals of extinction in the inhibitory microcircuit of the ventral midbrain. *Nat Neurosci*. 2013;16(1):71-78. doi:10.1038/nn.3283
 53. Dimpfel W. Rat electropharmacograms of the flavonoids rutin and quercetin in comparison to those of moclobemide and clinically used reference drugs suggest antidepressive and/or neuroprotective action. *Phytomedicine*. 2009;16(4):287-294. doi:10.1016/J.PHYMED.2009.02.005
 54. Dimpfel W, Spüler M, Koch R, Schatton W. Radioelectroencephalographic comparison of memantine with receptor-specific drugs acting on dopaminergic transmission in freely moving rats. *Neuropsychobiology*. 1987;18(4):212-218. doi:10.1159/000118420
 55. Kaag AM, Reneman L, Homberg J, van den Brink W, van Wingen GA. Enhanced

- amygdala-striatal functional connectivity during the processing of cocaine cues in male cocaine users with a history of childhood trauma. *Front Psychiatry*. 2018;9(MAR):1-13. doi:10.3389/fpsyt.2018.00070
56. Goutagny R, Gu N, Cavanagh C, et al. Alterations in hippocampal network oscillations and theta-gamma coupling arise before A β overproduction in a mouse model of Alzheimer's disease. *Eur J Neurosci*. 2013;37(12):1896-1902. doi:10.1111/ejn.12233
 57. Park JY, Lee YR, Lee J. The relationship between theta-gamma coupling and spatial memory ability in older adults. *Neurosci Lett*. 2011;498(1):37-41. doi:10.1016/j.neulet.2011.04.056
 58. Fell J, Axmacher N. The role of phase synchronization in memory processes. *Nat Rev Neurosci*. 2011;12(2):105-118. doi:10.1038/nrn2979
 59. Tort ABL, Kramer MA, Thorn C, et al. Dynamic cross-frequency couplings of local field potential oscillations in rat striatum and hippocampus during performance of a T-maze task. *Proc Natl Acad Sci U S A*. 2008;105(51):20517-20522. doi:10.1073/pnas.0810524105
 60. Stujenske JM, Likhtik E, Topiwala MA, Gordon JA. Fear and safety engage competing patterns of theta-gamma coupling in the basolateral amygdala. *Neuron*. 2014;83(4):919-933. doi:10.1016/j.neuron.2014.07.026
 61. Tan KR, Yvon C, Turiault M, et al. GABA neurons of the VTA drive conditioned place aversion. *Neuron*. 2012;73(6):1173-1183. doi:10.1016/j.neuron.2012.02.015
 62. Seno FZ, Sgobbib RF, Nobre MJ. Contributions of the GABAergic system of the prelimbic cortex and basolateral amygdala to morphine withdrawal-induced contextual fear. *Physiol Behav*. Published online 2022:113868. doi:10.1016/j.physbeh.2022.113868
 63. Taslimi Z, Sarihi A, Haghparast A. Glucocorticoid receptors in the basolateral amygdala mediated the restraint stress-induced reinstatement of methamphetamine-seeking behaviors in rats. *Behav Brain Res*. 2018;348:150-159. doi:10.1016/j.bbr.2018.04.022
 64. Der-Ghazarian TS, Charmchi D, Noudali SN, et al. Neural circuits associated with 5-HT 1B receptor agonist inhibition of methamphetamine seeking in the conditioned place preference model. Published online 2019. doi:10.1021/acscchemneuro.8b00709
 65. Young EJ, Lin H, Kamenecka TM, Rumbaugh G, Miller CA. Methamphetamine learning induces persistent and selective nonmuscle myosin II-dependent spine motility in the basolateral amygdala. *J Neurosci*. 2020;40(13):2695-2707. doi:10.1523/JNEUROSCI.2182-19.2020

66. Suhaimi FW, Yusoff NHM, Hassan R, et al. Neurobiology of kratom and its main alkaloid mitragynine. *Brain Res Bull.* 2016;126:29-40. doi:10.1016/j.brainresbull.2016.03.015
67. Yusoff NHM, Suhaimi FW, Vadivelu RK, et al. Abuse potential and adverse cognitive effects of mitragynine (kratom). *Addict Biol.* 2016;21(1):98-110. doi:10.1111/adb.12185
68. Adkins JE, Boyer EW, McCurdy CR. Mitragyna speciosa, a psychoactive tree from southeast asia with opioid activity. *Curr Top Med Chem.* 2011;11(9):1165-1175. doi:10.2174/156802611795371305
69. Kruegel AC, Grundmann O. The medicinal chemistry and neuropharmacology of kratom: A preliminary discussion of a promising medicinal plant and analysis of its potential for abuse. *Neuropharmacology.* 2018;134:108-120. doi:10.1016/j.neuropharm.2017.08.026
70. Jansen KL, Prast CJ. Psychoactive properties of mitragynine (kratom). *J Psychoactive Drugs.* 1988;20(4):455-457. doi:10.1080/02791072.1988.10472519
71. Chan KB, Pakiam C, Rahim RA. Psychoactive plant abuse: The identification of mitragynine in ketum and in ketum preparations. *Bull Narc.* 2007;57(1-2):249-256.
72. Foss JD, Nayak SU, Tallarida CS, Farkas DJ, Ward SJ, Rawls SM. Mitragynine, bioactive alkaloid of kratom, reduces chemotherapy-induced neuropathic pain in rats through α -adrenoceptor mechanism. *Drug Alcohol Depend.* 2020;209:1-9. doi:10.1016/j.drugalcdep.2020.107946
73. Idayu NF, Taufik Hidayat M, Moklas MAM, et al. Antidepressant-like effect of mitragynine isolated from Mitragyna speciosa Korth in mice model of depression. *Phytomedicine.* 2011;18(5):402-407. doi:10.1016/j.phymed.2010.08.011
74. Bourin MS, Fiocco AJ, Clenet F. How valuable are animal models in defining antidepressant activity? *Hum Psychopharmacol.* 2001;16(1):9-21. doi:10.1002/hup.178
75. Takahashi E, Katayama M, Niimi K, Itakura C. Additive subthreshold dose effects of cannabinoid CB1 receptor antagonist and selective serotonin reuptake inhibitor in antidepressant behavioral tests. *Eur J Pharmacol.* 2008;589(1-3):149-156. doi:10.1016/j.ejphar.2008.05.020
76. Reanmongkol W, Keawpradub N, Sawangjaroen K. Effects of the extracts from Mitragyna speciosa Korth. leaves on analgesic and behavioral activities in experimental animals. *Songklanakarinn J Sci Technol.* 2007;29:39-48.
77. Kumarnsit E, Vongvatcharanon U, Keawpradub N, Intasaro P. Fos-like immunoreactivity in rat dorsal raphe nuclei induced by alkaloid extract of Mitragyna speciosa. *Neurosci Lett.* 2007;416(2):128-132.

doi:10.1016/j.neulet.2007.01.061

78. Briley M, Moret C. Neurobiological mechanisms involved in antidepressant therapies. *Clin Neuropharmacol*. 1993;16(5):387-400. doi:10.1097/00002826-199310000-00002
79. Cheaha D, Keawpradub N, Sawangjaroen K, Phukpattaranont P, Kumarnsit E. Effects of an alkaloid-rich extract from *Mitragyna speciosa* leaves and fluoxetine on sleep profiles, EEG spectral frequency and ethanol withdrawal symptoms in rats. *Phytomedicine*. 2015;22(11):1000-1008. doi:10.1016/j.phymed.2015.07.008
80. Cheaha D, Sawangjaroen K, Kumarnsit E. Characterization of fluoxetine effects on ethanol withdrawal-induced cortical hyperexcitability by EEG spectral power in rats. *Neuropharmacology*. 2014;77:49-56. doi:10.1016/J.NEUROPHARM.2013.09.020
81. Eaimchaloay S, Kalayasiri R, Prechawit S. Characteristics and physical outcomes of kratom users at a substance abuse treatment center. *Chulalongkorn Med J*. 2019;63(3):179-185.
82. Munemura M, Eskay RL, Keabian JW, Long R. Release of α -melanocyte-stimulating hormone from dispersed cells of the intermediate lobe of the rat pituitary gland: Involvement of catecholamines and adenosine 3', 5'-monophosphate. *Endocrinology*. 1980;106(6):1795-1803. doi:10.1210/endo-106-6-1795
83. Boyer EW, Babu KM, Adkins JE, McCurdy CR, Halpern JH. Self-treatment of opioid withdrawal using kratom (*Mitragyna speciosa* korth). *Addiction*. 2008;103(6):1048-1050. doi:10.1111/j.1360-0443.2008.02209.x
84. Vijeepallam K, Pandey V, Kunasegaran T, Murugan DD, Naidu M. *Mitragyna speciosa* leaf extract exhibits antipsychotic-like effect with the potential to alleviate positive and negative symptoms of psychosis in mice. *Front Pharmacol*. 2016;7(DEC):1-11. doi:10.3389/fphar.2016.00464
85. Keawpradub N. *Alkaloids from the Fresh Leaves of Mitragyna Speciosa (Korth.) Havil*. 1990.
86. Kitajima M, Misawa K, Kogure N, et al. A new indole alkaloid, 7-hydroxyspeciociliatine, from the fruits of Malaysian *Mitragyna speciosa* and its opioid agonistic activity. *J Nat Med*. 2006;60(1):28-35. doi:10.1007/S11418-005-0001-7
87. Limsuwanchote S, Wungsintaweekul J, Keawpradub N, Putalun W, Morimoto S, Tanaka H. Development of indirect competitive ELISA for quantification of mitragynine in Kratom (*Mitragyna speciosa* (Roxb.) Korth.). *Forensic Sci Int*. 2015;244:70-77. doi:10.1016/j.forsciint.2014.08.011

88. Kumarnsit E, Keawpradub N, Nuankaew W. Effect of *Mitragyna speciosa* aqueous extract on ethanol withdrawal symptoms in mice. *Fitoterapia*. 2007;78(3):182-185. doi:10.1016/j.fitote.2006.11.012
89. Stahl SM, Pradko JF, Haight BR, Modell JG, Rockett CB, Learned-Coughlin S. A review of the neuropharmacology of bupropion, a dual norepinephrine and dopamine reuptake inhibitor. *Prim Care Companion J Clin Psychiatry*. 2004;06(04):159-166. doi:10.4088/pcc.v06n0403
90. Elkashef AM, Rawson RA, Anderson AL, et al. Bupropion for the treatment of methamphetamine dependence. *Neuropsychopharmacology*. 2008;33(5):1162-1170. doi:10.1038/sj.npp.1301481
91. Achat-Mendes C, Ali SF, Itzhak Y. Differential effects of amphetamines-induced neurotoxicity on appetitive and aversive Pavlovian conditioning in mice. *Neuropsychopharmacology*. 2005;30(6):1128-1137. doi:10.1038/sj.npp.1300675
92. Miles SW, Sheridan J, Russell B, et al. Extended-release methylphenidate for treatment of amphetamine/methamphetamine dependence: A randomized, double-blind, placebo-controlled trial. *Addiction*. 2013;108(7):1279-1286. doi:10.1111/add.12109
93. Amirabadi S, Pakdel FG, Shahabi P, Naderi S, Osalou MA, Cankurt U. Microinfusion of bupropion inhibits putative GABAergic neuronal activity of the ventral tegmental area. *Basic Clin Neurosci*. 2014;5(3):182-190.
94. Li JY, Kuo TBJ, Hsieh IT, Yang CCH. Changes in hippocampal theta rhythm and their correlations with speed during different phases of voluntary wheel running in rats. *Neuroscience*. 2012;213:54-61. doi:10.1016/J.NEUROSCIENCE.2012.04.020
95. Avery BA, Boddu SP, Sharma A, et al. Comparative pharmacokinetics of mitragynine after oral administration of *Mitragyna speciosa* (Kratom) leaf extracts in rats. *Planta Med*. 2019;85(4):340-346. doi:10.1055/a-0770-3683
96. Kamal MSA, Ghazali AR, Yahya N 'Ashikin, Wasiman MI, Ismail Z. Acute toxicity study of standardized *Mitragyna speciosa* Korth aqueous extract in sprague dawley rats. *J Plant Stud*. 2012;1(2):120-129. doi:10.5539/jps.v1n2p120
97. Harizal SN, Mansor SM, Hasnan J, Tharakan JKJ, Abdullah J. Acute toxicity study of the standardized methanolic extract of *Mitragyna speciosa* Korth in Rodent. *J Ethnopharmacol*. 2010;131(2):404-409. doi:10.1016/j.jep.2010.07.013
98. Ilmie MU, Jaafar H, Mansor SM, Abdullah JM. Subchronic toxicity study of standardized methanolic extract of *mitragyna speciosa* korth in sprague-dawley rats. *Front Neurosci*. 2015;9:1-6. doi:10.3389/fnins.2015.00189
99. Yusoff NHM, Mansor SM, Müller CP, Hassan Z. Opioid receptors mediate the acquisition, but not the expression of mitragynine-induced conditioned place

- preference in rats. *Behav Brain Res*. 2017;332:1-6. doi:10.1016/j.bbr.2017.05.059
100. Cunningham CL, Gremel CM, Groblewski PA. Drug-induced conditioned place preference and aversion in mice. *Nat Protoc*. 2006;1(4):1662-1670. doi:10.1038/nprot.2006.279
 101. Esmaeili MH, Kermani M, Parvishan A, Haghparast A. Role of D1/D2 dopamine receptors in the CA1 region of the rat hippocampus in the rewarding effects of morphine administered into the ventral tegmental area. *Behav Brain Res*. 2012;231(1):111-115. doi:10.1016/j.bbr.2012.02.050
 102. Westerink BHC, Kwint HF, DeVries JB. The pharmacology of mesolimbic dopamine neurons: A dual-probe microdialysis study in the ventral tegmental area and nucleus accumbens of the rat brain. *J Neurosci*. 1996;16(8):2605-2611. doi:10.1523/jneurosci.16-08-02605.1996
 103. Tan SE. Roles of hippocampal NMDA receptors and nucleus accumbens D1 receptors in the amphetamine-produced conditioned place preference in rats. *Brain Res Bull*. 2008;77(6):412-419. doi:10.1016/j.brainresbull.2008.09.007
 104. Trouche S, Koren V, Doig NM, et al. A hippocampus-accumbens tripartite neuronal motif guides appetitive memory in space. *Cell*. 2019;176(6):1393-1406.e16. doi:10.1016/j.cell.2018.12.037
 105. Taslimi Z, Arezoomandan R, Omranifard A, et al. Orexin A in the ventral tegmental area induces conditioned place preference in a dose-dependent manner: Involvement of D1/D2 receptors in the nucleus accumbens. *Peptides*. 2012;37(2):225-232. doi:10.1016/j.peptides.2012.07.023
 106. Lee RS, Steffensen SC, Henriksen SJ. Discharge profiles of ventral tegmental area GABA neurons during movement, anesthesia, and the sleep-wake cycle. *J Neurosci*. 2001;21(5):1757-1766. doi:10.1523/jneurosci.21-05-01757.2001
 107. Chatterjee M, Verma R, Ganguly S, Palit G. Neurochemical and molecular characterization of ketamine-induced experimental psychosis model in mice. *Neuropharmacology*. 2012;63(6):1161-1171. doi:10.1016/j.neuropharm.2012.05.041
 108. Sirota A, Csicsvari J, Buhl D, Buzsáki G. Communication between neocortex and hippocampus during sleep in rodents. *Proc Natl Acad Sci U S A*. 2003;100(4):2065-2069. doi:10.1073/pnas.0437938100
 109. Mitra A, Snyder AZ, Hacker CD, et al. Human cortical-hippocampal dialogue in wake and slow-wave sleep. *Proc Natl Acad Sci U S A*. 2016;113(44):E6868-E6876. doi:10.1073/pnas.1607289113
 110. Bamidis PD, Klados MA, Frantzidis C, et al. A framework combining delta event-related oscillations (EROs) and synchronisation effects (ERD/ERS) to study

- emotional processing. *Comput Intell Neurosci.* 2009;2009:1-16.
doi:10.1155/2009/549419
111. Herman JP, McKlveen JM, Ghosal S, et al. Regulation of the hypothalamic-pituitary- adrenocortical stress response. *Compr Physiol.* 2016;6(2):603-621.
doi:10.1002/cphy.c150015
 112. Wang JQ, McGinty JF. Differential effects of D1 and D2 dopamine receptor antagonists on acute amphetamine- or methamphetamine-induced up-regulation of zif/268 mRNA expression in rat forebrain. *J Neurochem.* 1995;65(6):2706-2715.
doi:10.1046/j.1471-4159.1995.65062706.x
 113. Bantick RA, De Vries MH, Grasby PM. The effect of a 5-HT1A receptor agonist on striatal dopamine release. *Synapse.* 2005;57(2):67-75. doi:10.1002/syn.20156
 114. Salgado S, Kaplitt MG. The nucleus accumbens: A comprehensive review. *Stereotact Funct Neurosurg.* 2015;93(2):75-93. doi:10.1159/000368279
 115. Vijeepallam K, Pandey V, Murugan DD, Naidu M. Methanolic extract of *Mitragyna speciosa* Korth leaf inhibits ethanol seeking behaviour in mice: Involvement of antidopaminergic mechanism. *Metab Brain Dis.* 2019;34:1712-1722.
doi:10.1007/s11011-019-00477-2
 116. Pandey V, Narasingam M, Mohamed Z. Antipsychotic-like activity of Noni (*Morinda citrifolia* Linn.) in mice. *BMC Complement Altern Med.* 2012;12.
doi:10.1186/1472-6882-12-186
 117. Pandey V, Narasingam M, Kunasegaran T, Murugan DD, Mohamed Z. Effect of noni (*Morinda citrifolia* Linn.) Fruit and its bioactive principles scopoletin and rutin on rat vas deferens contractility: An Ex vivo study. *Sci World J.* 2014;2014.
doi:10.1155/2014/909586
 118. Samerphob N, Cheaha D, Issuriya A, et al. Changes in neural network connectivity in mice brain following exposures to palatable food. *Neurosci Lett.* 2020;714:1-7.
doi:10.1016/j.neulet.2019.134542
 119. Oliveira JF, Dias NS, Correia M, et al. Chronic stress disrupts neural coherence between cortico-limbic structures. 2013;7:10-12. doi:10.3389/fncir.2013.00010
 120. Hasler G, Veen JW Van Der, Ph D, et al. Effect of acute psychological stress on prefrontal GABA concentration determined by proton magnet. 2010;(October):1226-1232.
 121. Losada MEO. Changes in central GABAergic function following acute and repeated stress. *Br J Pharmacol.* 1988;93(3):483. doi:10.1111/J.1476-5381.1988.TB10302.X
 122. Mark GP, Rada P V., Shors TJ. Inescapable stress enhances extracellular acetylcholine in the rat hippocampus and prefrontal cortex but not the nucleus

- accumbens or amygdala. *Neuroscience*. 1996;74(3):767-774. doi:10.1016/0306-4522(96)00211-4
123. Belujon P, Grace AA. Hippocampus, amygdala, and stress: Interacting systems that affect susceptibility to addiction. *Ann N Y Acad Sci*. 2011;1216(1):114-121. doi:10.1111/j.1749-6632.2010.05896.x
 124. Battaglia FP, Sutherland GR, McNaughton BL. Local sensory cues and place cell directionality: Additional evidence of prospective coding in the hippocampus. *J Neurosci*. 2004;24(19):4541-4550. doi:10.1523/JNEUROSCI.4896-03.2004
 125. Jones MW, Wilson MA. Theta rhythms coordinate hippocampal-prefrontal interactions in a spatial memory task. *PLoS Biol*. 2005;3(12):e402. doi:10.1371/journal.pbio.0030402
 126. Zhou Y, Yan E, Cheng D, et al. The projection from ventral CA1, not prefrontal cortex, to nucleus accumbens core mediates recent memory retrieval of cocaine-conditioned place preference. *Front Behav Neurosci*. 2020;14:1-13. doi:10.3389/fnbeh.2020.558074
 127. Lansink CS, Goltstein PM, Lankelma J V, Mcnaughton BL, Pennartz CMA. Hippocampus leads ventral striatum in replay of place-reward information. *PLoS Biol*. 2009;7(8):1000173. doi:10.1371/journal.pbio.1000173
 128. Ito R, Robbins TW, Pennartz CM, Everitt BJ. Functional interaction between the hippocampus and nucleus accumbens shell is necessary for the acquisition of appetitive spatial context conditioning. *J Neurosci*. 2008;28(27):6950-6959. doi:10.1523/JNEUROSCI.1615-08.2008
 129. Berke JD. Fast oscillations in cortical-striatal networks switch frequency following rewarding events and stimulant drugs. *Eur J Neurosci*. 2009;30(5):848-859. doi:10.1111/j.1460-9568.2009.06843.x
 130. Curic S, Andreou C, Nolte G, et al. Ketamine alters functional gamma and theta resting-state connectivity in healthy humans: Implications for schizophrenia treatment targeting the glutamate system. *Front Psychiatry*. 2021;12(June):1-13. doi:10.3389/fpsy.2021.671007
 131. Menne V, Chesworth R. Schizophrenia and drug addiction comorbidity: Recent advances in our understanding of behavioural susceptibility and neural mechanisms. *Neuroanat Behav*. 2020;2:e10. doi:10.35430/nab.2020.e10
 132. Li F, Fang Q, Liu Y, et al. Cannabinoid CB1 receptor antagonist rimonabant attenuates reinstatement of ketamine conditioned place preference in rats. *Eur J Pharmacol*. 2008;589(1-3):122-126. doi:10.1016/j.ejphar.2008.04.051
 133. Lorrain DS, Bacceti CS, Bristow LJ, Anderson JJ, Varney MA. Effects of ketamine and N-methyl-D-aspartate on glutamate and dopamine release in the rat prefrontal

cortex: Modulation by a group II selective metabotropic glutamate receptor agonist LY379268. *Neuroscience*. 2003;117(3):697-706. doi:10.1016/S0306-4522(02)00652-8

Appendices

Appendix A
Original article



Contents lists available at ScienceDirect

Neuroscience Letters

journal homepage: www.elsevier.com/locate/neulet

Research article



Spectral power and theta-gamma coupling in the basolateral amygdala related with methamphetamine conditioned place preference in mice

Jakkrit Nukitram^{a,c}, Dania Cheaha^{b,c}, Ekkasit Kumarnsit^{a,c,*}

^a Physiology Program, Division of Health and Applied Sciences, Faculty of Science, Prince of Songkla University, Hatyai Campus, Hatyai, Songkhla, 90110, Thailand

^b Biology Program, Division of Biological Science, Faculty of Science, Prince of Songkla University, Hatyai, Songkhla, 90112, Thailand

^c Biosignal Research Center for Health, Faculty of Science, Prince of Songkla University, Hatyai, Songkhla, 90112, Thailand

ARTICLE INFO

Keywords:

Basolateral amygdala
Conditioned place preference
Local field potential
Methamphetamine
Theta-gamma coupling

ABSTRACT

The basolateral amygdala (BLA) plays a crucial role in conditioned place preference (CPP) for addictive drugs. However, neural signaling associated with methamphetamine (METH) craving and seeking remained to be investigated. This study characterized local field potential (LFP) oscillatory patterns in the BLA and conditioned place preference induced by METH-related context. Male Swiss albino ICR mice were deeply anesthetized for LFP intracranial electrode implantation in the BLA. Control and METH groups received sessions to learn to associate saline-paired and METH-paired compartments of the CPP apparatus with saline and METH injections, respectively, for 10 days. LFP signals and exploring behavior were recorded simultaneously during pre- and post-conditioning phases. Time spent in METH-paired compartment was normalized and expressed as CPP scores. Fast Fourier Transform (FFT) algorithm was used to analyze LFP powers of 8 discrete frequency ranges (delta, theta, alpha, beta, gamma I-IV). During post-conditioning phase of METH CPP with METH cues, statistical analysis revealed that METH group significantly increased time spent in METH-paired compartment. Significant suppressions of theta and alpha powers were observed. Phase-amplitude cross frequency coupling analyses confirmed significant increases in maximal modulation index (MI), frequency for phase of slow wave and MI of theta-gamma II coupling. Taken together, LFP oscillation in the BLA was sensitive in association with METH CPP. These research findings might suggest the underlying mechanisms of drug reward learning and adaptive changes in the BLA in acquisition of METH CPP and dependence.

1. Introduction

The mesolimbic dopaminergic (DA) system with DA cell bodies located in the ventral tegmental area (VTA) is known to play a crucial role in addictive functions and pleasure behaviors. Fundamentally, several brain regions including the medial prefrontal cortex (mPFC), nucleus accumbens (NAc), hippocampus (HP), and the amygdala (AMY) are primarily innervated by DA pathways from the VTA [1]. In human, emotion and cognition were interrelated with neural processing from the AMY [2]. However, the feature of the AMY is not a complete single unit. Apparently, it comprises sub-regions e.g. the centromedial nuclei

(CMA) or basolateral nuclei (BLA) [3].

Neural processing in the BLA is related with reward learning and addiction [4]. Previously, permanent BLA lesion disrupted the effect of conditioned-cued reinstatement in cocaine self-administration. The attenuation of reinstatement was observable in a classical interference method that inactivated the BLA by using D1 receptor antagonist. This effect was reversible by intra-infusion of amphetamine, a psychostimulant drug, to the BLA directly [5,6]. It was found that decreased BLA activity by intra-injection with AP5, an NMDA receptor antagonist, was capable to block amphetamine conditioned place preference (CPP) acquisition and extinction [7]. These collective findings indicated that

Abbreviations: ANOVA, analysis of variance; AMY, amygdala; AP, antero-posterior; ARRIVE, Animal Research: Reporting of *in vivo* Experiments; BLA, basolateral amygdala; BSAFs, brain stress-activating factors; CFC, cross-frequency coupling; CMA, centromedial amygdala; CPP, conditioned place preference; D1, dopamine receptor type 1; DA, dopaminergic; DV, dorso-ventral; FFT, fast Fourier transform; HP, hippocampus; LFP, local field potential; METH, methamphetamine; MI, modulation index; ML, medio-lateral; mPFC, medial prefrontal cortex; NAc, nucleus accumbens; NaCl, sodium chloride; NOR, norepinephrine; PAC, phase-amplitude coupling; PSD, power spectral density; SEM, Standard Error Mean; VTA, ventral tegmental area.

* Corresponding author at: Physiology program, Division of Health and Applied Sciences, Faculty of Science, Prince of Songkla University, Hatyai Campus, Hatyai, Songkhla, 90110, Thailand.

E-mail address: kumarnsit.e@gmail.com (E. Kumarnsit).

<https://doi.org/10.1016/j.neulet.2021.135939>

Received 9 March 2021; Received in revised form 25 April 2021; Accepted 29 April 2021

Available online 1 May 2021

0304-3940/© 2021 Elsevier B.V. All rights reserved.

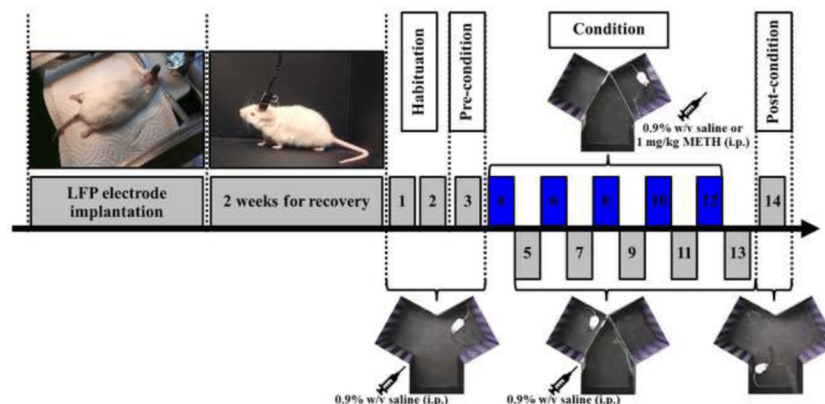


Fig. 1. The protocol for characterization of LFP pattern and PAC rhythm in the BLA of mice in METH-induced CPP. Animals were handled through the processes of electrode implantation, recover period and 3 phases of a CPP paradigm: habituation and pre-conditioning, conditioning, and post-conditioning phases during day 1-3, 4-13, and 14, respectively.

the BLA plays a critical role in neural mechanisms associated with some aspects of drug addiction and craving.

Although a significant role of the BLA engaged with addictive activities has been proposed, modulation of the BLA that facilitates drug seeking behaviors remained to be explored. Basically, most of previous studies were performed by using molecular techniques which the data outputs were limited in terms of temporal resolution and sensitivity. For example, it is impractical for the detection of brain activity modulated within a time fraction in milliseconds. Therefore, the solution of this problem has already been addressed by the previous demonstration using electrical brain wave recording and analyses [8].

Fundamentally, electrical transmission is a predominant feature of brain communication. Neuronal responses produced by substances such as drugs or neurotransmitters are mostly generated from interaction between functional domains of various biomolecular molecules (e.g. receptors, channels, enzymes) [9]. These substances change downstream signaling pathway modulation, alternate ion conductance pattern of neurons (e.g., increase or decrease firing rate) and elicit local field potential (LFP). Actually, LFP signal can be recorded, analyzed and depicted in various aspects such as LFP power and phase-amplitude coupling (PAC) which are extensively used to identify clinical profiles of drugs of interest in rodents [10] and human [11]. Moreover, unique LFP patterns can also be used to reflect and represent specific condition of stimulation or some certain tasks performed. Previously, elevated LFP powers in delta and theta bands as well as theta-high gamma PAC in the hippocampal CA1 of mice were detected in response to repeated chocolate consumptions [12]. Moreover, mPFC oscillation in theta and gamma frequency bands and theta-high gamma PAC were associated with heroin addiction validated by CPP behavioral method [13].

Altogether, several experiments were carried out by using CPP paradigm according to its highly standardized quality for testing addictive properties of drug candidates [14]. In particular, it has been widely used as a reliable model in animals for investigating brain mechanisms associated with drug seeking and rewarding behavior in laboratory animals induced by various psychomotor stimulants such as amphetamine, cocaine and methamphetamine (METH) [15–17]. For better understanding of addiction brain mechanism, it was important to characterize the LFP oscillation in the BLA related with METH seeking behavior. Therefore, this study aimed to investigate LFP spectral powers and PAC pattern in the BLA of mice using METH CPP paradigm.

2. Materials and methods

2.1. Animals

This animal study was conducted under the guidelines of the European Science Foundation (Use of Animals in Research, 2001) and ARRIVE (Animal Research: Reporting of *in vivo* Experiments) for the protection of animals used in scientific research. The experimental procedures and protocols were approved by the Institute Animal Care and Use Committee, Prince of Songkla University [project license number: MHESI 6800.11/845 and reference number: 57/2019]. Male Swiss albino ICR mice (7–8 weeks old) were obtained from the National Laboratory Animal Center, Mahidol University, Thailand. In order to acclimatize and minimize animal stress, all animals were pre-handled for one week prior to the initial of the experiment at the Southern Laboratory Animal Facility, Prince of Songkla University. The animals were housed in the individual stainless-steel cage ($17 \times 28.5 \times 17$ cm) with standard environment (12/12 h light/dark cycle, 22 ± 3 °C and 55 ± 10 % relative humidity). Commercial food pellets and water were available *ad libitum*. All experiments were carried out between 8 a.m. and 4 p.m.

2.2. Drugs and chemicals

METH hydrochloride was provided by the Food and Drug Administration, Thailand with a standard purity (95.8 %) for research purpose. In addition, METH at 1 mg/kg diluted in physiological saline solution (0.9 % w/v NaCl) was intraperitoneally injected with fixed volume per body weight of mice at 10 mL/kg. The concentration of METH was selected in accordance to dose that definitely produced conditioned place preference in this strain of mice [16].

2.3. Animal surgery for implanting the LFP electrodes

The process of intracranial electrode implantation has already been described previously [18]. At the start of the experiment, animals were approximately 4 months after birth with body weight 45.0 ± 2.4 g. They were deeply anesthetized with intraperitoneal injection of 16 mg/kg xylazine hydrochloride (Xylavet, Sigma-Aldrich International GmbH, Switzerland) and 50 mg/kg zolotil (Tiletamine – zolazepam, Vibac AH,

Inc., USA) cocktail. Following a period of unconsciousness, animal's heads were then fixed with stereotaxic apparatus. Lignocaine (20 mg/mL) (Lidocaine, M & H manufacturing Co., Ltd., Thailand), a local analgesic drug, was administered subcutaneously before making the midline incision of the scalp on the dorsal head to expose the skull. The position on the skull above the BLA was marked for drilling hole. Therefore, the electrode was stereotaxically positioned on the left hemisphere of the brain defined from bregma to the BLA (AP; -1.7 mm, ML; 3 mm; DV; 4.8 mm) according to the mouse brain atlas [19]. The reference that was also used as ground electrode was implanted on the skull at midline over the cerebellum (AP; -6.0 mm, ML; 0.0 mm; DV; 1.5 mm). Additional holes were drilled for stainless steel screws as anchors for extra stability. All silver wire electrodes (0.381 mm in diameter) were secured for permanent in place with dental acrylic (Unifast Trad, GC Dental Industrial Corp., Tokyo, Japan). The antibiotic ampicillin (100 mg/kg) (General Drug House Co., Ltd., Bangkok, Thailand) was applied intramuscularly once a day for 3 days to prevent infection. The animals were allowed to fully recover in individual cage for at least 2 weeks before the start of the experiment.

2.4. CPP apparatus and paradigm

CPP paradigm has been employed to assess environment-induced drug seeking behaviors in laboratory animals. The CPP apparatus was modified from the previous study [20] and made from plexiglass in a Y-shape (Fig. 1). There were 3 rectangular compartments (25cm × 18cm × 25 cm) connected with and separated from each other by removing or placing removable walls between each compartments and triangular central zone. Two compartments located laterally had the identical shape and size to that of central zone, but they had different floor textures and wall shading. One of the lateral compartments had

vertical strips lined on the wall and smooth floor. The other lateral compartment had grid strips attached to the wall and textured floor. The third compartment on the base was a neutral zone used as a starting position of the animal exploration. Overall time schedule of drugs injection was modified from the recent study [16]. The protocol of experiment was shown in time sequence (Fig. 1). In brief, CPP paradigm primarily began with habituation and continued with 3 phases of CPP which included pre-conditioning, conditioning, and post-conditioning phases.

2.4.1. Habituation and pre-conditioning phase

Animals were acclimatized with experimental room. They were brought to place in the room for at least 30 min prior to the start of the experiments. During the habituation (day 1 and 2), animals were intraperitoneally injected with normal saline solution and immediately placed to the starting position in the chamber. Then, animals were individually allowed to explore all compartments of the CPP apparatus freely for 15 min. During a period of pre-conditioning (day 3), the animals were treated and trained in the same manner to the habituation periods. Time that animals spent in each compartment was assessed and expressed as CPP score. CPP score each animal was calculated by subtraction of time that each animal spent in METH-paired compartment with time spent in normal saline-paired compartment. Tossing a coin was a method to divide all mice into 2 sub-groups to receive either normal saline or METH. Moreover, 2 sides of compartment were randomly paired with METH or saline to avoid bias.

2.4.2. Conditioning phase

Conditioning phase was taken for 10 consecutive days (day 4–13). Mice of METH group (n = 7) were given METH and saline injection in alternative days (1 mg/kg METH on odd day and saline on even day

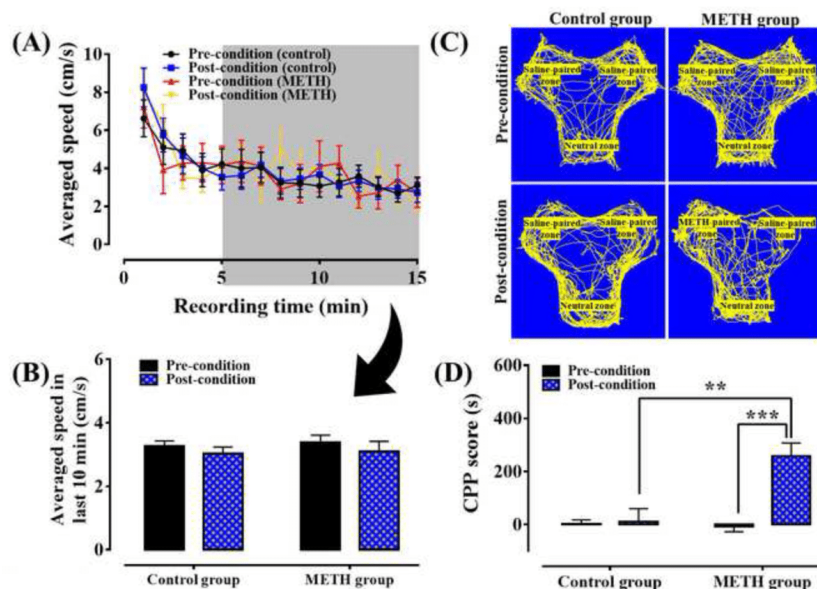


Fig. 2. Locomotor activity of animals in a CPP apparatus, Averaged speed during pre-conditioning and post-conditioning phases of control (n = 10) and METH (n = 7) groups were monitored. Values were calculated every 1-min bin (A). Averaged speed during 5–15 min were selected for investigation (B). Locomotor tracking of exploratory behavior of representative mice (C) and averaged CPP scores (D) of control and METH groups during pre- and post-conditioning phases in CPP apparatus are shown. Data were expressed as mean ± SEM. **, *** $P < 0.01$, 0.001 for comparisons with each paired result.

during this phase). Subsequently, they were confined to the assigned compartment for 30 min to learn to pair with different treatments (METH and saline) and specific details of the assigned compartments. On the other hand, control mice ($n = 10$) were administered with normal saline every day for both compartments. After animals completed the session in each day, they were moved back to their home cage.

2.4.3. Post-conditioning phase

Post-conditioning phase was done on day 14 (post-conditioning day1). The procedure of this phase was the same to that of pre-conditioning phase. For testing, mice from both groups were given neither METH nor normal saline. They were individually allowed to survey the entire CPP apparatus freely for 15 min. After that, the calculation of CPP score was carried out.

2.5. Recording of LFP signals and animal locomotor activity

LFP signals and locomotor activities of individual animals were recorded simultaneously during pre-conditioning and post-conditioning phases. For LFP signal recording, after 50 Hz power line and spontaneously electrical artifact rejection, signals were harvested with 1.024 s duration in sweeps and size of sampling frequency was 2 kHz. Therefore, sampling frequency was 2.048 kHz which was well over the Nyquist sampling rate. All LFP signals were amplified with low-pass 1 kHz and high-pass 0.3 Hz by Dual Bio Amp (AD Instruments, Castle Hill, NSW, Australia). The conversion from analog signals to digital data was performed by a PowerLab 16/35 system (AD Instruments, Castle Hill, NSW, Australia) with 16-bit A/D. LFP signal analysis was processed through 1–100 Hz band-pass digital filtering. For locomotor activity,

spontaneous animal movement was captured by webcam camera vertically fixed on the top of recording chamber. All data were deposited in a computer through LabChart 7.3.7 pro software. Data were specifically selected during 5–15 min of this recording to monitor LFP oscillations and PAC patterns of mice under addictive state induced by METH treatment.

2.5.1. Locomotor activity analysis

The analysis of locomotor activities of animals was validated by using open source toolbox OptiMouse [21] to capture body position of mice. The alternations of locomotor activity in assigned time period and time spent in each compartments of the apparatus were illustrated and expressed as mean \pm Standard Error Mean (SEM).

2.5.2. LFP signal analysis

For data analysis, Fast Fourier Transform (FFT) algorithm (Hanning window cosine transform) with 50 % window overlap and 0.976 Hz of power spectra resolution was used for generating power spectral density (PSD) from digitized data stored in a PC via the LabChart 7.3.7 pro software. Subsequently, each discrete frequency band of the PSD was averaged and depicted as log percentage total power in frequency domains with 8 defined signal frequency ranges (delta: 1.0–3.9 Hz, theta: 4.7–8.7 Hz, alpha: 9.8–12.7 Hz; beta: 13.6–29.3 Hz, gamma I-IV: 30–90 (increase in 15 Hz in order))

Cross-frequency coupling (CFC) was used for evaluating the interactions between different frequency ranges of neural signal. This study focused on phase-amplitude coupling (PAC), one of the most common representatives of CFC, to analyze the strength of coupling between 2 frequency bands of interest. The results were expressed as modulation index (MI) extracted from comodulograms or coupling maps

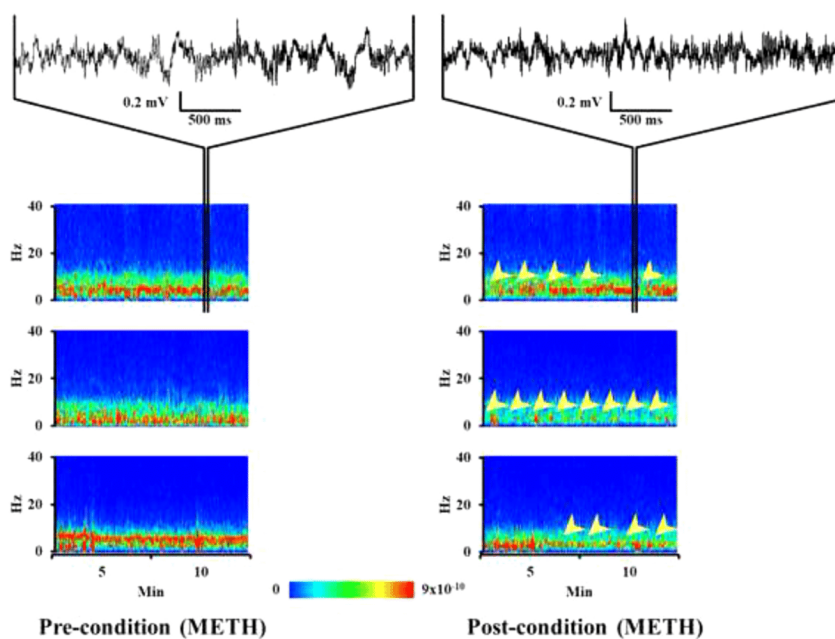


Fig. 3. Raw LFP signals of representative mice during pre-conditioning (A) and post-conditioning phases (B) of METH group. Raw signals were also converted and shown in spectrograms (lower panels). Frequency spectral power was demonstrated with color code. Blue and red colors represented the lowest and highest LFP powers, respectively. Arrow heads are used to indicate the disappearance of slow frequency oscillations particularly in theta and alpha ranges.

to present faster wave amplitude driven by slower frequency phase. Therefore, PAC was deployed to analyze LFP data during drug seeking behaviors. Theta-gamma coupling was specifically focused. All raw data were run via toolbox Brainstorm3 [22].

2.6. Statistical analyses

All parameters were shown and analyzed as mean \pm Standard Error Mean (SEM). All parameters were processed under the function of two-way repeated measure analysis of variance (ANOVA). Conditioning states or trials were used as within-subject factors, and with or without METH treatment considered as inter-subject factors defined as group. A P -value < 0.05 was defined statistically significant.

3. Results

3.1. Locomotor activity

Locomotor activity was monitored during a period of 15 min recording. Data were analyzed for a parameter of locomotor speed (Fig. 2A). Values during pre- and post-conditioning phases of control and METH groups were shown. The results showed high fluctuations particularly during the early period. The speed levels were relatively stable at the middle to the end of recording period of both control and METH groups. Statistical analysis revealed non-significant differences between groups and between pre- and post-conditioning phases (Fig. 2B). Therefore, raw signals from a period of 5–15 min recording were selected for analyses of all data in this study.

3.2. METH conditioned place preference

Times spent of animals in saline-paired and METH-paired

compartments during pre- and post-conditioning phases of control and METH groups were analyzed. During pre-conditioning phase, both control and METH animals explored all compartments relatively evenly. No obvious side preference in their exploratory patterns was seen (Fig. 2C). However, during post-conditioning phase, control group remained the same pattern of exploration whereas METH group clearly showed side preference for METH-paired compartment. Therefore, time spent values were converted into CPP scores and statistically analyzed. During pre-conditioning phase, control and METH groups had CPP score at 1.59 ± 16.03 s and -6.70 ± 20.42 s, respectively. During post-conditioning phase, control and METH groups produced CPP scores at 10.07 ± 50.20 s and 258.48 ± 48.83 s, respectively. Two-way repeated measure ANOVA revealed significant effects of trial [$F(1, 15) = 13.712, p = 0.002$], group [$F(1, 15) = 11.334, p = 0.004$] and group \times trial interactions [$F(1, 15) = 12.065, p = 0.003$]. Multiple comparisons revealed significant increases in CPP score during post-conditioning phase of METH group compared to pre-conditioning phase of METH group [$F(1, 15) = 21.888, p < 0.001$] and post-conditioning phase of control group [$F(1, 15) = 13.145, p = 0.002$] (Fig. 2D). No significant difference was found between pre- and post-conditioning phases of control group and between pre-conditioning phases of control and METH groups. Altogether, the present data confirmed the establishment of METH conditioned place preference.

3.3. LFP spectral powers in the BLA of METH conditioned place preference

Visual inspection was performed to observe the oscillatory patterns of raw LFP signals and spectrograms during pre- and post-conditioning phases (Fig. 3). Baseline LFP patterns of pre-conditioning phase were shown with normal components of frequency activity. During post-conditioning phase, slow wave activities were absent intermittently

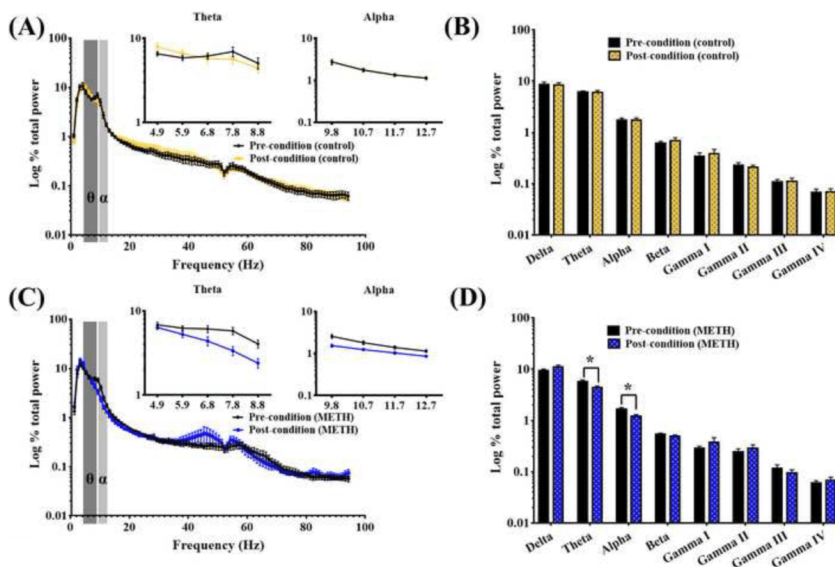


Fig. 4. Averaged LFP spectral powers of control (A) and METH groups (C). Data were normalized as percent total power and illustrated in log scale. Theta and alpha powers were depicted in small sub-plots. LFP powers of control (B) and METH groups (D) were divided into 8 discrete frequency bands ranging from delta (1.0–3.9 Hz), theta (4.7–8.7 Hz), alpha (9.8–12.7 Hz), beta (13.6–29.3 Hz), and gamma I–IV (30–90 Hz with increase in 15 Hz in order). Data were expressed as mean \pm SEM. Asterisks indicate significant differences at $^* P < 0.05$ performed by two-way repeated measure ANOVA.

from time domain signals of METH groups. No obvious change between pre- and post-conditioning phases was seen in control group. Therefore, LFP signals were transformed into frequency domain for quantitative analysis as LFP spectral powers (Fig. 4A and C for control and METH groups, respectively). Two-way repeated measures ANOVA demonstrated significant effects of trial [$F_{(1, 15)} = 4.776, p = 0.045$] and trial x group interactions [$F_{(1, 15)} = 5.342, p = 0.035$] but not effects of group on theta wave. Moreover, significant effect was found only on trial [$F_{(1, 15)} = 5.714, p = 0.030$] of alpha wave. Control group did not show any significant change following conditioning paradigm (Fig. 4B). In METH group, significant decreases in theta [$F_{(1, 15)} = 8.593, p = 0.010$] and alpha [$F_{(1, 15)} = 6.220, p = 0.025$] frequency powers during post-conditioning phase compared to pre-conditioning levels were seen (Fig. 4D). Taken together, the present data indicated specific changes in theta and alpha frequency ranges in the BLA during post-conditioning phase of METH CPP.

3.4. Phase-amplitude coupling in the BLA of METH conditioned place preference

Comodulograms of PAC from the BLA of mice during pre-conditioning and post-conditioning phases were visualized. In control group, no obvious change was seen. In METH group, different patterns between comodulograms of pre-conditioning and post-conditioning phases were found (Fig. 5A). Two-way repeated measures ANOVA demonstrated significant influence of trial [$F_{(1, 15)} = 15.195, p = 0.001$], group [$F_{(1, 15)} = 11.488, p = 0.004$], and trial x group interactions [$F_{(1, 15)} = 11.039, p = 0.005$] on maximal modulation index (MI). Pairwise

comparisons revealed significant increases in MI during post-conditioning phase compared to pre-conditioning phase of METH group [$F_{(1, 15)} = 24.620, p < 0.001$] and post-conditioning phase of control group [$F_{(1, 15)} = 12.254, p = 0.003$] (Fig. 5B). No significant difference was observed between pre-conditioning and post-conditioning phases of control group and between pre-conditioning phases of control and METH groups.

Additionally, significant effects of trial [$F_{(1, 15)} = 5.498, p = 0.033$], and trial x group interactions [$F_{(1, 15)} = 5.498, p = 0.033$], but not the effects of group, were seen in frequency for phase of slow wave. Multiple comparisons confirmed significant increase in METH group during post-conditioning phase compared to pre-conditioning phase [$F_{(1, 15)} = 10.386, p = 0.006$] and compared to post-conditioning phase of control group [$F_{(1, 15)} = 9.476, p = 0.008$] (Fig. 5C).

The analysis of frequency for amplitude of fast wave revealed a significant effect of group [$F_{(1, 15)} = 4.735, p = 0.046$] but not trial [$F_{(1, 15)} = 0.094, p = 0.764$] and trial x group interactions [$F_{(1, 15)} = 2.580, p = 0.129$]. Multiple comparisons indicated significant difference in frequency for amplitude of fast wave between post-conditioning levels of METH and control groups [$F_{(1, 15)} = 9.173, p = 0.008$] but not within any group (Fig. 5D).

Therefore, broad frequency ranges for phase and amplitude were sub-divided for testing PAC induced during post-conditioning phase. Frequency for phase was focused on theta and alpha ranges whereas frequency for amplitude was focused on gamma I, II and III. MI values were analyzed. The results displayed no significant difference between MI values of pre- and post-conditioning phases in control group (Fig. 6A–I). However, two-way repeated measure ANOVA revealed a

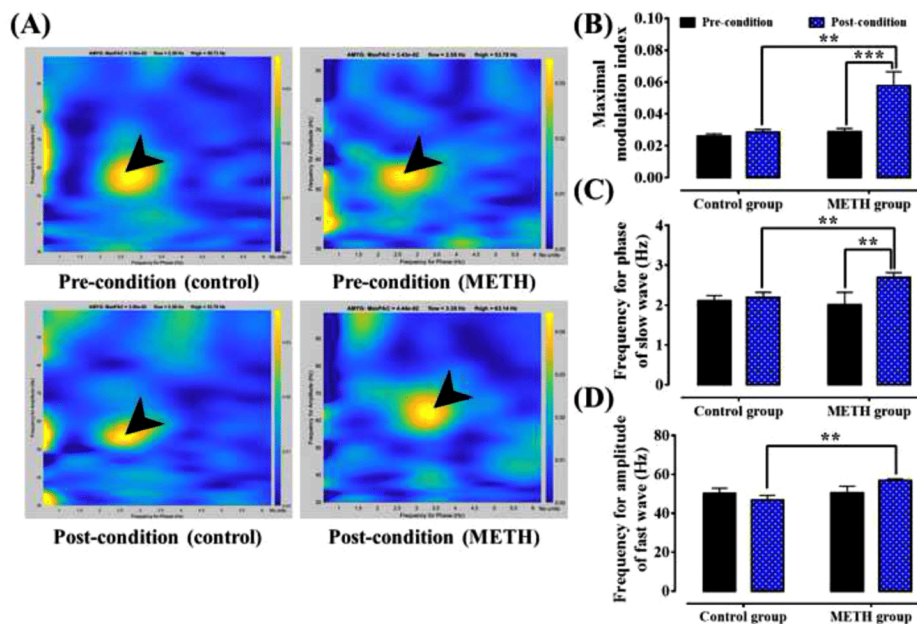


Fig. 5. Phase-amplitude cross (PAC) frequency couplings of METH group. Comodulograms of PAC in the BLA of representative mouse from control (left panel) and METH group (right panel) during pre-conditioning (top panel) and post-conditioning phase (bottom panel) are shown. Black arrows indicate the maximal modulation indices in each condition (A). PAC values were analyzed in terms of maximal modulation index (B), frequency for phase of slow oscillation (C), and frequency for amplitude of fast wave activity (D) extracted from comodulograms. All data were expressed as mean \pm SEM. A two-way repeated measure ANOVA was performed, ** $p < 0.01$, *** $p < 0.001$.

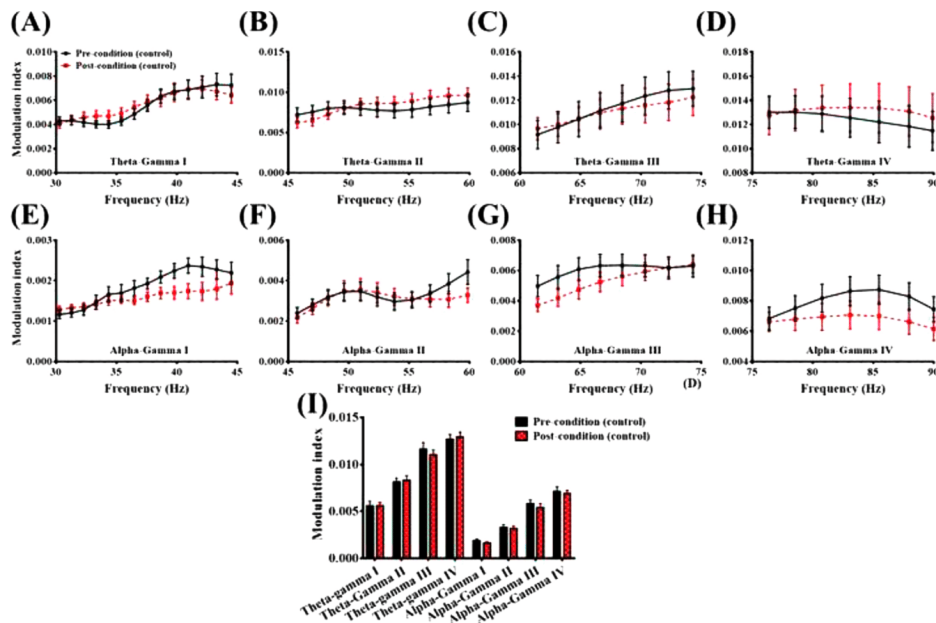


Fig. 6. Modulation indices of the BLA of control group during pre-conditioning and post-conditioning phases, Line graphs of modulation indices calculated from multiple couplings of frequency for amplitude of faster wave (gamma I–IV) (A–H) driven by phase of theta wave (A–D) and alpha wave (E–H), respectively. Modulation indices of each couplings were averaged and expressed as bar graphs for statistical analysis (I). Data are shown as mean \pm SEM and analyzed by two-way repeated measure ANOVA.

significant influence of trial [$F_{(1, 15)} = 10.670, p = 0.005$] but not trial \times group interaction [$F_{(1, 15)} = 2.830, p = 0.113$] and group [$F_{(1, 15)} = 0.259, p = 0.618$] on theta-gamma II (45–60 Hz) PAC. Moreover, a significant difference was seen in theta-gamma II [$F_{(1, 19)} = 8.294, p = 0.010$], but not other PAC couplings of METH group (Fig. 7A–D). The MI value of theta-gamma II was significantly increased during post-conditioning phase compared to pre-conditioning level. Altogether, these results indicated the enhanced MI of theta-gamma II PAC in the BLA of mice associated with METH CPP.

4. Discussion

The present study demonstrated METH CPP and changes in LFP activities of the BLA following repeated sessions of METH administration in CPP paradigm. METH CPP scores clearly confirmed addictive property of the drug. The increased time spent in METH-paired compartment induced by METH related cues in the CPP chamber was similar to that produced by standard drugs such as cocaine [15], heroin [23] or amphetamine [17]. The CPP score of METH and changes in LFP oscillatory pattern in the BLA were highlighted as neural processing of METH CPP through associative learning.

Basically, the BLA has a close functional connection with the mesolimbic DA system for neural processing in response to reward-related stimuli. Previously, a disruption of the brain reward circuitry was found to result in mood disorders [1]. Several experiments have been conducted to demonstrate a critical role of the BLA in addiction. Altogether, alleviation of drug-seeking behaviors was correlated with the BLA activity suppression [5–7]. The present data highlighted the decreased theta and alpha spectral powers and the increased MI of

theta-gamma II cross frequency coupling in the BLA. It is likely that these LFP oscillatory patterns would predict drug craving and seeking.

The expression of METH CPP was believed to be induced by memory-associated cue of METH administration. Basically, locomotor movement induced by psychostimulant drugs could interfere CPP outcomes. Previously, the fluctuation of animals' movement was found to have impacts on LFP signal generation and oscillation [24]. Therefore, data recorded during a stable period of 5–15 min were selectively analyzed.

Apart from the direct effect of addictive drugs, there are factors that facilitate addiction such as genetic vulnerability of the users and drug-associated conditions [25]. In particular, the latter factor is powerful for reward learning process of addictive drugs. Previously, the BLA was engaged with the reconsolidation of drug-associated memories [26]. It was involved in cocaine-related memory reconsolidation [27]. Moreover, the relationship between BLA action and drug seeking behaviors induced by drug related cue has been evidenced [28]. By using the CPP paradigm, the contextual cues of drug (e.g. drug paraphernalia) were demonstrated to elicit craving [29]. This could explain why the increase in CPP score was produced by METH associated cues during post-conditioning phase.

Side preference evaluated by METH CPP method in the present study may be related with neuroadaptive mechanism following repeated administrations of METH in the paradigm. Multiple brain mechanisms in response to learning process of drug-environment pairing have been well documented. During the development of drug dependence, neurochemical dysregulations including structural and functional changes in the reward brain circuits were observed [30]. The brain stress-activating factors (BSAFs) released from the AMY (e.g. corticotropin-releasing factor and norepinephrine (NOR)) was found to elicit negative

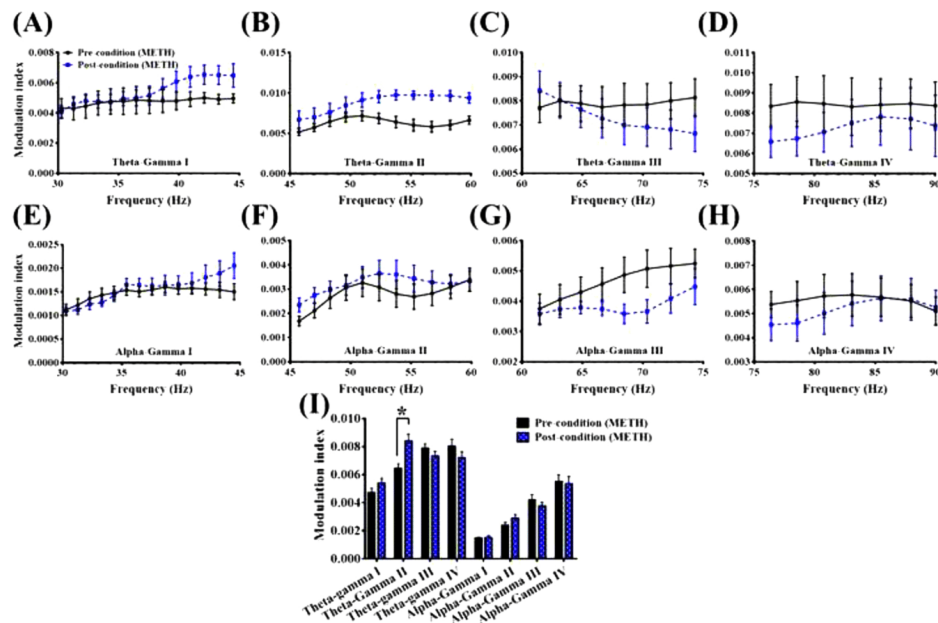


Fig. 7. Modulation indices of the BLA of METH group during pre-conditioning and post-conditioning phases. Line graphs of modulation indices calculated from multiple couplings of frequency for amplitude of faster wave (gamma I–IV) (A–H) driven by phase of theta wave (A–D) and alpha wave (E–H), respectively. Modulation indices of each couplings were averaged and expressed as bar graphs for statistical analysis (I). Data are shown as mean \pm SEM and analyzed by two-way repeated measure ANOVA, * $P < 0.05$.

emotional state and promote addiction, respectively [31]. It is possible that METH produces CPP through these mechanisms after repeated METH exposures until withdrawal in physiological adaptation to maintain hedonic homeostasis.

The present study highlighted the LFP oscillation and PAC rhythm of the BLA in response to METH CPP. Normally, the specific patterns of brain oscillation are known to reflect unique neuronal functions related with task performance [12,13]. LFP oscillatory patterns are widely used to specify clinical profiles of some drugs of interest that act on the CNS both in animals and human [10,11]. Previously, theta frequency oscillation was believed to mediate encoding of working and episodic memory and retrieval processes [32]. Multiple brain regions were interconnected in synchronization with theta frequency range to integrate spatial information transmission [33,34]. The AMY was demonstrated to produce and release NOR, one of BSAs, mostly during dependence or withdrawal periods [31]. Moreover, adrenergic alpha2 receptor activity was correlated with theta wave function [35]. Therefore, the decrease in theta power during post-conditioning phase might be related with change in adrenergic alpha2 receptor activity to modulate cognitive function, sleep, anxiety, and aches during withdrawal period [36,37].

Alpha power was decreased during post-conditioning phase. Normally, alpha oscillation can be observed in various brain regions including the amygdala and its functional roles have been proposed. Basically, it is involved in processing emotional information, filtering of inhibitory input of selective attention and probably supporting cognitive function [38,39]. Previously, METH was found to impair spatial learning and memory process in rodent [40]. Reduced alpha power during post-conditioning phase might be one of METH direct effects that could

affect learning. The CPP paradigm is practical to directly monitor that METH group accessed METH-paired compartment as a side preference. These phenomena may be resulted from the ideal concept that brain is capable to maintain homeostasis and dampen drug reward effects in adaptation to disturbances automatically [41,42].

Phase-amplitude coupling (PAC), one of the most studied type of cross frequency coupling, was analyzed following METH repeated exposures in the CPP paradigm. The increase in theta-gamma sub-band II (45–60 Hz) was observed. Actually, theta-gamma PAC has been mainly recognized as a key maker of neural processing that supports learning and memory both in animals [43] and human [44] and appeared to be associated with memory formation and synaptic plasticity [45]. So far, the important role of theta-gamma coupling in the brain reward circuits implicated with drug dependence has not been well described. Previously, neural communication between the BLA and the mPFC via glutamatergic neurons was also detected in particular [46]. These connections are believed to engage with craving induced by drug cue stimuli [47]. Previously, a significantly remarkable elevation in theta-gamma coupling (6–8 Hz with 50–55 Hz) was seen in the mPFC following cocaine treatment [13]. In addition, cross-frequency coupling appeared to mediate network-level dynamical computations during performance of T-maze task [48]. Collectively, the couplings in the mPFC and BLA may be considered as functional interactions that motivate drug-seeking behaviors. By the way, gamma range coupled with theta mentioned above was below 60 Hz. On the other hand, theta-high gamma (60–100 Hz) coupling was also involved in other motivated behaviors such as food seeking induced by chocolate cues after repeated chocolate sessions [12]. These data may suggest the underlying brain mechanisms in different degrees of motivation for food- or drug-induced

seeking behaviors. Altogether, the present PAC results might suggest possible changes in the brain circuits of memory and cognitive functions induced by METH dependence. Moreover, these findings may provide new information of LFP rhythmic oscillations in the BLA as evidence-based mechanisms in consistency with METH-induced neural plasticity, neuronal transmission, and the transduction of intracellular pathways during METH dependence [49–51].

In summary, this study demonstrated the LFP spectral powers and PAC in the BLA during post-conditioning phase of METH CPP. These findings were found in parallel with the induced METH CPP that could reflect METH craving and seeking behavior of mice in CPP paradigm. These electrical brain signals in the BLA are believed to support the process of learning association between METH effects and the assigned environment paired with METH administration. These BLA LFP oscillations might represent brain mechanisms that underlie drug craving and seeking behavior.

Author contributions

Jakkrit Nukitram: Methodology, Software, Validation, Formal analysis, Investigation, Resources, Data Curation, Writing - Original Draft, Visualization, Funding acquisition. **Dania Cheaha:** Software, Resources. **Ekkasit Kumarnsit:** Conceptualization, Writing - Review & Editing, Supervision, Project administration.

Declaration of Competing Interest

The authors report no declarations of interest.

Acknowledgments

This investigation was financially provided by the professional development project under the Science Achievement Scholarship of Thailand (SAST). Partially financial support was also from the Program of Physiology, Division of Health and Applied Science, Faculty of Science, Prince of Songkla University, Thailand.

References

- [1] S.J. Russo, E.J. Nestler, The brain reward circuitry in mood disorders, *Nat. Rev. Neurosci.* 14 (2013) 609–625, <https://doi.org/10.1038/nrn3381>.
- [2] E.A. Phelps, Emotion and cognition: Insights from studies of the human amygdala, *Annu. Rev. Psychol.* 57 (2006) 27–53, <https://doi.org/10.1146/annurev.psych.56.091103.070234>.
- [3] K. Amunts, O. Kedo, M. Kindler, P. Pieperhoff, H. Mohlberg, N.J. Shah, U. Habel, F. Schneider, K. Zilles, Cytoarchitectonic mapping of the human amygdala, hippocampal region and entorhinal cortex: intersubject variability and probability maps, *Anat. Embryol. (Berl.)* 210 (2005) 343–352, <https://doi.org/10.1007/s00429-005-0025-5>.
- [4] K.M. Wassum, A. Izquierdo, The basolateral amygdala in reward learning and addiction, *Neurosci. Biobehav. Rev.* 57 (2015) 271–283, <https://doi.org/10.1016/j.neubiorev.2015.08.017>.
- [5] R.E. See, R.A. Fuchs, C.C. Ledford, J. McLaughlin, Drug addiction, relapse, and the amygdala, *Ann. N. Y. Acad. Sci.* 985 (2003) 294–307, <https://doi.org/10.1111/j.1749-6632.2003.tb07089.x>.
- [6] W.M. Meil, R.E. See, Lesions of the basolateral amygdala abolish the ability of drug associated cues to reinstate responding during withdrawal from self-administered cocaine, *Behav. Brain Res.* 87 (1997) 139–148, [https://doi.org/10.1016/S0166-4328\(96\)02270-X](https://doi.org/10.1016/S0166-4328(96)02270-X).
- [7] J. Goodman, E. Hsu, M.G. Packard, NMDA receptors in the basolateral amygdala mediate acquisition and extinction of an amphetamine conditioned place preference, *Behav. Neurosci.* 133 (2019) 428–436, <https://doi.org/10.1037/bne0000323>.
- [8] W. Dimpfel, Pharmacological classification of herbal extracts by means of comparison to spectral EEG signatures induced by synthetic drugs in the freely moving rat, *J. Ethnopharmacol.* 149 (2013) 583–589, <https://doi.org/10.1016/j.jep.2013.07.029>.
- [9] W. Dimpfel, L. Schombert, N. Gericke, Electropharmacogram of Scelenium tortuosum extract based on spectral local field power in conscious freely moving rats, *J. Ethnopharmacol.* 177 (2016) 140–147, <https://doi.org/10.1016/j.jep.2015.11.036>.
- [10] E.P. Christian, D.H. Snyder, W. Song, D.A. Gurley, J. Smolka, D.L. Maier, M. Ding, F. Gharahdaghi, X.F. Liu, M. Chopra, M. Ribadeneira, M.J. Chapdelaine, A. Dudley, J.L. Arriza, C. Maciag, M.C. Quirk, J.J. Doherty, EEG/ spectral power elevation in rat: a translatable biomarker elicited by GABA A2/3-positive allosteric modulators at nonseating anxiolytic doses, *J. Neurophysiol.* 113 (2015) 116–131, <https://doi.org/10.1152/jn.00539.2013-Benzodiazepine>.
- [11] J.F. Alonso, S. Romero, M.A. Mañanas, M. Rojas, J. Riba, M.J. Barbano, Evaluation of multiple comparison correction procedures in drug assessment studies using LORETA maps, *Med. Biol. Eng. Comput.* 53 (2015) 1011–1023, <https://doi.org/10.1007/s11517-015-1315-6>.
- [12] N. Samerhob, D. Cheaha, S. Chatpun, E. Kumarnsit, Hippocampal CA1 local field potential oscillations induced by olfactory cue of liked food, *Neurobiol. Learn. Mem.* 142 (2017) 173–181, <https://doi.org/10.1016/j.nlm.2017.05.011>.
- [13] Z. Zhu, Z. Ye, H. Wang, T. Hua, Q. Wen, C. Zhang, Theta-gamma coupling in the prelimbic area is associated with heroin addiction, *Neurosci. Lett.* 701 (2019) 26–31, <https://doi.org/10.1016/j.neulet.2019.02.020>.
- [14] K. Vijeeppallam, V. Pandey, D. Murugan, M. Kuppusamy, Methanolic extract of *Mitragyna speciosa* Korth leaf exhibits place preference only at higher doses in mice, *Pharmacogn. Mag.* 16 (2020) 449–454, <https://doi.org/10.4103/pm.pm.62.20>.
- [15] M. Shen, C. Jiang, P. Liu, F. Wang, L. Ma, Mesolimbic leptin signaling negatively regulates cocaine-conditioned reward, *Transl. Psychiatry* 6 (2016) 1–10, <https://doi.org/10.1038/tp.2016.223>.
- [16] V. Pandey, Y.C. Wai, N.F. Amira Roslan, A. Sajat, A.H. Abdulla Jalib, K. Vijeeppallam, Methanolic extract of *Morinda citrifolia* Linn. Unripe fruit attenuates methamphetamine-induced conditioned place preferences in mice, *Biomed. Pharmacother.* 107 (2018) 368–373, <https://doi.org/10.1016/j.biopha.2018.08.008>.
- [17] M.E. Bardgett, T. Downen, C. Crane, E.C. Bales Thompson, B. Muncie, S. A. Steffen, J.R. Yates, J.R. Pauly, Chronic Risperidone administration leads to greater amphetamine-induced conditioned place preference, *Neuropharmacology* 179 (2020), 108276, <https://doi.org/10.1016/j.neuropharm.2020.108276>.
- [18] D. Cheaha, C. Reakkamuan, J. Nukitram, S. Chittrakarn, P. Phukattarant, N. Keawpradub, E. Kumarnsit, Effects of alkaloid-rich extract from *Mitragyna speciosa* (Korth.) Havil. on naloxone-precipitated morphine withdrawal symptoms and local field potential in the nucleus accumbens of mice, *J. Ethnopharmacol.* 208 (2017) 129–137, <https://doi.org/10.1016/j.jep.2017.07.008>.
- [19] G. Paxinos, K.B.J. Franklin, *The Mouse Brain in Stereotaxic Coordinates*, 2001, p. 120.
- [20] S. Caillé, E.F. Espejo, J.P. Renier, M. Cador, G.F. Koob, L. Stinus, Total neurochemical lesion of noradrenergic neurons of the locus ceruleus does not alter either naloxone-precipitated or spontaneous opiate withdrawal nor does it influence ability of clonidine to reverse opiate withdrawal, *J. Pharmacol. Exp. Ther.* 290 (1999) 881–892.
- [21] Y. Ben-Shaul, OptiMouse: A comprehensive open source program for reliable detection and analysis of mouse body and nose positions, *BMC Biol.* 15 (2017) 1–22, <https://doi.org/10.1186/s12915-017-0377-3>.
- [22] F. Tadel, S. Baillet, J.C. Mosher, D. Pantazis, R.M. Leahy, Brainstorm: a user-friendly application for MEG/EEG analysis, *Comput. Intell. Neurosci.* 2011 (2011) 1–13, <https://doi.org/10.1155/2011/879716>.
- [23] E. Galaj, M. Manuszak, S. Babic, S. Ananthan, R. Ranaldi, The selective dopamine D3 receptor antagonist, SR 21502, reduces cue-induced reinstatement of heroin seeking and heroin conditioned place preference in rats, *Drug Alcohol Depend.* 156 (2015) 228–233, <https://doi.org/10.1016/j.drugalcdep.2015.09.011>.
- [24] C. Reakkamuan, D. Cheaha, E. Kumarnsit, Nucleus accumbens local field potential power spectrums, phase-amplitude couplings and coherences following morphine treatment, *Acta Neurobiol. Exp. (Wars)* 77 (2017) 214–224, <https://doi.org/10.21307/ane-2017-055>.
- [25] R.J. Cadoret, T.W. O'gorman, E. Troughton, E. Heywood, Alcoholism and Antisocial Personality: Interrelationships, Genetic and Environmental Factors, *Arch. Gen. Psychiatry* 42 (1985) 161–167, <https://doi.org/10.1001/archpsyc.1985.01790250055007>.
- [26] K.G.C. Hellemans, B.J. Everitt, J.L.C. Lee, Disrupting reconsolidation of conditioned withdrawal memories in the basolateral amygdala reduces suppression of heroin seeking in rats, *J. Neurosci.* 26 (2006) 12694–12699, <https://doi.org/10.1523/JNEUROSCI.3101-06.2006>.
- [27] H.S. Shi, Y.X. Luo, X. Yin, H.H. Wu, G. Xue, X.H. Geng, Y.N. Hou, Reconsolidation of a cocaine associated memory requires DNA methyltransferase activity in the basolateral amygdala, *Sci. Rep.* 5 (2015) 1–13, <https://doi.org/10.1038/srep13327>.
- [28] A. Servonnet, G. Hernandez, C. El Hage, P.P. Rompré, A.N. Samaha, Optogenetic activation of the basolateral amygdala promotes both appetitive conditioning and the instrumental pursuit of reward cues, *J. Neurosci.* 40 (2020) 1732–1743, <https://doi.org/10.1523/JNEUROSCI.2196-19.2020>.
- [29] K.C. Kirby, R.J. Lamb, M.Y. Iguchi, S.D. Husband, J.J. Platt, Situations occasioning cocaine use and cocaine abstinence strategies, *Addiction* 90 (1995) 1241–1252, <https://doi.org/10.1046/j.1360-0443.1995.90912418.x>.
- [30] E.R. Korpi, B. den Hollander, U. Farooq, E. Vashchinkina, R. Rajkumar, D.J. Nutt, P. Hyttä, G.S. Dawe, Mechanisms of action and persistent neuroplasticity by drugs of abuse, *Pharmacol. Rev.* 67 (2015) 872–1004, <https://doi.org/10.1124/pr.115.010967>.
- [31] G.F. Koob, Neuroadaptive mechanisms of addiction: studies on the extended amygdala, *Eur. Neuropsychopharmacol.* 13 (2003) 442–452, <https://doi.org/10.1016/j.euroneuro.2003.08.005>.
- [32] L.T. Hsieh, C. Ranganath, Frontal midline theta oscillations during working memory maintenance and episodic encoding and retrieval, *Neuroimage* 85 (2014) 721–729, <https://doi.org/10.1016/j.neuroimage.2013.08.003>.
- [33] P.-K. O'neill, J.A. Gordon, T. Sigurdsson, Theta oscillations in the medial prefrontal cortex are modulated by spatial working memory and synchronize with the

- Hippocampus through its ventral subregion, *J. Neurosci.* 33 (2013) 14211–14224, <https://doi.org/10.1523/JNEUROSCI.2378-13.2013>.
- [34] M.W. Jones, M.A. Wilson, Theta rhythms coordinate hippocampal–prefrontal interactions in a spatial memory task, *PLoS Biol.* 3 (2005) e402, <https://doi.org/10.1371/journal.pbio.0030402>.
- [35] F. Dimpfel, W. Schober, Norepinephrine, EEG theta waves and sedation, *Brain Pharmacol.* 1 (2001) 89–97.
- [36] L.A. Newman, J. Darling, J. McGaughy, Atomoxetine reverses attentional deficits produced by noradrenergic deafferentation of medial prefrontal cortex, *Psychopharmacology (Berl.)* 200 (2008) 39–50, <https://doi.org/10.1007/s00213-008-1097-8>.
- [37] L. Gowing, M. Farrell, R. Ali, J.M. White, Alpha2-adrenergic agonists for the management of opioid withdrawal, *Cochrane Database Syst. Rev.* 2016 (2016), <https://doi.org/10.1002/14651858.CD002024.pub5>.
- [38] L.M. Schönfeld, L. Wojtecki, Beyond emotions: oscillations of the amygdala and their implications for electrical neuromodulation, *Front. Neurosci.* 13 (2019), <https://doi.org/10.3389/fnins.2019.00366>.
- [39] W. Klimesch, Alpha-band oscillations, attention, and controlled access to stored information, *Trends Cogn. Sci.* 16 (2012) 606–617, <https://doi.org/10.1016/j.tics.2012.10.007>.
- [40] M. Saeed, A. Ghadiri, F. Hadizadeh, A. Attarazadeh, M.S. Alavi, L. Etemad, Cinnamaldehyde improves methamphetamine-induced spatial learning and memory deficits and restores ERK signaling in the rat prefrontal cortex, *Iran. J. Basic Med. Sci.* 21 (2018) 1316–1321, <https://doi.org/10.22038/IJBMS.2018.35368.8427>.
- [41] G.F. Koob, M. Le Moal, Neurobiological mechanisms for opponent motivational processes in addiction, *Philos. Trans. R. Soc. B Biol. Sci. Royal Soc.* (2008) 3113–3123, <https://doi.org/10.1098/rstb.2008.0094>.
- [42] G.F. Koob, L. Stinus, M. Le Moal, F.E. Bloom, Opponent process theory of motivation: neurobiological evidence from studies of opiate dependence, *Neurosci. Biobehav. Rev.* 13 (1989) 135–140, [https://doi.org/10.1016/S0149-7634\(89\)80022-3](https://doi.org/10.1016/S0149-7634(89)80022-3).
- [43] R. Goutagny, N. Gu, C. Cavanagh, J. Jackson, J.G. Chabot, R. Quirion, S. Krantic, S. Williams, Alterations in hippocampal network oscillations and theta-gamma coupling arise before A β overproduction in a mouse model of Alzheimer's disease, *Eur. J. Neurosci.* 37 (2013) 1896–1902, <https://doi.org/10.1111/ejn.12233>.
- [44] J.Y. Park, Y.R. Lee, J. Lee, The relationship between theta-gamma coupling and spatial memory ability in older adults, *Neurosci. Lett.* 498 (2011) 37–41, <https://doi.org/10.1016/j.neulet.2011.04.056>.
- [45] J. Fell, N. Axmacher, The role of phase synchronization in memory processes, *Nat. Rev. Neurosci.* 12 (2011) 105–118, <https://doi.org/10.1038/nrn2979>.
- [46] S.J. Bacon, A.J.N. Headlam, P.L.A. Gabbott, A.D. Smith, Amygdala input to medial prefrontal cortex (mPFC) in the rat: a light and electron microscope study, *Brain Res.* 720 (1996) 211–219, [https://doi.org/10.1016/0006-8993\(96\)00155-2](https://doi.org/10.1016/0006-8993(96)00155-2).
- [47] G.F. Koob, The neurobiology of addiction: a neuroadaptational view relevant for diagnosis, *Addiction* 101 (2006) 23–30, <https://doi.org/10.1111/j.1360-0443.2006.01586.x>.
- [48] A.B.L. Tort, M.A. Kramer, C. Thorn, D.J. Gibson, Y. Kubota, A.M. Graybiel, N. J. Kopell, Dynamic cross-frequency couplings of local field potential oscillations in rat striatum and hippocampus during performance of a T-maze task, *Proc. Natl. Acad. Sci. U. S. A.* 105 (2008) 20517–20522, <https://doi.org/10.1073/pnas.0810524105>.
- [49] Z. Taslimi, A. Sarihi, A. Haghparast, Glucocorticoid receptors in the basolateral amygdala mediated the restraint stress-induced reinstatement of methamphetamine-seeking behaviors in rats, *Behav. Brain Res.* 348 (2018) 150–159, <https://doi.org/10.1016/j.bbr.2018.04.022>.
- [50] T.S. Der-Ghazarian, D. Charmchi, S.N. Noudali, S.N. Scott, M.C. Holter, J. M. Newbern, J.L. Neisewander, Neural circuits associated with 5-HT1B receptor agonist inhibition of methamphetamine seeking in the conditioned place preference model, *ACS Chem. Neurosci.* 10 (2019) 3271–3283, <https://doi.org/10.1021/acscchemneuro.8b00709>.
- [51] E.J. Young, H. Lin, T.M. Kamenecka, G. Rumbaugh, C.A. Miller, Methamphetamine learning induces persistent and selective nonmuscle myosin II-dependent spine motility in the Basolateral Amygdala, *J. Neurosci.* 40 (2020) 2695–2707, <https://doi.org/10.1523/JNEUROSCI.2182-19.2020>.



Contents lists available at ScienceDirect

Journal of Ethnopharmacology

journal homepage: www.elsevier.com/locate/jethpharm

Ameliorative effects of alkaloid extract from *Mitragyna speciosa* (Korth.) Havil. Leaves on methamphetamine conditioned place preference in mice

Jakkrit Nukitram^{a,e}, Dania Cheaha^{b,e}, Narumon Sengnon^d, Juraithip Wungsintaweekul^d, Supattra Limsuwanchote^c, Ekkasit Kumarnsit^{a,e,*}

^a Physiology Program, Division of Health and Applied Sciences, Faculty of Science, Prince of Songkla University, Hatyai Campus, Hatyai, Songkhla, 90112, Thailand

^b Biology Program, Division of Biological Science, Faculty of Science, Prince of Songkla University, Hatyai Campus, Hatyai, Songkhla, 90112, Thailand

^c Pharmacology Program, Division of Health and Applied Sciences, Faculty of Science, Prince of Songkla University, Hatyai Campus, Hatyai, Songkhla, 90112, Thailand

^d Department of Pharmacognosy and Pharmaceutical Botany, Faculty of Pharmaceutical Sciences, Prince of Songkla University, Hatyai Campus, Hatyai, Songkhla, 90112, Thailand

^e Biosignal Research Center for Health, Faculty of Science, Prince of Songkla University, Hatyai Campus, Hatyai, Songkhla, 90112, Thailand

ARTICLE INFO

Keywords:

Bupropion
Coherence analysis
Conditioned place preference
Local field potential methamphetamine
Mitragyna speciosa

ABSTRACT

Ethnopharmacological relevance: *Mitragyna speciosa* (Korth.) Havil., popularly known as Kratom (KT), is a medicinal plant used for pain suppression in Southeast Asia. It has been claimed to assist drug users withdraw from methamphetamine (METH) dependence. However, its use was controversial and not approved yet.

Aim of the study: This study was conducted to characterize local field potential (LFP) patterns in the nucleus accumbens (NAc) and the hippocampus (HP) in mice with METH conditioned place preference (CPP) that were treated with KT alkaloid extract.

Materials and methods: Male Swiss albino ICR mice were implanted with intracranial electrodes into the NAc and HP. To induce METH CPP, animals were injected intraperitoneally once a day with METH (1 mg/kg) and saline (0.9% w/v) alternately and put into METH/saline compartments to experience the associations between drug/saline injection and the unique environmental contexts for 10 sessions. Control group received saline injection paired with both saline/saline compartments. On post-conditioning day, effects of 40 (KT40), 80 (KT80) mg/kg KT alkaloid extract and 20 mg/kg bupropion (BP) on CPP scores and LFP powers and NAc-HP coherence were tested.

Results: Two-way ANOVA revealed significant induction of CPP by METH sessions ($P < 0.01$). Multiple comparisons indicated that METH CPP was completely abolished by KT80 ($P < 0.001$). NAc gamma 1 (30.0–44.9 Hz) and HP delta (1.0–3.9 Hz) powers were significantly increased in mice with METH CPP ($P < 0.01$). The elevated NAc gamma 1 was significantly suppressed by KT80 ($P < 0.05$) and the increased HP delta was significantly reversed by KT40 ($P < 0.01$) and KT80 ($P < 0.001$). In addition, NAc-HP coherence was also significantly increased in gamma 1 (30.0–44.9 Hz) frequency range ($P < 0.05$) but it was reversed by KT80 ($P < 0.05$). Treatment with BP did not produce significant effect on these parameters.

Conclusions: These findings demonstrated that KT alkaloid extract significantly reversed CPP scores and LFP patterns induced by METH administration. The ameliorative effects of the extract might be beneficial for treatment of METH craving and addiction.

1. Introduction

The evidence of public health problems from misuse and overdose of methamphetamine (METH) does exist (Halpin et al., 2013). METH is a stimulant drug acting on the central nervous system (CNS) as a

sympathomimetic agent. Chronic METH administration produced adverse effects on body functions (Turnipseed et al., 2003) and psychological consequences including depression and schizophrenia (Wearne and Cornish, 2018). These psychological disorders are partially resulted from the elevation of monoamine neurotransmission-induced monoamine neurotransmitter (NT) remodeling known as

* Corresponding author. Physiology program, Division of Health and Applied Sciences, Faculty of Science, Prince of Songkla University, Hatyai Campus, Hatyai, Songkhla, 90112, Thailand.

E-mail address: ekkasit.k@psu.ac.th (E. Kumarnsit).

<https://doi.org/10.1016/j.jep.2021.114824>

Received 23 March 2021; Received in revised form 21 September 2021; Accepted 5 November 2021

Available online 8 November 2021

0378-8741/© 2021 Elsevier B.V. All rights reserved.

Abbreviations:			
7-HMT	7-hydroxymitragynine	HP	Hippocampus
ANOVA	Analysis of variance	HPA axis	Hypothalamic-Pituitary-Adrenal axis
AP	Antero-posterior	HPLC	High performance liquid chromatography
ARRIVE	Animal Research: Reporting of <i>In Vivo</i> Experiments	IR	Infrared
BP	Bupropion	KBr	Potassium bromide
CHCl ₃	Chloroform	KT	Kratom
CMC	Sodium carboxymethyl cellulose	LFP	Local field potential
CNS	Central nervous system	MeOH	Methanol
COR	Corticosterone	METH	Methamphetamine
CPP	Conditioned place preference	ML	Medio-Lateral
D1	Dopamine receptor type 1	MT	Mitragynine
D2	Dopamine receptor type 2	MTPD	Methylphenidate
DA	Dopamine	Nac	Nucleus accumbens
DAT	Dopamine transporter	NaCl	Sodium chloride
DRn	Dorsal raphe nuclei	NMR	Nuclear magnetic resonance
DV	Dorso-ventral	NT	Neurotransmitter
EIMS	Electron impact mass spectrometry	PSD	Power spectral density
FFT	Fast Fourier Transform	SEM	Standard Error Mean
		STR	Striatum
		VTA	Ventral tegmental area

neuroplasticity (Korpi et al., 2015). Additionally, negative consequences of METH use were found to affect behavioral and social aspects of the adolescent population (Embry et al., 2009). Although the impacts of METH use on health and social are critical, the current interventions are not satisfactory especially the pharmacotherapy for handling of METH craving. The use of medicinal plant extract is one of alternative treatments for drug addiction. Many parts of various plant species including *Mitragyna speciosa* (Korth.) Havil. have been tested for possible curative effects on drug addiction (Cheaha et al., 2017; Kumarsit et al., 2007a; Pandey et al., 2018; Vijeeppallam et al., 2019).

Mitragyna speciosa (Korth.) Havil., commonly known as Kratom (KT), is a medicinal plant of the family Rubiaceae. It is abundantly found in Malaysia and Thailand (Suhaimi et al., 2016). It has been widely used in folk medicines to cure many illness for several decades (Yusoff et al., 2016). KT leaves contain varieties of indole alkaloids that have been isolated and chemically identified such as mitragynine (MT), a major alkaloid, or 7-hydroxymitragynine (7-HMT), a minor constituent. These molecules exert their functions partially via opioid receptor activation in both peripheral and central organs (Adkins et al., 2011; Kruegel and Grundmann, 2018). Traditionally, KT leaf consumption produces remedy in the mitigation of chronic musculoskeletal pain and fatigue, attenuation of inflammatory response and reduction of diarrhea and mood swing (Chan et al., 2007; Jansen and Prast, 1988). Recently, MT was found to reduce the neuropathic pain in rat via α -adrenoceptor mechanism (Foss et al., 2020).

Moreover, during the past decades, KT alkaloid extract has been consistently studied. It exhibited beneficial effects in various aspects such as reducing severity of ethanol and morphine withdrawal symptoms and showing similar local field potential (LFP) patterns of electrical brain wave to that of a standard anti-depressant drug fluoxetine (Cheaha et al., 2015, 2017). Fundamentally, local people in the communities consume whole alkaloid contents in KT leaves by chewing or drinking tea from its leaves. The evidence-based study indicated the potential of KT to reduce craving in poly-drug users including METH addicts in Malaysia (Singh et al., 2020). Previously, the KT extract produced more beneficial effects than MT in animal models of addiction (Cheaha et al., 2017). By oral route, the pharmacokinetics of KT extract were more preferable than that of MT alone (Avery et al., 2019). Therefore, the present study used KT alkaloid extract instead of MT to represent the use of KT plant in communities.

Previously, KT alkaloid extract at effective dose did not activate the nucleus accumbens (NAc), the brain reward center that is normally

activated by standard addictive drugs such as morphine (Cheaha et al., 2017; Reakkammuan et al., 2017). Moreover, reward effects induced by MT was demonstrated using conditioned place preference (CPP) paradigm (Yusoff et al., 2017, 2018). These findings raised concerns of possible dependence produced by MT. Hence, the utilization of MT for therapeutic purposes is not recommended. Previously, KT leaves were chewed by METH addicts to attenuate craving and some other withdrawal symptoms (Assanangkornchai et al., 2007; Saref et al., 2019, 2020). However, this remained uninvestigated in a well-controlled research particularly in animal models. It is important to examine the effect of KT alkaloid extract on addictive behaviors induced by METH.

The CPP paradigm has been widely used as a reliable model in animals for testing drug seeking behavior and rewarding property produced by stimuli associated with administration of psychoactive drugs such as METH, amphetamine or cocaine (Bardgett et al., 2020; Nukitram et al., 2021; Pandey et al., 2018; Shen et al., 2016). Basically, this paradigm is involved with the effects of environment cues of drug associated stimuli (e.g. drug paraphernalia) which dramatically elicited craving (Foltin and Haney, 2000). Addictive behaviors are primarily regulated by the hippocampus (HP) and the NAc (Ito et al., 2008). The processing of spatial information and the formation and retrieval of addictive-related memory were believed to link with the main functions of the HP (Jones and Wilson, 2005; Masuoka et al., 2006). The spatial information while animals exploring each compartment in CPP paradigm was produced and stored. The NAc would possibly receive the information of contextual cue from the HP. Moreover, the crucial roles between the HP and the NAc in acquisition of CPP have been demonstrated (Ito et al., 2008). These evidences suggest that the memory of drug associated environment is necessary to induce drug-craving behaviors. Suppression of drug craving in addiction treatment would hint the success of drug therapy. Better understanding of brain mechanisms and neural signaling associated with drug seeking and craving from CPP paradigm is important and might be useful particularly in clinical management for drug addicts.

Summated excitatory and inhibitory potentials from neuronal population located in the cortical area or other deep brain nuclei can be recorded as LFP signals. LFP oscillation also provides an effective platform to identify brain mechanism in correlation with task performing as clinical profile of drugs of interest (Cheaha et al., 2015; Dimpfel et al., 2016). For LFP signal interpretation, many algorithms and computational techniques have been deployed to analyze LFP signals for quantitative measurement of electrical activity in each brain region. LFP signal can be processed as a form of power spectral density (PSD) to

represent the intensity of signal energy of different frequencies (Unde and Shriram, 2014). PSD has been generally analyzed to detect the brain injury (Goldfine et al., 2011), cognitive function (Samerphob et al., 2017), and the fluctuation of NT systems (Dimpfel, 2008). Moreover, coherence activity can be analyzed to clarify the communication between different brain regions. Previously, high coherence values suggested that electrical activity across brain areas synchronized to each other and vice versa (Murias et al., 2007).

Mostly, the addicts are vulnerable to relapse in response to the stimuli associated with drug intake. Drug craving and seeking behavior are induced by the contextual stimuli related with drug administration. Therefore, this study was designed to establish the association between environmental context and METH injection through conditioning paradigm. Animal behavior and LFP signals were monitored during pre-conditioning and post-conditioning phases to investigate craving and neural activity. After that, the efficacy of alkaloid extract from KT leaves on induced addictive behaviors was examined by using METH CPP paradigm in a mouse model. Changes in LFP pattern and coherence values were also monitored in purpose to clarify neural signaling associated with CPP in response to treatment with KT alkaloid extract.

2. Materials and methods

2.1. Plant materials

Mature leaves of KT were collected from natural sources in Songkhla and Satun provinces, Thailand. Plant materials were then identified by Assist. Prof. Dr. Chatchai Wattanapiromsakul and stored at the herbarium in the Department of Pharmacognosy and Pharmaceutical Botany, Faculty of Pharmaceutical Sciences, Prince of Songkla University, Thailand where a voucher specimen (no. PCOG/MS001-002) has been deposited.

2.2. Instrumentals

Infrared (IR) absorption spectrum was performed on PerkinElmer Spectrum One FT-IR spectrometer (MA, USA). The materials were examined in potassium bromide (KBr) disc. Mass spectrum was recorded on Thermo Finnigan MAT 95 XL (MA, USA) for the electron impact mass spectrometry (EIMS). Nuclear magnetic resonance (NMR) spectra were recorded on FT-NMR Varian® Unity Inova 500 spectrometer (CA, USA) at 500 and 125 MHz for ^1H and ^{13}C -NMR, respectively. The chemical shifts were reported in ppm (δ) scale with referenced to the solvent signals including chloroform-*d* (7.24 ppm of residual CHCl_3 for ^1H -NMR and 77.0 ppm for ^{13}C -NMR).

2.3. Preparation of crude alkaloid extract and phytochemical characterization

The extraction and isolation of KT alkaloid extract were performed as described previous study (Keawpradub, 1990) with the following modifications. In brief, KT leaves were cleaned, dried at 45–50 °C, powdered, and macerated with methanol. The filtrate was evaporated in vacuo. The residue was dissolved in 10% (v/v) acetic acid solution, filtrated, and washed with petroleum ether, then made into alkaline (pH 9) with 25% (v/v) ammonia solution and extracted with chloroform. The combined chloroform fractions were washed with brine solution, dried over anhydrous sodium sulfate. After evaporated to dryness, the KT alkaloid extract was obtained with the yield of 0.25% (w/w) based on dried weight. The authentic MT was isolated. The crude alkaloid extract was loaded on the top of the silica-gel column eluting with CHCl_3 : MeOH (95:5). The structure of MT was identified using spectroscopic methods (MS, IR, ^1H NMR, and ^{13}C NMR). The results were in agreement with the data from previous investigations (Keawpradub, 1990; Kitajima et al., 2006). The MT purity was estimated at approx. 98% pure (Supp. Figure 1).

The characteristic of the KT alkaloid extract was determined using the validated HPLC method as described (Limsuwanchote et al., 2015). The HPLC Shimadzu Prominence i 2030C (Kyoto, Japan) connected with VertiSep™ USP C18 HPLC column (4.6 × 250 mm, 5 μm ; Vertical, Bangkok, Thailand) was used. The column was eluted isocratically with 20 mM ammonium acetate (pH 6): acetonitrile; 35:65 (% v/v). The flow rate was 1 ml/min. The injection volume was 20 μL . The photodiode array detector-UV was set at 225 nm (Supp. Figure 4).

2.4. Animals

This investigation was carried out under the guidelines of the European Science Foundation (Use of Animals in Research, 2001) (Van Zutphen, 2004) and the ARRIVE (Animal Research: Reporting of *In Vivo* Experiments) (Kilkenny et al., 2010) for the protection of animals used in scientific research. The experimental procedures and protocols were approved by the Institute Animal Care and Use Committee, Prince of Songkla University [project license number: MHESI 6800.11/845 and reference number: 57/2019]. Male Swiss albino ICR mice (7–8 weeks old) were obtained from the Nomura Siam International Company, Bangkok, Thailand. In order to minimize the stress in animals, all animals were handled for one week prior to the beginning of the experiment at the Southern Laboratory Animal Facility, Prince of Songkla University. The animals were individually housed in single stainless-steel cages (17 × 28.5 × 17 cm) with the standard environmental condition (12/12 h light/dark cycle, 22 ± 3 °C and 55 ± 10% relative humidity). Commercial food pellets and water were available *ad libitum*. All experiments were conducted between 8 a.m. and 4 p.m.

2.5. Drugs and chemicals

METH hydrochloride with a standard purity (95.8%) for research purpose was provided by the Food and Drug Administration, Thailand. Moreover, 1 mg/kg METH dissolved in 0.9% w/v NaCl was used for intraperitoneal (i.p.) injection. METH concentration was selected in accordance to the dose that definitely produced addictive behavior in the same strain of mice (Nukitram et al., 2021; Pandey et al., 2018). The 40 (KT40) and 80 (KT80) mg/kg KT alkaloid extracts and a standard drug bupropion (BP) at 20 mg/kg (Sigma-Aldrich, St.Louis, MO, USA) were diluted in 1%w/v of sodium carboxymethyl cellulose (CMC) solution and administered orally (p.o). Intragastric administration was accomplished by using a smooth ball tipped stainless steel gavage needle with fixed volume per body weight of mice at 10 ml/kg.

2.6. Animal surgery for implanting the LFP electrodes

The process of intracranial electrode implantation was modified from the previous study (Cheaha et al., 2017; Nukitram et al., 2021). At approximately 4 months after birth, mice with initial body weight 45.0–52.0 g were deeply anesthetized with intramuscular injection of a mixed solution of 16 mg/kg xylazine hydrochloride (Xylavet, Sigma-Aldrich International GmbH, Switzerland) and 50 mg/kg zoletil (Tiletamine – zolazepam, Vibac Ah, Inc., USA). Animals' head were then held with stereotaxic apparatus. Lignocaine (20 mg/ml) (Lidocaine, M & H manufacturing Co., Ltd., Thailand), a local analgesic drug, was applied subcutaneously before making the incision to the midline of the scalp on the dorsal head. The skull was drilled for the electrodes to be stereotaxically positioned on the left hemisphere of the brain defined from bregma to the HP in dorsal part (the CA1 region) (AP; –2.5 mm, ML; 2 mm; DV; 1.5 mm), and the NAc (AP; +1.3 mm, ML; 1.0 mm; DV; 4.2 mm) according to the mouse brain atlas (Paxinos and Franklin, 2001). The reference and ground electrodes were implanted at the midline skull over the cerebellum (AP; –6.0 mm, ML; 0.0 mm; DV; 1.5 mm). After that, holes were drilled for stainless steel screws as anchors. All electrodes (0.381 mm diameter, coated) were secured in place for permanent with dental acrylic (Unifast Trad, GC Dental Industrial Corp.,

Tokyo, Japan). The antibiotic ampicillin (100 mg/kg) (General Drug House Co., Ltd., Bangkok, Thailand) and carprofen (10 mg/kg) (Best Equipment Center Co., Ltd., Thailand) were administered subcutaneously once a day for three days to prevent infection and alleviate pain, respectively. The animals were allowed for at least two weeks to fully recover from the surgery in their separated cages.

2.7. CPP apparatus and paradigm

The equipment has been employed to evaluate condition-induced drug craving behaviors in CPP paradigm known as CPP apparatus. The CPP apparatus in this experiment was modified from the previous investigations (Caillé et al., 1999; Nukitram et al., 2021). In brief, it was made from plexiglass to have 3 rectangular compartments (25 cm × 18 cm × 25 cm) (compartment A, B, and C) which were arranged radially in 120° to each other. Each rectangular compartment was accessible from a triangular zone located centrally. The compartments had identical shape and size but different floor texture and wall shading. The ornamentation for floor texture and wall shading were designed as following details, respectively: A) medium rough, vertical strips; B) rough, grid strips; and C) smooth, black color (Fig. 1). Compartment C was defined as a starting or neutral zone where individual animals were placed and allowed to freely explore the CPP apparatus. Overall time schedule of drug administration was modified from the previous experiment (Nukitram et al., 2021; Pandey et al., 2018) as depicted in Fig. 1. Briefly, after habituation, CPP paradigm mainly consisted of 3 consecutive periods initiating from pre-conditioning to conditioning and post-conditioning phases in sequence.

2.7.1. Habituation and pre-conditioning phase

Mice were brought to a recording room for at least a half an hour prior to the initiation of the experiments. During the habituation (day 1 and 2) period, animals were intraperitoneally injected with normal saline solution in order to attenuate the stress from pain of drug injection and then immediately placed on the starting zone. Next, they were allowed to explore all compartments of the CPP apparatus freely for 15 min. During pre-conditioning phase (day 3), the animals were subjected to the same protocol of the habituation period. Time that animals spent in each compartment was recorded and expressed as CPP score. CPP score was calculated from the difference of time that each animal spent in METH-paired and normal saline-paired compartment. Tossing a coin was a method to randomly divide all mice into 5 groups defined as control, METH + CMC, METH + KT40, METH + KT80 and METH + BP groups. Each group contained 10 mice. However, 3 n number of METH + CMC and METH + KT40 group and 2 n number of METH + KT80 and METH + BP groups showed initial bias of side preference. They spent the time in one compartment more than 80% of a total time. Altogether, 10 mice were rejected from the CPP procedure after pre-conditioning phase.

2.7.2. Conditioning phase

Animals were subjected for training sessions that took 10 consecutive days (from day 4–13) that began the day after pre-conditioning phase. To trigger the addictive behavior, mice were given intraperitoneal (i.p.) injection of 1 mg/kg METH and normal saline solution in alternative days (odd and even days for METH and saline, respectively). Animals were immediately confined to the assigned compartment for 30 min to learn to associate between the context of unique condition of each compartment and the specific effect of METH or saline injection. Animals in control group were administered with normal saline (both odd and even days) for pairing with all compartments. After animals completed the session in each day, they were brought back to their home cage.

2.7.3. Post-conditioning phase

Post-conditioning phase was taken on day 14 to evaluate the efficacy

of KT alkaloid extract and BP on the expression of METH CPP. 40 mg/kg KT (n = 7), 80 mg/kg KT (n = 8), 20 mg/kg BP (n = 8) and 10 ml/kg 1% w/v CMC (n = 7) were administered orally to the assigned groups of mice 60 min before CPP testing. After that, time spent in each compartment was analyzed for CPP score.

2.8. The processing of LFP signals and locomotor activity of animals

During pre-conditioning and post-conditioning phases, LFP signals and locomotor activities of individual mice in the CPP apparatus were recorded simultaneously for 15 min. For LFP signal processing, raw LFP signals were amplified and converted from analog to digital data by Dual Bio Amp (AD Instruments, Castle Hill, NSW, Australia) and a PowerLab 16/35 system (AD Instruments, Castle Hill, NSW, Australia) with 16-bit A/D, respectively. Additionally, signals were harvested with 1.024 s duration in sweeps and sampling frequency was 2 kHz. Notch filtering at 50 Hz was deployed to reject the noise from power line artifacts. LFP signal analysis was processed through 1–100 Hz band-pass digital filtering. For locomotor activity, a webcam mounted vertically on the top of CPP apparatus was used to capture and monitor spontaneous movement of animals. All data were stored in a PC computer through LabChart 7.3.7 Pro software for offline analysis.

2.8.1. Locomotor activity analysis

Each video record of locomotor activities from individual mouse deposited in a PC computer was analyzed to evaluate the animal movement. The method was validated by using open source toolbox OptiMouse (Ben-Shaul, 2017) to detect the translocation of center position of animal body. The basic principle of animal detection was designed based on the contrast between black color of background (floor & wall of the CPP apparatus) and white color of animals' body. The alternations of locomotor activity, tracking of animal exploration and time spent in each compartment of the apparatus during the assigned time period were the parameters to be specifically focused.

2.8.2. LFP signal analysis

PSD values were computed from LFP raw data stored in the LabChart software by using the function of the Hanning window cosine transform with 50% window overlap and 0.976 Hz of power spectra resolution. The analysis of frequency power was processed by using Fast Fourier transform (FFT) algorithm and expressed in powers of frequency domain in 6 discrete frequency bands which included delta (1.0–3.9 Hz), theta (4.7–8.7 Hz), alpha (9.8–12.7 Hz), beta (13.6–29.3 Hz), low gamma or gamma I (30.0–44.9 Hz), and high gamma or gamma II (60.5–95.7 Hz). Data were normalized as percent relative powers of particular frequency range ($P_{(f)}$) by the following equation;

$$\% \text{ Relative power} = \frac{P_{(f)} \text{ at Post-condition} - P_{(f)} \text{ at Pre-condition}}{P_{(f)} \text{ at Post-condition} + P_{(f)} \text{ at Pre-condition}} \times 100$$

For coherence analysis, the values were obtained by running raw data via toolbox Brainstorm3 (Tadel et al., 2011). Then, data were normalized as percent relative coherence to quantify the strength of signal communication between 2 separate brain regions in particular frequency ($C_{(f)}$) according to the provided equation;

$$\% \text{ Relative coherence} = \frac{C_{(f)} \text{ at Post-condition} - C_{(f)} \text{ at Pre-condition}}{C_{(f)} \text{ at Post-condition} + C_{(f)} \text{ at Pre-condition}} \times 100$$

2.9. Statistical analyses

All parameters were analyzed and illustrated as mean ± Standard

Error Mean (SEM). For locomotor activities and CPP scores, two-way repeated analysis of variance (ANOVA) was used to determine the influence of an interaction between two factors (Treatment x Condition) followed by *post hoc* Bonferroni test for multiple comparisons. Conditioning states were used as within-subject factors, and with or without METH treatment considered as inter-subject factors defined as treatment. The rest of parameters from considered brain regions induced by drug treatment with statistically significant output were specified using one-way ANOVA in comparison to data of control condition. Different symbols were used to indicate significant differences at $p < 0.05$ according to Tukey's *post hoc*. Multiple comparisons were performed for data expressed in %relative power and %relative coherence. All data were analyzed using the temporarily available software GraphPad 7.0 (Graphpad Software, Inc., USA).

3. Results

3.1. Characteristic of KT alkaloid extract

The KT alkaloid extract appeared as a dark brown mass. The MT was in-house isolated using silica gel column (Supp. Figure 1) and elucidated. Details of MT structure elucidation were also described and interpreted. The spectroscopic data are shown in Supp. Figure 2-3 and Supp. Table 1. By HPLC analysis, the amount of MT accounted for 47.1 mg per g of the KT alkaloid extract. The HPLC fingerprint of KT alkaloid extract is summarized in Supp. Figure 4. Amounts of 40 mg and 80 mg of KT alkaloid extract were equivalent to 1.9 and 3.8 mg MT, respectively.

3.2. Animal movement and locomotor activity

The spontaneous movement of each animal was recorded for 15 min for both pre-conditioning and post-conditioning phases. Videos that captured mice exploration in the CPP apparatus were next analyzed and displayed for locomotor tracking patterns and parameters of velocity and time spent in each compartment. Locomotor speeds of each group were averaged with 1 min-bin and illustrated (Fig. 2A). The results revealed relatively higher speed during the first 5 min and slow down movement after that. In order to avoid movement related effects on LFP signal generation, the analysis of averaged speed during 15 min of data recording was next performed. The results found that no alternation of

speed in pre-conditioning and post-conditioning phases in all treatment was seen. Two-way repeated measures ANOVA also confirmed a non-significant difference of locomotor speed among groups [$F_{(4, 35)} = 0.152, P = 0.961$] and between pre-conditioning and post-conditioning phases [$F_{(4, 35)} = 0.475, P = 0.754$] (Fig. 2B).

3.3. CPP score

The effects of KT alkaloid extract and BP were measured during the expression of METH CPP. Data were analyzed as locomotor tracking patterns and CPP scores. Representative locomotor tracking of 5 groups were shown in comparisons between different treatments and between pre-conditioning and post-conditioning phases (Fig. 3A). During pre-conditioning phases, all five groups appeared to explore and visit all 3 compartments relatively equally. During post-conditioning period, control animals remained the same pattern exploring all 3 compartments equally whereas METH + CMC group clearly preferred to visit neutral and METH-paired compartments more than saline-paired compartment. METH + KT40 group also visited saline-paired compartment less than control group but more than METH + CMC group. However, normal patterns were found in METH + KT80 group which animals visited all 3 compartments equally. Unexpectedly, METH + BP group clearly preferred METH-paired compartment more than the other 2 compartments.

Therefore, CPP scores were statistically analyzed (Fig. 3B). Two-way repeated measures ANOVA revealed significant effects of condition [$F_{(4, 35)} = 34.576, P < 0.001$], treatment [$F_{(4, 35)} = 4.545, P = 0.005$] and treatment x condition interaction [$F_{(4, 35)} = 6.486, P < 0.001$]. Multiple comparisons using a *post hoc* Bonferroni test indicated significant in CPP scores during post-conditioning phase in METH + CMC ($P = 0.002$), METH + KT40 ($P = 0.001$) and METH + BP ($P < 0.001$) but not METH + KT80 group compared with pre-conditioning score of each group. In comparisons among groups during post-conditioning phase, significant increases in CPP score were seen in METH + CMC ($P = 0.001$), METH + KT40 ($P < 0.001$) and METH + BP ($P < 0.001$) but not METH + KT80 group compared to control level. Interestingly, addiction-related mice treated with KT80 (METH + KT80) significantly attenuated the CPP score as compared to post-conditioning phase of METH + CMC group ($P < 0.001$). These data confirmed that METH at 1 mg/kg significantly produced addictive behaviors. However, 80 mg/kg KT significantly

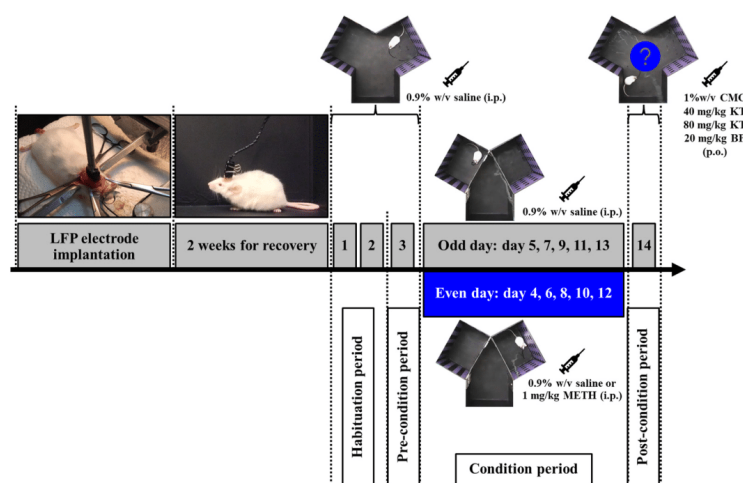


Fig. 1. Experimental protocol for investigation of KT alkaloid extract effects on METH CPP. Animals were handled through the processes of a surgery for LFP electrode implantation into the brain and a recovery period for at least 2 weeks. Following the habituation, the CPP paradigm consisted of 3 phases: habituation and pre-conditioning, conditioning, and post-conditioning period scheduled on day 1-3, 4-13, and 14, respectively. On post-conditioning phase, animals were administered orally with either 2 concentrations of KT alkaloid extract or a standard drug bupropion (BP) 60 min prior to testing of METH CPP and LFP patterns.

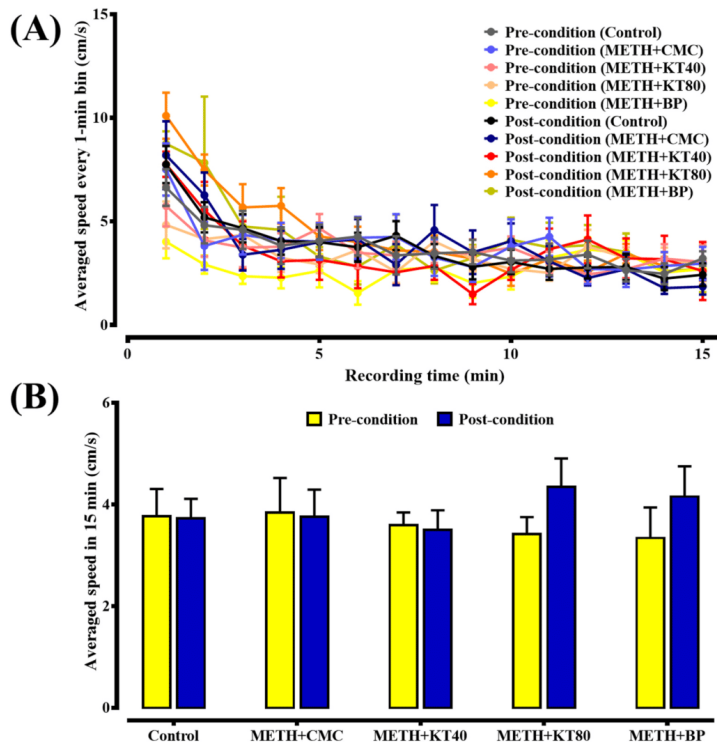


Fig. 2. Locomotor activity of mice during pre-conditioning and post-conditioning phases of control group ($n = 10$) and METH groups treated with solvent (METH + CMC) ($n = 7$), 40 mg/kg KT alkaloid (METH + KT40) ($n = 7$), 80 mg/kg KT alkaloid (METH + KT80) ($n = 8$), and a standard drug bupropion (BP) (METH + BP) ($n = 8$). Mean values of locomotor speed in each group were calculated every 1-min bin (A). Averaged speed in during a 15-min of exploration in CPP apparatus was analyzed (B).

ameliorated METH CPP in mice whereas a standard drug BP at 20 mg/kg failed to suppress the CPP score.

3.4. LFP oscillation in the NAc and the HP

The effects of KT alkaloid extract and BP on LFP pattern in the NAc and the HP during METH CPP were illustrated. Visual inspection was performed to overview the oscillations of raw LFP signals (Fig. 4). General patterns in the NAc were similar among groups during pre-conditioning phase. Therefore, the patterns appeared to be different during post-conditioning phase in which additional fast wave activity were superimposed in METH + CMC and METH + BP groups. In the HP, relatively similar patterns of LFP oscillation were seen among groups both during pre-conditioning and post-conditioning phases.

Therefore, raw LFP signals in the NAc during post-condition in time domain were computed and transformed into LFP power spectra (% Relative power) in frequency domain. LFP power spectra of control, METH + CMC, METH + KT40, METH + KT80, and METH + BP groups were shown for comparison (Fig. 5A). Statistical analysis confirmed significant differences found in delta [$F_{(4, 35)} = 4.458, P = 0.005$], theta [$F_{(4, 35)} = 5.194, P = 0.002$], alpha [$F_{(4, 35)} = 3.306, P = 0.021$], gamma I [$F_{(4, 35)} = 11.547, P < 0.001$], and gamma II [$F_{(4, 35)} = 5.512, P = 0.002$] bands (Fig. 5B). Tukey's post hoc analysis indicated a significant increase in gamma I ($P = 0.001$) and decrease in gamma II ($P = 0.012$) induced by METH conditioning. However, 80 mg/kg KT alkaloid extract significantly reversed the increased gamma I power ($P = 0.033$). No significant different was seen among control, METH + KT40 and METH

+ KT80 group for both gamma I and II. It was noted that METH + KT80 group significantly produced opposite effects to that of METH + CMC in delta ($P = 0.002$), theta ($P = 0.001$), and alpha ($P = 0.015$) bands. Moreover, METH + BP group produced significant differences from control levels in gamma I ($P < 0.001$) and gamma II ($P = 0.001$). The standard drug BP failed to reverse the effects of METH conditioning seen in gamma I and II powers of METH + CMC group.

In the HP, LFP power spectra of these 5 groups were shown for comparison. Dramatical differences among groups appeared to be seen in slow frequency activities below 20 Hz (Fig. 6A). Relatively equal powers were seen for higher frequency waves. One-way ANOVA revealed significant differences only in delta wave [$F_{(4, 35)} = 10.660, P < 0.001$]. Multiple comparisons confirmed significant increases in delta power seen in METH + CMC ($P = 0.001$) and METH + BP ($P = 0.003$) groups compared to that of control and METH + KT80 groups, respectively (Fig. 6B). Interestingly, this elevated delta power seen METH + CMC group was significantly suppressed by the treatment with both 40 mg/kg ($P = 0.001$) and 80 mg/kg ($P < 0.001$) KT alkaloid extract. Altogether, KT extract was found to prevent the increase in delta power induced by METH-conditioning. This LFP pattern in the HP was positively correlated with the data of CPP scores that might reflect the attenuation effect of the extract on the intensity of METH CPP.

3.5. The activities of the HP-NAc coherence

The effects of KT alkaloid extract and BP on coherence activity between the NAc and the HP during post-conditioning phase were

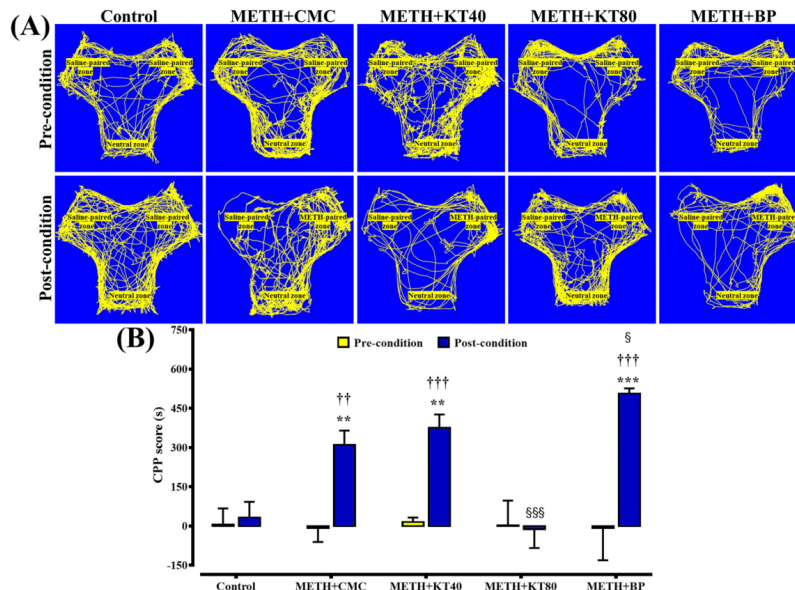


Fig. 3. Locomotor tracking of animal exploration in CPP apparatus during pre-conditioning and post-conditioning phases. Locomotor tracking of representative animals from each group were shown for comparison (A). Data of time spent in specific compartment were calculated and expressed as CPP scores for statistical analysis for the effects of 40 mg/kg KT alkaloid (METH + KT40) ($n = 7$), 80 mg/kg KT alkaloid (METH + KT80) ($n = 8$), and a reference drug BP at 20 mg/kg (METH + BP) ($n = 8$), compared to that treated with vehicle (METH + CMC) ($n = 7$) (B). CPP scores were calculated by the subtraction of time that mice spent in METH-paired zone with time spent in saline-paired zone. Data were expressed as mean \pm SEM. **, *** $P < 0.01, 0.001$ for significant analyses using two-way repeated ANOVA followed by *post hoc* Bonferroni test for multiple comparisons between pre-conditioning and post-conditioning phases. † $P < 0.01$, †† $P < 0.001$ compared with post-conditioning phase of control group. ††† $P < 0.005$, †††† $P < 0.001$ compared with post-conditioning phase of the METH + CMC group.

analyzed and compared among groups. Data were expressed as percent relative coherence in frequency domain (Fig. 7A). The results showed obvious differences in coherence activity mostly in a frequency range approximately between 30 and 50 Hz. Therefore, statistical analyses revealed significant differences only in gamma I band [$F_{(4, 35)} = 9.934$, $P < 0.001$] (Fig. 7B). Tukey's *post hoc* test confirmed significantly increased coherence values in gamma I band of METH + CMC group ($P = 0.022$). However, this increased coherence was significantly reversed only by treatment with KT80 ($P = 0.031$). No such effect was produced by treatment with BP, a standard drug for METH withdrawal treatment. Instead, METH + BP group was found to dramatically enhance the coherence activity in gamma I band compared to control ($P < 0.001$). The increased coherence produced by BP treatment was even further than in METH + CMC group.

4. Discussion

The effects of KT alkaloid extract and BP were measured during the expression of METH CPP. The present study highlighted that KT extract completely prevented METH CPP and changes in LFP oscillations induced by METH conditioning. At 80 mg/kg, KT alkaloid extract exhibited significant effects on all parameters, which might suggest its efficacies on both physical and mental symptoms. CPP score reflects drug craving and seeking behaviors. In contrast, neural signaling induced during the post-conditioning phase suggests the brain mechanism underlying withdrawal symptoms.

Several mental disorders, including depression and anxiety, were detected during METH and ethanol withdrawal periods (Embry et al.,

2009; Halpin et al., 2013; Kumarnsit et al., 2007a; Wearne and Cornish, 2018). Thus, potential substances for drug addiction treatment need to be determined whether they have CNS action with anti-depressive and anxiolytic effects. Previously, KT alkaloid extract was found to produce an LFP pattern and effectively attenuate the severity of ethanol withdrawal symptoms similarly to standard antidepressant drug fluoxetine (Cheaha et al., 2015). KT aqueous extract also attenuated ethanol withdrawal-induced depressive behavior, probably through its antidepressant-like activity (Kumarnsit et al., 2007a). Therefore, KT alkaloid extract and BP were hypothesized to effectively treat METH dependence in this CPP paradigm.

In this study, the antidepressant BP was deployed as a reference drug to compensate for dopamine (DA) depletion induced by METH exposures. Changes in behavior, emotion, learning, and the cognitive process are normally in response to DA depletion. BP was used to cure METH dependent patients as a dopamine transporter (DAT) inhibitor, and increases DA concentration in the synaptic cleft for stronger receptor activation (Stahl et al., 2004). It was also expected to improve depressive symptoms and mood swings during METH withdrawal period (Elkashaf et al., 2008). However, the present data showed that BP did not prevent or attenuate behavioral change and neural signaling induced METH conditioning (Figs. 3, 5 and 7). This may be discussed in terms of METH concentration used for the CPP paradigm. Previously, side preference in CPP paradigm induced by METH at 0.125–1.0 mg/kg was diminished by pretreatment with high dose METH that would induce neurotoxicity and decrease DA level in the striatum (STR) (Achat-Mendes et al., 2005). The dose of METH at 1.0 mg/kg in the present study was not likely to produce DA deficiency. It is possible that

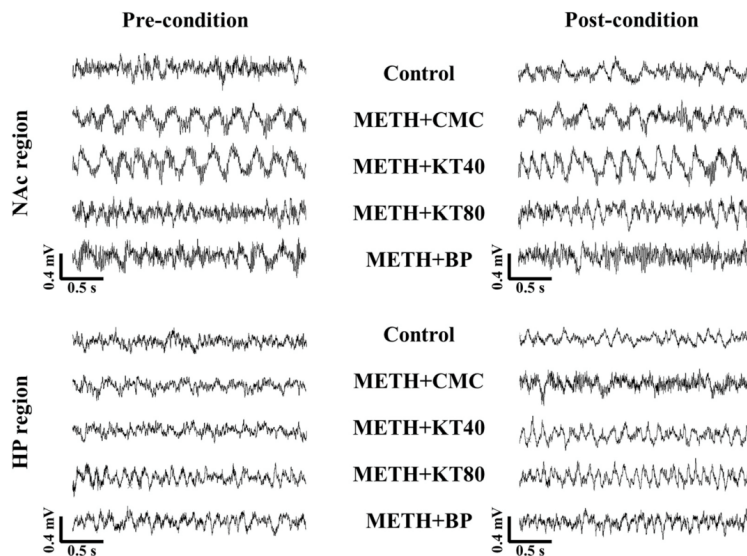


Fig. 4. Raw LFP signals of representative mice from each group during pre-conditioning (left panel) and post-conditioning (right panel) phases of control and METH groups treated with vehicle (CMC), 40 mg/kg KT alkaloid, 80 mg/kg KT alkaloid and 20 mg/kg BP. Raw signals were recorded from the nucleus accumbens (NAc) (top panel) and the hippocampus (HP) (bottom panel).

treatment with the DAT blocker could elicit excessively long lasting and overstimulation on DA receptors in METH + BP group as seen in CPP scores and LFP oscillatory patterns. Taken together, the alterations of parameters during the post-conditioning phase might partially be mediated through modulation in the DA system. Moreover, the present findings were consistent with a previous report that the other DAT blocker, methylphenidate (MTPD), also failed to produce beneficial results in the treatment of amphetamine/METH dependence (Miles et al., 2013). These data may suggest that DAT blockers (e.g., BP and/or MTPD) may be carefully used only in specific conditions of METH dependence.

The expression of METH CPP has been found in response to a memory-associated cue of METH exposures. Any drugs that alter animal movement could have some impacts on CPP outcomes. Apart from affecting CPP score, the fluctuation of animal's locomotor activity was also found to interfere with LFP signal generation and oscillation (Li et al., 2012; Reakkamnuan et al., 2017). Therefore, it was necessary to exclude this confounding factor. Previous data revealed that 80 mg/kg KT alkaloid extract *per se* did not alter the animal's locomotor activity (Cheaha et al., 2017). It means that the KT alkaloid extract at this concentration was clearly effective on METH CPP and clean from disturbance produced by the motor activity of mice.

In traditional use, whole alkaloid constituents of KT are ingested by chewing and drinking tea from KT leaves. The HPLC chromatograms (Supp. Figure 4) illustrate the fingerprints of compound of the extract. The phytochemical analysis confirmed the presence of MT as a major alkaloid in the KT extract which is in agreement with previous investigation (Cheaha et al., 2017). It has been reported that lyophilized tea (containing 25 mg/g MT) exhibited better oral bioavailability than feeding with MT alone (Avery et al., 2019). KT alkaloid extract, prepared in this study, had 47.1 mg MT per gram extract and was also administered orally to the mice.

CPP paradigm is a standard model routinely used for screening drug candidates or herbal extract on addictive substances-induced reward

behaviors in experimental animals. Various psychostimulant drugs such as METH, amphetamine, and cocaine were used as positive substances that produced addictive behaviors (Bardgett et al., 2020; Nukitram et al., 2021; Pandey et al., 2018; Shen et al., 2016). CPP is a form of Pavlovian conditioning used to measure the motivational effects of learning experiences (Cunningham et al., 2006). Pairing repeated drug use with a specific environment is believed to link with the conditioning context that the drug is delivered. Allowing animals to re-expose with drug-related context after the condition development is able to trigger craving behaviors. Animals were found to spend more time in the environment that has contextual cue paired with addictive drug delivery. The present study clearly showed the increased CPP score of METH + CMC group during post-conditioning phase. Fundamentally, this phenomenon appeared to have underlying mechanisms in many brain regions including the HP and the NAc functioning together as neural networks (Ito et al., 2008). Previously, reward-seeking behavior driven by the modulation of the HP-NAc axis has been also proposed (Trouche et al., 2019).

LFP spectral powers have been extensively analyzed as quantitative data for screening of unidentified new drug compounds in comparison to that of standard drugs with known CNS action (Cheaha et al., 2015; Dimpfel et al., 2016). In the present experiment, the increased gamma I LFP power in the NAc and CPP scores were induced by METH contextual cue. However, these parameters were significantly ameliorated by the treatment with 80 mg/kg KT alkaloid extract. The activity of the gamma I frequency range in the NAc is believed to be related with DA release and addiction. Basically, opioid receptor activation by its agonists such as a significant KT alkaloid composition MT or even morphine, a standard addictive drug, in the ventral tegmental area (VTA) was found to promote the over-release of DA as well as to increase gamma I in the NAc. However, these phenomena were abolished by pretreatment with naloxone, an opioid receptor blocker (Reakkamnuan et al., 2017). A psychoactive substance such as pseudoephedrine was demonstrated to have sites of action in both the NAc and STR of the dopamine pathway

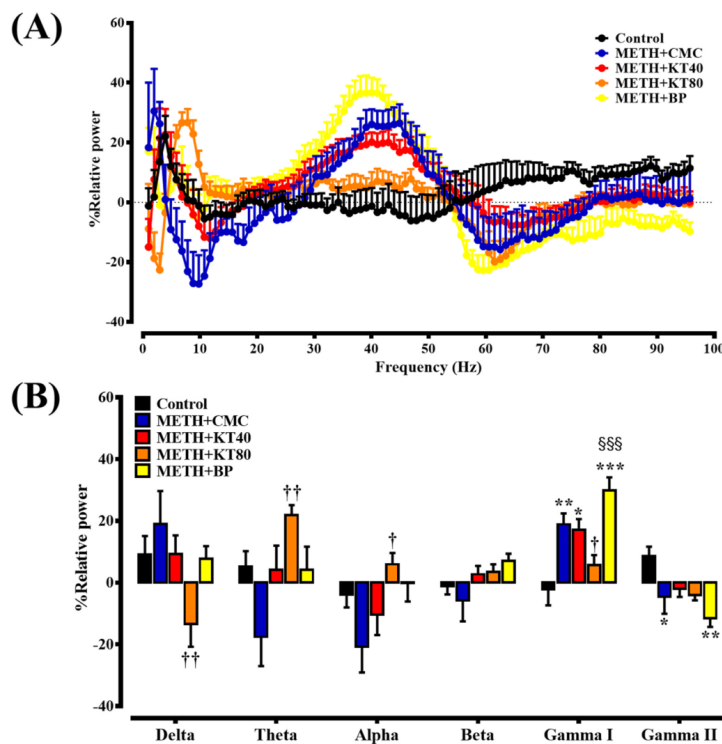


Fig. 5. Effects of the treatments on LFP spectral powers in the NAc. Animals were treated with KT alkaloid extract (40 and 80 mg/kg) and BP (20 mg/kg). Data were normalized as percent relative power (A). LFP spectral powers were divided into powers of 6 discrete frequency bands (B). All data were expressed as mean \pm SEM and statistically analyzed using one-way ANOVA followed by Tukey's *post hoc* test. * $P < 0.05$, ** $P < 0.01$, *** $P < 0.001$ compared with the control group. † $P < 0.05$, †† $P < 0.01$ compared with the METH + CMC. ‡ $P < 0.05$, ‡‡ $P < 0.001$ compared with the METH + KT80.

(Kumarnsit et al., 1999). Amphetamine and METH also activate gene expression in the mesolimbic/mesostriatal pathways via D1 and D2 dopamine receptors (Wang and McGinty, 1995). Previously, the dorsal raphe nuclei (DRn) is an origin of serotonergic projections that inhibit dopaminergic nigrostriatal neurons (Bantick et al., 2005). A previous report confirmed that the DRn was activated by KT extract (Kumarnsit et al., 2007b) that would result in decreased dopamine release in the NAc because the NAc is a major component of the ventral STR (Salgado and Kaplitt, 2015). Additionally, the involvement of antidopaminergic mechanism from methanolic extract of KT leaves evaluated by measuring the DA level in the NAc was also evidenced (Vijeeppallam et al., 2019). Thus, KT extract might alleviate withdrawal symptoms and decrease gamma I activity via reduced DA release in the NAc as a mechanism.

The present study also showed the decreases in gamma II oscillation in the NAc during post-conditioning phase only in METH + vehicle and METH + BP groups. Actually, a wide range of gamma II activities in the NAc have been evidenced (Reakkamnuan et al., 2017; Samerphob et al., 2020). Gamma II oscillation was induced by palatable food cue in CPP paradigm (Samerphob et al., 2020). This frequency band activity may be associated with brain mechanism that supports seeking behavior driven by CPP. Moreover, the positive correlation between gamma II oscillation and neuronal coding of movement was also reported (Reakkamnuan et al., 2017). The present CPP data clearly demonstrated that KT alkaloid extract at the effective dose did not induce spontaneous psychoactive effect. This was consistent with the previous report that 80 mg/kg KT alkaloid extract did not alter the motor activities (Cheaha et al., 2017).

Altogether, these findings proposed the attenuation effects of KT alkaloid extract on METH-induced addiction partially through dopaminergic modulation. Gamma I and II oscillations were sensitive to METH repeated exposures and treatment with KT alkaloid extract but not BP.

Following multiple exposures to METH sessions, significant changes in delta oscillation in the HP were also highlighted. METH-induced significant increase in HP delta power was consistent with the previous findings (Yusoff et al., 2016). The olfactory cue of palatable food was found to increase delta power in the CA1, the sub-area of the HP (Samerphob et al., 2017). HP delta activity was associated with memory encoding through neocortical–hippocampal crosstalk both in animals (Sirota et al., 2003) and human (Mitra et al., 2016). Delta oscillation in the HP was hypothesized to be part of neural mechanisms related with cognition and motivation. Changes in delta oscillation can be seen in human in response to emotional stimuli (Bamidis et al., 2009) and in the processing of reward-related condition (Yusoff et al., 2016). However, the enhanced HP delta power in this experiment was significantly reversed by KT alkaloid extract treatment. This result may partially be the outcome of the CNS action of KT alkaloid extract on the hypothalamic-pituitary-adrenal (HPA) axis. Basically, the HP is an important brain region known to regulate stress response via the HPA axis modulation (Herman et al., 2016). Having to face emotional stress during post-conditioning phase would result in drug craving behaviors as well as corticosterone (COR) secretion (De Vries et al., 1998). These stress responses especially the HPA axis hyperactivity and forced swimming-induced COR secretion were reduced by the treatment with MT, a major alkaloid from KT leaves (Jdayu et al., 2011). Moreover, MT

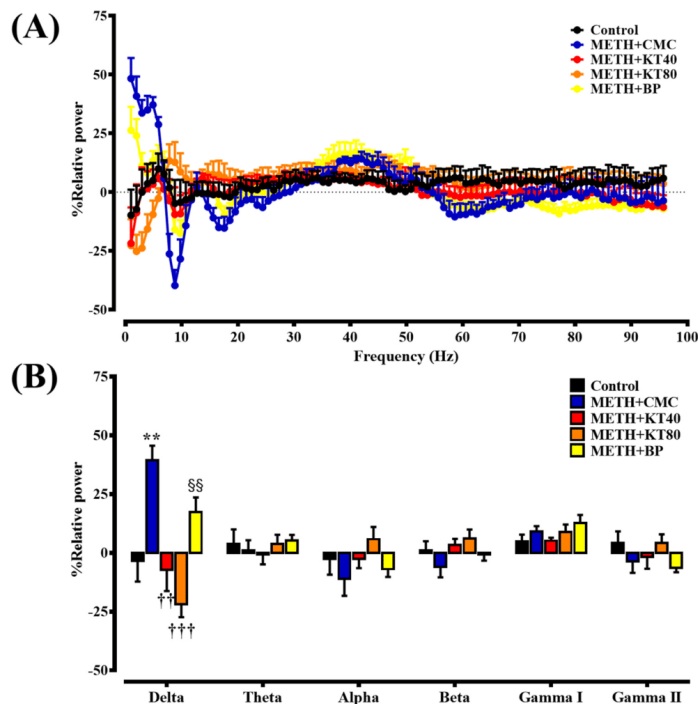


Fig. 6. Effects of the treatments with KT alkaloid extract on LFP spectral powers in the HP. Animals were treated with KT alkaloid extract (40 and 80 mg/kg) and BP (20 mg/kg). Data were normalized as percent relative power (A). LFP spectral powers were divided into powers of 6 discrete frequency bands (B). All data were expressed as mean \pm SEM and statistically analyzed using one-way ANOVA followed by Tukey's *post hoc* test. $^{**}P < 0.01$ compared with the control group. $^{\dagger\dagger}P < 0.01$ compared with the METH + CMC. $^{\dagger\dagger\dagger}P < 0.001$ compared with the METH + KT80.

was able to suppress HP delta and CPP score (Yusoff et al., 2016). These findings may suggest the alternative mechanism that the HP delta rhythm reflect the brain mechanism of motivation for METH seeking behavior. With the mechanism of MT, KT alkaloid extract which contains MT as a major alkaloid constituent would reduce stress, CPP score and neural signaling patterns induced during METH post-conditioning phase.

The regulation of each behavior may involve multiple brain areas functioning in coordination. The interrelationship of the HP-NAC axis was believed to mediate drug-related cue induced seeking behaviors (Trouche et al., 2019). To assess the communication between separate brain regions following drug treatment, coherence analysis, a mathematical algorithm, was used to measure the strength of neural connection. The present data revealed that METH + CMC group increased both percent relative coherence in gamma I frequency range and CPP score. However, this coherence activity was completely reversed by 80 mg/kg KT alkaloid extract. Previously, the HP was demonstrated to contain neuronal population of place cells that selectively burst in response to specific spatial contexts (Battaglia et al., 2004). This is the evidence-based finding that strongly suggests the involvement of the HP in the processing of spatial navigation (Jones and Wilson, 2005). With the coherence activity, signaling information could be sent through the projection from the CA1 region of the HP to the NAc (Zhou et al., 2020). The analysis of firing rate confirmed that place cells in the HP fired preferentially before reward-related neurons in the NAc. This finding indicated that place-reward information was carried from the HP to the NAc (Lansink et al., 2009). Ultimately, the interaction between the HP and the NAc also plays a significant role in CPP acquisition (Ito et al., 2008). Moreover, a modern investigation in this experiment also found

that LFP in the dorsal HP relatively exhibited high coherence value at gamma I band with the LFP in the NAc. This may be associated with the processing of information in decision making and reinforcement-based learning (Berke, 2009). This study suggests that the elevated CPP score and coherence in gamma I frequency range were triggered by neural signal of METH-associated cue sent from the HP to the NAc. Therefore, KT80 treatment may help attenuate METH dependence and reduce the inter-region connectivity.

5. Conclusion

In summary, the present study proposed beneficial effects of 80 mg/kg KT alkaloid extract for treatment of METH dependence. The data from CPP paradigm revealed that the extract successfully reversed METH CPP scores. This would suggest therapeutic property of KT plant in treatment of abnormal behaviors induced by METH dependence. Moreover, the analyses of LFP power spectra and coherence also provided additional data for better understanding of possible brain mechanisms of KT alkaloid extract in attenuation of METH CPP. Taken together, these findings strongly suggested that the KT alkaloid extract has promising effects for further development as an alternative compound for possible use in METH addicted patients.

CRedit authorship contribution statement

Jakkrit Nukitram: Methodology, Software, Validation, Formal analysis, Investigation, Resources, Data curation, Writing – original draft, Visualization, Funding acquisition. **Dania Cheaha:** Software, Resources. **Narumon Sengnon:** Methodology, Validation. **Juraithip**

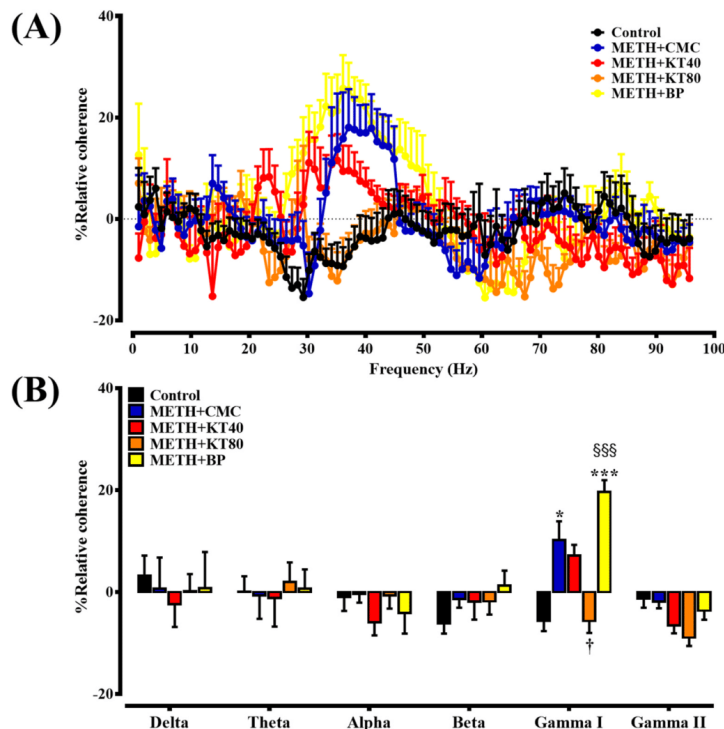


Fig. 7. Effects of the treatments with KT alkaloid extract on LFP spectral coherence between the HP and the NAc in frequency domain (1–100 Hz). Animals were treated with KT alkaloid extract (40 and 80 mg/kg) and BP (20 mg/kg). Data were normalized as percent relative coherence and expressed as mean \pm SEM (A). Data of each group were averaged in 6 discrete frequency bands (B). Statistical analyses were performed using one-way ANOVA followed by Tukey's *post hoc* test. ** $P < 0.05$, *** $P < 0.001$ compared with the control group. † $P < 0.05$ compared with the METH + CMC. §§§ $P < 0.001$ compared with the METH + KT80.

Wungsintaweekul: Methodology, Validation, and. **Supattra Limsuwanchote:** Methodology, Validation. **Ekkasit Kumarnsit:** Conceptualization, Writing – review & editing, Supervision, Project administration.

Declaration of competing interest

The authors declare that there are no conflicts of interest.

Acknowledgment

The carry out in this experiment was supported by a grant from the professional development project under the Science Achievement Scholarship of Thailand (SAST). Partially financial support was also from the Program of Physiology, Division of Health and Applied Science, Faculty of Science, Prince of Songkla University, Thailand.

Appendix A. Supplementary data

Supplementary data to this article can be found online at <https://doi.org/10.1016/j.jep.2021.114824>.

References

Achat-Mendes, C., Ali, S.F., Itzhak, Y., 2005. Differential effects of amphetamines-induced neurotoxicity on appetitive and aversive Pavlovian conditioning in mice. *Neuropsychopharmacology* 30, 1128–1137. <https://doi.org/10.1038/sj.npp.1300675>.

Adkins, J.E., Boyer, E.W., McCurdy, C.R., 2011. *Mitragyna speciosa*, a psychoactive tree from southeast asia with opioid activity. *Curr. Top. Med. Chem.* 11, 1165–1175. <https://doi.org/10.2174/156802611795371305>.

Assanangkornchai, S., Muekthong, A., Sam-Angsri, N., Pattanasattayawong, U., 2007. The use of *Mitragyna speciosa* ("Kratom"), an addictive plant. *Thailand. Subst. Use Misuse* 42, 2145–2157. <https://doi.org/10.1080/10826080701205869>.

Avery, B.A., Boddu, S.P., Sharma, A., Furr, E.B., Leon, F., Cutler, S.J., McCurdy, C.R., 2019. Comparative pharmacokinetics of mitragynine after oral administration of *Mitragyna speciosa* (Kratom) leaf extracts in rats. *Planta Med.* 85, 340–346. <https://doi.org/10.1055/a-0770-3683>.

Bamidis, P.D., Kladou, M.A., Frantidis, C., Vivas, A.B., Papadelis, C., Lithari, C., Pappas, C., 2009. A framework combining delta event-related oscillations (EROs) and synchronisation effects (ERD/ERS) to study emotional processing. *Comput. Intell. Neurosci.* 1–16. <https://doi.org/10.1155/2009/549419>, 2009.

Bantick, R.A., De Vries, M.H., Grashy, P.M., 2005. The effect of a 5-HT1A receptor agonist on striatal dopamine release. *Synapse* 57, 67–75. <https://doi.org/10.1002/syn.20156>.

Bardgett, M.E., Downen, T., Crane, C., Baltes Thompson, E.C., Muncie, B., Steffen, S.A., Yates, J.R., Pauly, J.R., 2020. Chronic risperidone administration leads to greater amphetamine-induced conditioned place preference. *Neuropharmacology* 179, 108276. <https://doi.org/10.1016/j.neuropharm.2020.108276>.

Battaglia, F.P., Sutherland, G.R., McNaughton, B.L., 2004. Local sensory cues and place cell directionality: additional evidence of prospective coding in the hippocampus. *J. Neurosci.* 24, 4541–4550. <https://doi.org/10.1523/JNEUROSCI.4896-03.2004>.

Ben-Shaul, Y., 2017. OptiMouse: a comprehensive open source program for reliable detection and analysis of mouse body and nose positions. *BMC Biol.* 15, 1–22. <https://doi.org/10.1186/s12915-017-0377-3>.

Berke, J.D., 2009. Fast oscillations in cortical-striatal networks switch frequency following rewarding events and stimulant drugs. *Eur. J. Neurosci.* 30, 848–859. <https://doi.org/10.1111/j.1460-9568.2009.06843.x>.

Caillé, S., Espejo, E.F., Reneric, J.P., Cadot, M., Koob, G.F., Stinus, L., 1999. Total neurochemical lesion of noradrenergic neurons of the locus ceruleus does not alter either naloxone-precipitated or spontaneous opiate withdrawal nor does it influence ability of clonidine to reverse opiate withdrawal. *J. Pharmacol. Exp. Therapeut.* 290, 881–892.

- Chan, K.B., Pakiam, C., Rahim, R.A., 2007. Psychoactive plant abuse: the identification of mitragynine in ketum and in ketum preparations. *Bull. Narc.* 57, 249–256.
- Cheaha, D., Keawpradub, N., Sawangjaroen, K., Phukpattaranont, P., Kumarnsit, E., 2015. Effects of an alkaloid-rich extract from *Mitragyna speciosa* leaves and fluoxetine on sleep profiles, EEG spectral frequency and ethanol withdrawal symptoms in rats. *Phytomedicine* 22, 1000–1008. <https://doi.org/10.1016/j.phymed.2015.07.008>.
- Cheaha, D., Reakkamuan, C., Nukitram, J., Chittrakarn, S., Phukpattaranont, P., Keawpradub, N., Kumarnsit, E., 2017. Effects of alkaloid-rich extract from *Mitragyna speciosa* (Korth.) Havil. on naloxone-precipitated morphine withdrawal symptoms and local field potential in the nucleus accumbens of mice. *J. Ethnopharmacol.* 208, 129–137. <https://doi.org/10.1016/j.jep.2017.07.008>.
- Cunningham, C.L., Gremel, C.M., Groblewski, P.A., 2006. Drug-induced conditioned place preference and aversion in mice. *Nat. Protoc.* 1, 1662–1670. <https://doi.org/10.1038/nprot.2006.279>.
- De Vries, A.C., Taymans, S.E., Sundstrom, J.M., Pert, A., 1998. Conditioned release of corticosterone by contextual stimuli associated with cocaine is mediated by corticotropin-releasing factor. *Brain Res.* 786, 39–46. [https://doi.org/10.1016/S0006-8993\(97\)01328-0](https://doi.org/10.1016/S0006-8993(97)01328-0).
- Dimpfel, W., 2008. Pharmacological modulation of dopaminergic brain activity and its reflection in spectral frequencies of the rat electroencephalogram. *Neuropsychobiology* 58, 178–186. <https://doi.org/10.1159/000191124>.
- Dimpfel, W., Schombert, L., Gericke, N., 2016. Electroencephalogram of Sceletium tortuosum extract based on spectral local field power in conscious freely moving rats. *J. Ethnopharmacol.* 177, 140–147. <https://doi.org/10.1016/j.jep.2015.11.036>.
- Elkashaf, A.M., Rawson, R.A., Anderson, A.L., Li, S.H., Holmes, T., Smith, E.V., Chiang, N., Kahy, R., Vocci, F., Ling, W., Pearce, V.J., McCann, M., Campbell, J., Gorodetsky, C., Haning, W., Carlton, B., Mawhinney, J., Weis, D., 2008. Bupropion for the treatment of methamphetamine dependence. *Neuropsychopharmacology* 33, 1162–1170. <https://doi.org/10.1038/sj.npp.1301481>.
- Embry, D., Hankins, M., Biglan, A., Boles, S., 2009. Behavioral and social correlates of methamphetamine use in a population-based sample of early and later adolescents. *Addict. Behav.* 34, 343–351. <https://doi.org/10.1016/j.addbeh.2008.11.019>.
- Foltin, R.W., Haney, M., 2000. Conditioned effects of environmental stimuli paired with smoked cocaine in humans. *Psychopharmacology (Berlin)* 149, 24–33. <https://doi.org/10.1007/s002139900340>.
- Foss, J.D., Nayak, S.U., Tallarida, C.S., Farkas, D.J., Ward, S.J., Rawls, S.M., 2020. Mitragynine, bioactive alkaloid of kratom, reduces chemotherapy-induced neuropathic pain in rats through α -adrenoceptor mechanism. *Drug Alcohol Depend.* 209, 1–9. <https://doi.org/10.1016/j.drugalcdep.2020.107946>.
- Goldfine, A.M., Victor, J.D., Conte, M.M., Bardin, J.C., Schiff, N.D., 2011. Determination of awareness in patients with severe brain injury using EEG power spectral analysis. *Clin. Neurophysiol.* 122, 2157–2168. <https://doi.org/10.1016/j.clinph.2011.03.022>.
- Halpin, L.E., Collins, S.A., Yamamoto, B.K., 2013. Neurotoxicity of methamphetamine and 3,4-methylenedioxymethamphetamine. *Life Sci.* 97, 37–44. <https://doi.org/10.1016/j.lfs.2013.07.014>.
- Herman, J.P., McKlveen, J.M., Ghosal, S., Kopp, B., Wulsin, A., Makinson, R., Scheimann, J., Myers, B., 2016. Regulation of the hypothalamic-pituitary-adrenocortical stress response. *Comp. Physiol.* 6, 603–621. <https://doi.org/10.1002/cphy.e150015>.
- Idayu, N.F., Taufik Hidayat, M., Moklas, M.A.M., Sharida, F., Nurul Raudzah, A.R., Shamima, A.R., Apryani, E., 2011. Antidepressant-like effect of mitragynine isolated from *Mitragyna speciosa* Korth in mice model of depression. *Phytomedicine* 18, 402–407. <https://doi.org/10.1016/j.phymed.2010.08.011>.
- Ito, R., Robbins, T.W., Pennartz, C.M., Everitt, B.J., 2008. Functional interaction between the hippocampus and nucleus accumbens shell is necessary for the acquisition of appetitive spatial context conditioning. *J. Neurosci.* 28, 6950–6959. <https://doi.org/10.1523/JNEUROSCI.1615-08.2008>.
- Jansen, K.L., Prast, C.J., 1988. Psychoactive properties of mitragynine (kratom). *J. Psychoact. Drugs* 20, 455–457. <https://doi.org/10.1080/02791072.1988.10472519>.
- Jones, M.W., Wilson, M.A., 2005. Theta rhythms coordinate hippocampal-prefrontal interactions in a spatial memory task. *PLoS Biol.* 3, e402 <https://doi.org/10.1371/journal.pbio.0030402>.
- Keawpradub, N., 1990. Alkaloids from the fresh leaves of *Mitragyna speciosa* (Korth.) Havil. *Grad. Sch. Chulalongkorn Univ. Bangkok*.
- Kilkenny, C., Browne, W.J., Cuthill, I.C., Emerson, M., Altman, D.G., 2010. Improving bioscience research reporting: the arrive guidelines for reporting animal research. *PLoS Biol.* 8, 6–10. <https://doi.org/10.1371/journal.pbio.1000412>.
- Kitajima, M., Misawa, K., Kogure, N., Said, I.M., Horie, S., Hatori, Y., Murayama, T., Takayama, H., 2006. A new indole alkaloid, 7-hydroxyspeciocillatine, from the fruits of Malaysian *Mitragyna speciosa* and its opioid agonistic activity. *J. Nat. Med.* 60, 28–35. <https://doi.org/10.1007/S11418-005-0001-7>.
- Korpi, E.R., den Hollander, B., Faraoo, U., Vashchinkina, E., Rajkumar, R., Nutt, D.J., Hyttia, P., Dawe, G.S., 2015. Mechanisms of action and persistent neuroplasticity by drugs of abuse. *Pharmacol. Rev.* 67, 872–1004. <https://doi.org/10.1124/pr.115.010967>.
- Kruegel, A.C., Grundmann, O., 2018. The medicinal chemistry and neuropharmacology of kratom: a preliminary discussion of a promising medicinal plant and analysis of its potential for abuse. *Neuropharmacology* 134, 108–120. <https://doi.org/10.1016/j.neuropharm.2017.08.026>.
- Kumarnsit, E., Harnyuttananakorn, P., Meksurien, D., Govitrapong, P., Baldwin, B.A., Kotchabhakdi, N., Casalotti, S.O., 1999. Pseudoephedrine, a sympathomimetic agent, induces Fos-like immunoreactivity in rat nucleus accumbens and striatum. *Neuropharmacology* 38, 1381–1387. [https://doi.org/10.1016/S0028-3908\(99\)00054-4](https://doi.org/10.1016/S0028-3908(99)00054-4).
- Kumarnsit, E., Keawpradub, N., Nuankae, W., 2007a. Effect of *Mitragyna speciosa* aqueous extract on ethanol withdrawal symptoms in mice. *Pitoterapia* 78, 182–185. <https://doi.org/10.1016/j.froete.2006.11.012>.
- Kumarnsit, E., Vongvatcharanon, U., Keawpradub, N., Intasaro, P., 2007b. Fos-like immunoreactivity in rat dorsal raphe nuclei induced by alkaloid extract of *Mitragyna speciosa*. *Neurosci. Lett.* 416, 128–132. <https://doi.org/10.1016/j.neulet.2007.01.061>.
- Lansink, C.S., Goltstein, P.M., Lankelma, J.V., McNaughton, B.L., Pennartz, C.M.A., 2009. Hippocampus leads ventral striatum in replay of place-reward information. *PLoS Biol.* 7, 1000173. <https://doi.org/10.1371/journal.pbio.1000173>.
- Li, J.Y., Kuo, T.B.J., Hsieh, I.T., Yang, C.C.H., 2012. Changes in hippocampal theta rhythm and their correlations with speed during different phases of voluntary wheel running in rats. *Neuroscience* 213, 54–61. <https://doi.org/10.1016/j.neuroscience.2012.04.020>.
- Limsuwanchote, S., Wungintaweekul, J., Keawpradub, N., Patalun, W., Morimoto, S., Tanaka, H., 2015. Development of indirect competitive ELISA for quantification of mitragynine in Kratom (*Mitragyna speciosa* (Roxb.) Korth.). *Forensic Sci. Int.* 244, 70–77. <https://doi.org/10.1016/j.forsciint.2014.08.011>.
- Masuoka, T., Fujii, Y., Kamei, C., 2006. Participation of the hippocampal theta rhythm in memory formation for an eight-arm radial maze task in rats. *Brain Res.* 1103, 159–163. <https://doi.org/10.1016/j.brainres.2006.04.003>.
- Miles, S.W., Sheridan, J., Russell, B., Kydd, R., Wheeler, A., Walters, C., Gamble, G., Hardley, P., Jensen, M., Kuoppasalmi, K., Tuomola, P., Föhr, J., Kuikamäki, O., Vorm, H., Salokangas, R., Mikkonen, A., Kallio, M., Kauhanen, J., Kiviniemi, V., Tiikonen, J., 2013. Extended-release methylphenidate for treatment of amphetamine/methamphetamine dependence: a randomized, double-blind, placebo-controlled trial. *Addiction* 108, 1279–1286. <https://doi.org/10.1111/add.12109>.
- Mitra, A., Snyder, A.Z., Hacker, C.D., Pahwa, M., Tagliazucchi, E., Laufs, H., Leuthardt, E.C., Raichle, M.E., 2016. Human cortical-hippocampal dialogue in wake and slow-wave sleep. *Proc. Natl. Acad. Sci. U.S.A.* 113, E6868–E6876. <https://doi.org/10.1073/pnas.1607289113>.
- Murias, M., Webb, S.J., Greenson, J., Dawson, G., 2007. Resting state cortical connectivity reflected in EEG coherence in individuals with autism. *Biol. Psychiatry* 62, 270–273. <https://doi.org/10.1016/j.biopsych.2006.11.012>.
- Nukitram, J., Cheaha, D., Kumarnsit, E., 2021. Spectral power and theta-gamma coupling in the basolateral amygdala related with methamphetamine conditioned place preference in mice. *Neurosci. Lett.* 756, 1–10. <https://doi.org/10.1016/j.neulet.2021.135939>.
- Pandy, V., Wai, Y.C., Amira Roslan, N.F., Sajat, A., Abdulla Jalil, A.H., Vijeeppallam, K., 2018. Methanolic extract of *Morinda citrifolia* Linn. unripe fruit attenuates methamphetamine-induced conditioned place preferences in mice. *Biomed. Pharmacother.* 107, 368–373. <https://doi.org/10.1016/j.biopha.2018.08.008>.
- Paxinos, G., Franklin, K.B.J., 2001. *The Mouse Brain in Stereotaxic Coordinates*. Reakkamuan, C., Cheaha, D., Kumarnsit, E., 2017. Nucleus accumbens local field potential power spectrums, phase-amplitude couplings and coherences following morphine treatment. *Acta Neurobiol. Exp.* 77, 214–224. <https://doi.org/10.21307/ane-2017-055>.
- Salgado, S., Kaplitt, M.G., 2015. The nucleus accumbens: a comprehensive review. *Stereotact. Funct. Neurosurg.* 93, 75–93. <https://doi.org/10.1159/000368279>.
- Samerphob, N., Cheaha, D., Chatpun, S., Kumarnsit, E., 2017. Hippocampal CA1 local field potential oscillations induced by olfactory cue of liked food. *Neurobiol. Learn. Mem.* 142, 173–181. <https://doi.org/10.1016/j.nlm.2017.05.011>.
- Samerphob, N., Cheaha, D., Issuriya, A., Chatpun, S., Lertwittayanon, W., Jensen, O., Kumarnsit, E., 2020. Changes in neural network connectivity in mice brain following exposures to palatable food. *Neurosci. Lett.* 714, 1–7. <https://doi.org/10.1016/j.neulet.2019.134542>.
- Saref, A., Suraya, S., Singh, D., Grundmann, O., Narayanan, S., Swogger, M.T., Prozialek, W.C., Boyer, E., Balasingam, V., 2020. Self-report data on regular consumption of illicit drugs and HIV risk behaviors after kratom (*Mitragyna speciosa* korth.) initiation among illicit drug users in Malaysia. *J. Psychoact. Drugs* 52, 138–144. <https://doi.org/10.1080/02791072.2019.1686553>.
- Saref, A., Suraya, S., Singh, D., Grundmann, O., Narayanan, S., Swogger, M.T., Prozialek, W.C., Boyer, E., Chear, N.J.Y., Balasingam, V., 2019. Self-reported prevalence and severity of opioid and kratom (*Mitragyna speciosa* korth.) side effects. *J. Ethnopharmacol.* 238, 1–8. <https://doi.org/10.1016/j.jep.2019.111876>.
- Shen, M., Jiang, C., Liu, P., Wang, F., Ma, L., 2016. Mesolimbic leptin signaling negatively regulates cocaine-conditioned reward. *Transl. Psychiatry* 6, 1–10. <https://doi.org/10.1038/tp.2016.223>.
- Singh, D., Yeou Chear, N.J., Narayanan, S., Leon, F., Sharma, A., McCurdy, C.R., Avery, B.A., Balasingam, V., 2020. Patterns and reasons for kratom (*Mitragyna speciosa*) use among current and former opioid poly-drug users. *J. Ethnopharmacol.* 249, 112462. <https://doi.org/10.1016/j.jep.2019.112462>.
- Sirota, A., Csicsvari, J., Buhl, D., Buzsáki, G., 2003. Communication between neocortex and hippocampus during sleep in rodents. *Proc. Natl. Acad. Sci. U.S.A.* 100, 2065–2069. <https://doi.org/10.1073/pnas.0437938100>.
- Stahl, S.M., Pradko, J.F., Haight, B.R., Modell, J.G., Rockett, C.B., Learned-Coughlin, S., 2004. A review of the neuropharmacology of bupropion, a dual norepinephrine and dopamine reuptake inhibitor. *Prim. Care Companion J. Clin. Psychiatry* 159–166. <https://doi.org/10.4088/pcp.v06n0403.06>.
- Suhaimi, F.W., Yusoff, N.H.M., Hassan, R., Mansor, S.M., Navaratnam, V., Müller, C.P., Hassan, Z., 2016. Neurobiology of kratom and its main alkaloid mitragynine. *Brain Res. Bull.* 126, 29–40. <https://doi.org/10.1016/j.brainresbull.2016.03.015>.

- Tadel, F., Baillet, S., Mosher, J.C., Pantazis, D., Leahy, R.M., 2011. Brainstorm: a user-friendly application for MEG/EEG analysis. *Comput. Intell. Neurosci.* 1–13. <https://doi.org/10.1155/2011/879716>, 2011.
- Trouche, S., Koren, V., Doig, N.M., Ellender, T.J., El-Gaby, M., Lopes-dos-Santos, V., Reeve, H.M., Perestenko, P.V., Garas, F.N., Magill, P.J., Sharott, A., Dupret, D., 2019. A hippocampus-accumbens tripartite neuronal motif guides appetitive memory in space. *Cell* 176, 1393–1406. <https://doi.org/10.1016/j.cell.2018.12.037> e16.
- Turnipseed, S.D., Richards, J.R., Kirk, J.D., Diercks, D.B., Amsterdam, E.A., 2003. Frequency of acute coronary syndrome in patients presenting to the emergency department with chest pain after methamphetamine use. *J. Emerg. Med.* 24, 369–373. [https://doi.org/10.1016/S0736-4679\(03\)00031-3](https://doi.org/10.1016/S0736-4679(03)00031-3).
- Unde, S.A., Shriram, R., 2014. PSD based coherence analysis of EEG signals for stroop task. *Int. J. Comput. Appl.* 95, 975–8887. <https://doi.org/10.5120/16675-6778>.
- Van Zutphen, B.F.M., 2004. The European science foundation: three Rs policy and education. *ATLA Altern. to Lab. Anim.* 32, 533–537. <https://doi.org/10.1177/026119290403201s86>.
- Vijeeppallam, K., Pandey, V., Murugan, D.D., Naidu, M., 2019. Methanolic extract of *Mitragyna speciosa* Korth leaf inhibits ethanol seeking behaviour in mice: involvement of antidopaminergic mechanism. *Metab. Brain Dis.* 34, 1712–1722. <https://doi.org/10.1007/s11011-019-00477-2>.
- Wang, J.Q., McGinty, J.F., 1995. Differential effects of D1 and D2 dopamine receptor antagonists on acute amphetamine- or methamphetamine-induced up-regulation of zif/268 mRNA expression in rat forebrain. *J. Neurochem.* 65, 2706–2715. <https://doi.org/10.1046/j.1471-4159.1995.65062706.x>.
- Wearne, T.A., Cornish, J.L., 2018. A comparison of methamphetamine-induced psychosis and schizophrenia: a review of positive, negative, and cognitive symptomatology. *Front. Psychiatr.* 9, 1–21. <https://doi.org/10.3389/fpsyg.2018.00491>.
- Yusoff, N.H.M., Mansor, S.M., Müller, C.P., Hassan, Z., 2018. Baclofen blocks the acquisition and expression of mitragynine-induced conditioned place preference in rats. *Behav. Brain Res.* 345, 65–71. <https://doi.org/10.1016/j.bbr.2018.02.039>.
- Yusoff, N.H.M., Mansor, S.M., Müller, C.P., Hassan, Z., 2017. Opioid receptors mediate the acquisition, but not the expression of mitragynine-induced conditioned place preference in rats. *Behav. Brain Res.* 332, 1–6. <https://doi.org/10.1016/j.bbr.2017.05.059>.
- Yusoff, N.H.M., Suhaimi, F.W., Vadivelu, R.K., Hassan, Z., Rümmler, A., Rotter, A., Amato, D., Dringenberg, H.C., Mansor, S.M., Navaratnam, V., Müller, C.P., 2016. Abuse potential and adverse cognitive effects of mitragynine (kratom). *Addiction Biol.* 21, 98–110. <https://doi.org/10.1111/adb.12185>.
- Zhou, Y., Yan, E., Cheng, D., Zhu, H., Liu, Z., Chen, X., Ma, L., Liu, X., 2020. The projection from ventral CA1, not prefrontal cortex, to nucleus accumbens core mediates recent memory retrieval of cocaine-conditioned place preference. *Front. Behav. Neurosci.* 14, 1–13. <https://doi.org/10.3389/fnbeh.2020.558074>.

Appendix B
Ethical approval of using the animal for scientific purposes



PRINCE OF SONGKLA UNIVERSITY
15 Karnjanawanij Road, Hat Yai, Songkhla 90110, Thailand
Tel (66-74) 286940 Fax (66-74) 286961
Website : www.psu.ac.th

MHESI 6800.11/ 845

Ref.57/2019

July 22, 2019

This is to certify that the research project entitled "Effects of cannabinoid (*Cannabis sativa* L.) and kratom (*Mitragyna speciosa* (Korth.) Havil) extracts on behaviors and electrical brain activity of mice induced by methamphetamine and 3,4-methylenedioxy-methamphetamine" conducted by Assoc. Prof. Dr. Ekkasit Kumarnsit, Faculty of Science, Prince of Songkla University, has been approved by Institutional Animal Care and Use Committee, Prince of Songkla University.

Wandee Udomuksorn

Wandee Udomuksorn, Ph.D.
Chairman,
Institutional Animal Care and Use Committee, Prince of Songkla University

VITAE

Name Mr. Jakkrit Nukitram

Student ID 6110230003

Academic background

Degree	Name of Institution	Year of Graduation
Bachelor of Science Program in Biology (First-Class Honours)	Khon Kaen University	2017

Scholarships and awards:

- Human Resource Development in Science Project (Science Achievement Scholarship of Thailand, SAST), Thailand
- Krung Thai Bank Scholarship, Thailand
- Outstanding undergraduate student award in the Biology program with the highest GPA from Professor Tab Nilaniti Foundation, Thailand
- Canada-ASEAN Scholarships and Educational Exchanges for Development (SEED), Canada (Cancellation)

International Meetings:

- **Oral presentation** – **Nukitram, J.**, Cheaha, D., & Kumarnsit, E. Medial prefrontal cortex local field potential oscillations and attenuated craving behaviors in methamphetamine-induced addictive-like behaviors mice in response to *Mitragyna speciosa* (Korth.) Havil. leaves extract treatment. *The 8th International BioScience Conference (IBSC)*, November 25-26, 2021, Novi Sad, Serbia
- **Poster presentation** - **Nukitram, J.**, Cheaha, D., & Kumarnsit, E. Neural signaling in the VTA-accumbens axis correlated with cannabis extract effects on methamphetamine conditioned place preference in mice. *The 13th FENS Forum of Neuroscience*, July 9-13, 2022, Paris, France.

Publications:

- Cheaha, D., Reakkamnuan, C., **Nukitram, J.**, Chittrakarn, S., Phukpattaranont, P., Keawpradub, N., & Kumarnsit, E. (2017). Effects of alkaloid-rich extract from *Mitragyna speciosa* (Korth.) Havil. on naloxone-precipitated morphine withdrawal symptoms and local field potential in the nucleus accumbens of mice. *Journal of Ethnopharmacology*, 208, 129-137.
- **Nukitram, J.**, Cheaha, D., & Kumarnsit, E. (2021). Spectral power and theta-gamma coupling in the basolateral amygdala related with methamphetamine conditioned place preference in mice. *Neuroscience letters*, 756, 135939.
- Niyomrat, K., Cheaha, D., **Nukitram, J.**, & Kumarnsit, E. (2021). Locomotor activity and resting local field potential oscillatory rhythms of 6-OHDA mouse model of Parkinson's disease in response to acute and repeated treatments with L-dopa. *Neuroscience Letters*, 759, 136007.
- **Nukitram, J.**, Cheaha, D., Sengnon, N., Wungsintaweekul, J., Limsuwanchote, S., & Kumarnsit, E. (2022). Ameliorative effects of alkaloid extract from *Mitragyna speciosa* (Korth.) Havil. Leaves on methamphetamine conditioned place preference in mice. *Journal of Ethnopharmacology*, 284, 114824.